

ออกซิเดชันเชิงเร่งปฏิกิริยาด้วยไฟฟ้าของเมทานอลด้วยตัวเร่งปฏิกิริยาโลหะ-ฟ่อนาโนคาร์บอน

นางสาวรัตนา จีระประดิษฐ์

วิทยานิพนธ์นี้เป็นส่วนหนึ่งของการศึกษาตามหลักสูตรปริญญาวิทยาศาสตรมหาบัณฑิต

สาขาวิชาวิชาปิโตรเคมีและวิทยาศาสตร์พอลิเมอร์

คณะวิทยาศาสตร์ จุฬาลงกรณ์มหาวิทยาลัย

ปีการศึกษา 2551

ลิขสิทธิ์ของจุฬาลงกรณ์มหาวิทยาลัย

ELECTROCATALYTIC OXIDATION OF METHANOL BY METAL-CARBON  
NANOTUBE CATALYSTS

Miss Rattana Cheerapradit

A Thesis Submitted in Partial Fulfillment of the Requirements  
for the Degree of Master of Science Program in Petrochemistry and Polymer Science  
Faculty of Science  
Chulalongkorn University  
Academic Year 2008  
Copyright of Chulalongkorn University

Thesis Title                    ELECTROCATALYTIC OXIDATION OF METHANOL BY  
METAL-CARBON NANOTUBE CATALYSTS  
By                                    Rattana Cheerapradit  
Field of Study                 Petrochemistry and Polymer Science  
Thesis Advisor                Associate Professor Orawon Chailapakul, Ph.D.  
Thesis Co-advisor            Parichatr Vanalabhpataana, Ph.D.

---

Accepted by the Faculty of Science, Chulalongkorn University in  
Partial Fulfillment of the Requirements for the Master's Degree

.....Dean of the Faculty of Science  
(Professor Supot Hannongbua, Dr. rer. nat.)

#### THESIS COMMITTEE

..... Chairman  
(Associate Professor Sirirat Kokpol, Ph.D.)

..... Thesis Advisor  
(Associate Professor Orawon Chailapakul, Ph.D.)

..... Thesis Co-advisor  
(Parichatr Vanalabhpataana, Ph.D.)

..... Examiner  
(Associate Professor Wimonrat Trakarnpruk, Ph.D.)

..... External Examiner  
(Weena Siangproh, Ph.D.)

รัตนา จีระประดิษฐ์ : ออกซิเดชันเชิงเร่งปฏิกิริยาด้วยไฟฟ้าของเมทานอลด้วยตัวเร่งปฏิกิริยาโลหะ-  
 ท่อนาโนคาร์บอน (ELECTROCATALYTIC OXIDATION OF METHANOL BY METAL-  
 CARBON NANOTUBE CATALYSTS) อ. ที่ปรึกษาวิทยานิพนธ์หลัก : รศ.ดร.อรรณพ ชัยลภากุล,  
 อ. ที่ปรึกษาวิทยานิพนธ์ร่วม : อ. ดร. ปาริฉัตร วณลาภพัฒนา, 81 หน้า

งานวิจัยนี้ มีการพัฒนาอนุภาคนาโนของโลหะ 1, 2, และ 3 ชนิด บนท่อนาโนคาร์บอนเพื่อเป็น  
 ตัวเร่งปฏิกิริยาเชิงไฟฟ้าเคมีสำหรับปฏิกิริยาออกซิเดชันของเมทานอล โดยใช้การสังเคราะห์ด้วย  
 กระบวนการโพสิเออ์ ใช้แพลทินัมร่วมกับโลหะอื่น ได้แก่ รูทีเนียม โคโรเนียม โมลิบดีนัม และนิกเกิลเป็น  
 ตัวเร่งปฏิกิริยา ข้อมูลโครงสร้างของตัวเร่งปฏิกิริยาโลหะบนท่อนาโนคาร์บอนยืนยันด้วยเทคนิคเอ็กซ์เรย์  
 ดิฟแฟรกชันและเอเนอร์จีดีสเพอร์ซีฟเอ็กซ์เรย์ฟลูออเรสเซนส์สเปกโทรสโกปี ผลของการศึกษาทางทราเคมีส  
 ชั้นอิเล็กตรอนไมโครสโกปีแสดงว่าโลหะอนุภาคระดับนาโนเมตรกระจายตัวอย่างสม่ำเสมอบนท่อนาโน  
 คาร์บอน สมบัติการเร่งปฏิกิริยาทางไฟฟ้าของอนุภาคโลหะระดับนาโนที่มีแพลทินัมเป็นหลักบนท่อนาโน  
 คาร์บอนต่อการออกซิเดชันของเมทานอลศึกษาโดยวิธีไซคลิกโวลแทมเมตรีที่อัตราเร็วในการสแกน  
 50 มิลลิโวลต์ต่อวินาที จากตัวเร่งปฏิกิริยาทั้งหมดที่สังเคราะห์ขึ้นพบว่า 2:1:0.5 แพลทินัม-รูทีเนียม-โม-  
 ลิบดีนัม ที่ยึดเกาะบนท่อนาโนคาร์บอนแสดงการเร่งปฏิกิริยาทางไฟฟ้าที่ดีที่สุดโดยให้กระแสแอโนดิก  
 เท่ากับ 77.5 แอมแปร์ต่อกรัมของตัวเร่งปฏิกิริยา สำหรับเมทานอล 1 โมลาร์ ใน 0.5 โมลาร์ กรดซัลฟูริก  
 นอกจากนี้ แพลทินัม-รูทีเนียม-โมลิบดีนัมบนท่อนาโนคาร์บอนนี้สามารถเร่งปฏิกิริยาออกซิเดชันของ  
 เมทานอลซ้ำโดยให้กระแสใกล้เคียงกันทุกครั้งและมีความเสถียรที่ยาวนาน

สาขาวิชา..ปิโตรเคมีและวิทยาศาสตร์พอลิเมอร์..ลายมือชื่อผู้คิด.....  
 ปีการศึกษา.....2551..... ลายมือชื่ออาจารย์ที่ปรึกษาวิทยานิพนธ์หลัก.....  
 ลายมือชื่ออาจารย์ที่ปรึกษาวิทยานิพนธ์ร่วม.....

# # 4972455723: MAJOR MAJOR PETROCHEMISTRY AND POLYMER SCIENCE

KEY WORD: ELECTRO-OXIDATION / ELECTROCATALYTIC OXIDATION / METHANOL OXIDATION / CARBON NANOTUBE (CNT) / DIRECT METHANOL FUEL CELL (DMFC)

RATTANA CHEERAPRADIT : ELECTROCATALYTIC OXIDATION OF METHANOL BY METAL-CARBON NANOTUBE CATALYSTS. THESIS ADVISOR : ASSOC. PROF. ORAWON CHAILAPAKUL, Ph.D., THESIS COADVISOR : PARICHATR VANALABHPATANA, Ph.D., 81 pp.

In this research, the mono-, di-, and tri-metal nanoparticles supported on carbon nanotube (CNT) have been developed as electrocatalysts for the oxidation of methanol using polyol process synthesis. Pt, accompanied by other metals including Ru, Cr, Mo, and Ni, were used as catalysts. Structural information of the metal catalysts on CNT was confirmed by X-ray diffraction (XRD) technique and energy dispersive X-ray fluorescence spectroscopy (XRF-EDX). Transmission electron microscopic (TEM) observation showed that the metal nanoparticles were evenly distributed on CNT. Electrocatalytic properties of the Pt-based metal nanoparticles on CNT towards methanol oxidation were investigated by means of cyclic voltammetry at the scan rate of  $50 \text{ mV}\cdot\text{s}^{-1}$ . Among all of the synthesized catalysts, 2:1:0.5 PtRuMo supported on CNT showed the best electrocatalytic performance with the anodic current of  $77.5 \text{ A}\cdot(\text{g catalyst})^{-1}$  for 1.0 M methanol containing 0.5 M sulfuric acid. In addition, the optimized PtRuMo on CNT had high reproducibility and long term stability.

Field of study...Petrochemistry and Polymer Science...Student's signature.....

Academic year .....2008..... Advisor's signature.....

Co-advisor's signature .....

## ACKNOWLEDGEMENTS

Firstly, I would like to express my gratitude to my advisor, Assoc. Prof. Dr. Orawan Chailapakul and my co-advisor, Dr. Parichatr Vanalabhpataana, for continuously providing important guidance and unwavering encouragement throughout my three years of graduate study at Chulalongkorn University. I also would like to thank my thesis examination committee members, Assoc. Prof. Dr. Sirirat Kokpol, Assoc. Prof. Dr. Wimonrat Trakarnpruk, and Dr. Weena Siangproh, who give helpful comments and advice in this thesis.

I especially want to thank all members of the Electrochemical Research Group for their great friendship and help during my study.

I am grateful to the financial supports from Center of Excellence for Petroleum, Petrochemicals, and Advanced Materials (CE-PPAM), Sensor Research Unit of Chemistry Department, and Energy Policy and Planning Office under Energy Conservation Promotion Fund

Finally, I am affectionately thankful to my Cheerapradit Family and my friends for their unlimited support, belief, and encouragement throughout my education.

# CONTENTS

	<b>PAGE</b>
<b>ABSTRACT IN THAI</b> .....	iv
<b>ABSTRACT IN ENGLISH</b> .....	v
<b>ACKNOWLEDGEMENT</b> .....	vi
<b>CONTENTS</b> .....	vii
<b>LIST OF TABLES</b> .....	xi
<b>LIST OF FIGURES</b> .....	xii
<b>ABBREVIATIONS</b> .....	xvii
<b>CHAPTER I INTRODUCTION</b> .....	1
1.1 Introduction.....	1
1.2 Literature Review: Development of Direct Methanol Fuel Cell (DMFC) Anode.....	5
1.3 Objective and Scopes of The Thesis.....	10
<b>CHAPTER II THEORY</b> .....	11
2.1 Carbon Nanotube (CNT).....	11
2.1.1 Single-Walled Carbon Nanotube (SWCNT).....	11
2.1.2 Multi-Walled Carbon Nanotube (MWCNT).....	11
2.2 Polyol Process.....	12
2.3 Electrochemical Techniques.....	13
2.3.1 Cyclic Voltammetry.....	13
2.3.2 Chronoamperometry.....	15
2.4 Real Surface Area.....	15
2.4.1 Hydrogen Adsorption Method.....	16
2.5 Characterization Techniques.....	18
2.5.1 Infrared (IR) Spectroscopy.....	18
2.5.2 X-ray Diffraction (XRD) Technique .....	19
2.5.3 Transmission Electron Microscopy (TEM).....	20
2.5.4 Energy Dispersive X-ray Fluorescence Spectroscopy (XRF- EDX) .....	20
<b>CHAPTER III EXPERIMENTAL</b> .....	22
3.1 Instruments and Apparatus.....	22

	<b>PAGE</b>
3.1.1 Electrochemical Instruments.....	22
3.1.2 Characterization Instruments.....	23
3.2 Chemicals.....	23
3.3 Preparation of Reagents.....	24
3.3.1 Solutions for pH Adjustment .....	24
3.3.1.1 Sodium Hydroxide (1.0 M).....	24
3.3.1.2 Hydrochloric acid (2.0 M).....	24
3.3.2 Solutions of Catalyst Precursors.....	25
3.3.2.1 Platinum and Platinum-Ruthenium Solutions .....	25
3.3.2.2 Platinum-Chromium, Platinum-Cobalt, Platinum-Gold Platinum-Iron, Platinum-Manganese, Platinum-Molyb- denum, and Platinum-Nickel Solutions at Mole Ratios of 2:1.5.....	25
3.3.2.3 Platinum-Chromium Solutions .....	26
3.3.2.4 Platinum-Molybdenum Solutions .....	26
3.3.2.5 Platinum-Nickel Solutions.....	27
3.3.2.6 Platinum-Ruthenium-Chromium Solutions .....	28
3.3.2.7 Platinum-Ruthenium-Molybdenum Solutions .....	28
3.3.2.8 Platinum-Ruthenium-Nickel Solutions.....	29
3.3.3 Electrolyte Solution.....	29
3.3.3.1 Sulfuric Acid Solution (0.5 M).....	29
3.4 Experimental Procedures.....	29
3.4.1 Modification of Carbon Nanotube .....	29
3.4.2 Preparation of Metal Catalysts Supported on Carbon Nano- tube (Metal/CNT Catalysts).....	30
3.4.3 Morphology of CNT and Metal/CNT Catalysts .....	30
3.4.4 Electrode Preparation.....	30
3.4.4.1 Glassy Carbon Electrode .....	30
3.4.4.2 CNT Modified Glassy Carbon Electrodes .....	30
3.4.4.3 Metal/CNT Catalysts Modified Glassy Carbon Electrodes.....	31



	<b>PAGE</b>
3.4.5 Electrochemical Characterization of CNT and Metal/CNT Catalyst Modified Glassy Carbon Electrodes.....	31
3.4.5.1 Electrochemical Set-up.....	31
3.4.5.2 Background Current.....	31
3.4.6 Catalytic Activity of Metal/CNT Catalyst Modified Glassy Carbon Electrodes.....	32
3.4.7 Stability of Metal/CNT Catalyst Modified Glassy Carbon Electrodes.....	32
<b>CHAPTER IV RESULTS AND DISCUSSION.....</b>	<b>33</b>
4.1 Modification of Carbon Nanotube (CNT) .....	33
4.1.1 Fourier Transform Infrared Spectroscopic Analysis.....	33
4.1.2 X-ray Diffraction Analysis.....	34
4.1.3 Transmission Electron Microscopic Analysis.....	35
4.2 Morphological Information of Metal/CNT Catalysts.....	36
4.2.1 X-Ray Diffraction Analysis.....	36
4.2.2 Transmission Electron Microscopic Analysis.....	37
4.2.3 Energy Dispersive X-ray Fluorescence Spectroscopic Analysis.....	40
4.3 CNT Modified Glassy Carbon (CNT/GC) Electrode .....	41
4.3.1 Background Current.....	41
4.3.2 Methanol Oxidation by CNT Modified Glassy Carbon Electrode .....	41
4.4 Pt/CNT Modified Glassy Carbon Electrode .....	43
4.4.1 Background Current.....	43
4.4.2 Catalytic Activity of Pt/CNT Modified Glassy Carbon Electrode .....	44
4.5 Pt-Based Di-metal/CNT Modified Glassy Carbon Electrodes.....	45
4.5.1 Background Current.....	46
4.5.2 Catalytic Activity of Pt-based Di-metal/CNT Modified Glassy Carbon Electrodes .....	48
4.5.2.1 PtRu/CNT Modified Glassy Carbon Electrodes.....	49

	<b>PAGE</b>
4.5.2.2 PtCr/CNT Modified Glassy Carbon Electrodes.....	50
4.5.2.3 PtMo/CNT Modified Glassy Carbon Electrodes.....	51
4.6 Pt-based Tri-Metal/CNT Modified Glassy Carbon Electrodes.....	52
4.6.1 Background Current.....	52
4.6.2 Catalytic Activity of Tri-metal/CNT Modified Glassy Carbon Electrodes.....	54
4.6.2.1 PtRuCr/CNT Modified Glassy Carbon Electrodes..	54
4.6.2.2 PtRuMo/CNT Modified Glassy Carbon Electrodes..	55
4.6.2.3 PtRuNi/CNT Modified Glassy Carbon Electrodes...	56
4.7 Effect of Methanol Concentration.....	57
4.8 Repeatability of Metal/CNT Modified Glassy Carbon Electrodes.....	59
4.9 Stability of Metal/CNT Modified Glassy Carbon Electrodes.....	60
<b>CHAPTER V CONCLUSIONS</b> .....	<b>64</b>
5.1 Conclusions.....	64
5.2 Suggestion.....	65
<b>REFERENCES</b> .....	<b>66</b>
<b>APPENDIX</b> .....	<b>71</b>
<b>VITA</b> .....	<b>81</b>

## LIST OF TABLES

TABLE		PAGE
3.1	Electrochemical instruments.....	22
3.2	Characterization instruments.....	23
3.3	Chemicals.....	23
3.4	Platinum and platinum-ruthenium composite solutions.....	25
3.5	Platinum-chromium, platinum-cobalt, platinum-gold, platinum-iron, platinum-manganese, platinum-molybdenum, and platinum-nickel solutions at mole ratios of 2:1.5.....	26
3.6	Platinum-chromium composite solutions .....	26
3.7	Platinum-molybdenum composite solutions .....	27
3.8	Platinum-nickel composite solutions.....	27
3.9	Platinum-ruthenium-chromium composite solutions .....	28
3.10	Platinum-ruthenium-molybdenum composite solutions .....	28
3.11	Platinum-ruthenium-nickel composite solutions.....	29
3.12	Potentials for the metal/CNT/GC electrodes in chronoamperometric measurement.....	32
4.1	Percentage of weight (wt.%) for Pt/CNT and PtRu/CNT catalysts.....	40
4.2	Percentage of weight (wt.%) for PtRuM/CNT (M = Cr, Mo, and Ni) .....	41
4.3	Mass activity of the optimized PtRu/CNT/GC, PtRuCr/CNT/GC, and PtRu-Mo/CNT/GC electrodes for 4.0 M methanol in 0.5 M H <sub>2</sub> SO <sub>4</sub> recorded at the scan rate of 50 mV·s <sup>-1</sup> .....	59

## LIST OF FIGURES

FIGURE		PAGE
2.1	Potential-time excitation signal in cyclic voltammetry.....	13
2.2	Typical cyclic voltammogram for a reversible redox process.....	14
2.3	Potential-time waveform of chronoamperometry.....	15
2.4	Adsorbate particles packing with (a) physisorption and (b) chemisorption.....	16
2.5	Cyclic voltammetric current potential curve for a Pt electrode in contact with acid solution. The inset shows the different charge contributions in the hydrogen region.....	18
2.6	Sketch of one possible configuration of the XRD instrument .....	19
2.7	Schematic representation of an energy-dispersive spectrometer...	21
3.1	Electrochemical cell for cyclic voltammetry.....	31
4.1	FTIR spectra of (a) unmodified and (b) modified CNT.....	34
4.2	XRD patterns of (a) unmodified and (b) modified CNT .....	34
4.3	TEM images of unmodified CNT ((a) and (b)) and modified CNT ((c) and (d)) with the magnification power of 50,000 ((a) and (c)) and 800,000 ((b) and (d)).....	35
4.4	XRD patterns of (a) Pt/CNT, (b) PtRu/CNT (2:1), (c) PtRu/CNT (2:1.25), (d) PtRu/CNT (2:1.5), (e) PtRu/CNT (2:2), and (f) PtRu/CNT (2:4).....	36
4.5	XRD patterns of (a) PtRuCr/CNT (2:0.5:1), (b) PtRuMo/CNT (2:1:0.5), and (c) PtRuNi/CNT (2:1:0.5).....	37
4.6	TEM images of (a) Pt/CNT, (b) PtRu/CNT (2:1), (c) PtRu/CNT (2:1.25), (d) PtRu/CNT (2:1.5), (e) PtRu/CNT (2:2), (f) PtRu/CNT (2:4), (g) PtRuCr/CNT (2:0.5:1), (h) PtRuMo/CNT (2:1:0.5), and (i) PtRuNi/CNT (2:1:0.5) with the magnification power of 6,000, 50,000, and 800,000.....	38
4.7	Cyclic voltammograms for 0.5 M H <sub>2</sub> SO <sub>4</sub> recorded with GC electrode (solid line) and CNT/GC electrode (dash line) at the scan rate of 50 mV·s <sup>-1</sup> .....	42

<b>FIGURE</b>	<b>PAGE</b>
4.8	Cyclic voltammograms for 0.5 M H <sub>2</sub> SO <sub>4</sub> solution recorded with CNT/GC electrode in the absence (solid line) and presence of 1.0 M methanol (dash line) at the scan rate of 50 mV·s <sup>-1</sup> ..... 42
4.9	Cyclic voltammogram for 0.5 M H <sub>2</sub> SO <sub>4</sub> solution recorded with Pt/CNT/GC electrode at the scan rate of 50 mV·s <sup>-1</sup> ..... 43
4.10	Cyclic voltammogram for 1.0 M methanol in 0.5 M H <sub>2</sub> SO <sub>4</sub> solution recorded with Pt/CNT/GC electrode at the scan rate of 50 mV·s <sup>-1</sup> ..... 44
4.11	Mass activity vs. methanol concentration curve of Pt/CNT/GC electrode recorded in 0.5 M H <sub>2</sub> SO <sub>4</sub> solution at the scan rate of 50 mV·s <sup>-1</sup> ..... 45
4.12	Cyclic voltammograms for 0.5 M H <sub>2</sub> SO <sub>4</sub> solution recorded by Pt/CNT/GC electrode (solid lines) in comparison with (a) PtRu/CNT/GC, (b) PtCr/CNT/GC, (c) PtCo/CNT/GC, (d) PtAu/CNT/GC, (e) PtFe/CNT/GC, (f) PtMn/CNT/GC, (g) PtMo/CNT/GC, and (h) PtNi/CNT/GC electrodes (dash lines) with Pt-to-co-catalyst ratio of 2:1.5 at the scan rate of 50 mV·s <sup>-1</sup> ..... 47
4.13	Current vs. methanol concentration curves of Pt/CNT/GC, PtRu/CNT/GC, PtCr/CNT/GC, PtCo/CNT/GC, PtAu/CNT/GC, PtFe/CNT/GC, PtMn/CNT/GC, PtMo/CNT/GC, and PtNi/CNT/GC electrodes recorded in 0.5 M H <sub>2</sub> SO <sub>4</sub> at the scan rate of 50 mV·s <sup>-1</sup> ..... 48
4.14	Mass activity vs. methanol concentration curves of Pt/CNT/GC and PtRu/CNT/GC electrodes with (a) 2:1, (b) 2:1.25, (c) 2:1.5, (d) 2:2, and (e) 2:4 Pt-to-Ru mole ratios recorded in 0.5 M H <sub>2</sub> SO <sub>4</sub> at the scan rate of 50 mV·s <sup>-1</sup> ..... 49
4.15	Current vs. methanol concentration curves of Pt/CNT/GC and PtCr/CNT/GC electrodes with (a) 2:1, (b) 2:1.25, (c) 2:1.5, and (d) 2:2 Pt-to-Cr mole ratios recorded in 0.5 M H <sub>2</sub> SO <sub>4</sub> at the scan rate of 50 mV·s <sup>-1</sup> ..... 50

<b>FIGURE</b>	<b>PAGE</b>	
4.16	Current vs. methanol concentration curves of Pt/CNT/GC electrode and PtMo/CNT/GC electrodes with (a) 2:1, (b) 2:1.25, (c) 2:1.5, and (d) 2:2 Pt-to-Mo mole ratios recorded in 0.5 M H <sub>2</sub> SO <sub>4</sub> at the scan rate of 50 mV·s <sup>-1</sup> .....	51
4.17	Cyclic voltammograms for 0.5 M H <sub>2</sub> SO <sub>4</sub> solution recorded at the scan rate of 50 mV·s <sup>-1</sup> by PtRu/CNT/GC electrode (dash lines) and (a) PtRuCr/CNT/GC, (b) PtRuMo/CNT/GC, and (c) PtRu-Ni/CNT/GC electrodes with Pt-to-Ru-to-the third metal mole ratio of 2:1:0.5 (solid lines).....	53
4.18	Mass activity vs. methanol concentration curves of PtRu/CNT/GC electrode with Pt to Ru mole ratio of 2:1.5 and PtRuCr/CNT/GC electrodes with Pt-to-Ru-to-Cr mole ratios of (a) 2:1:0.5, (b) 2:0.5:1, and (c) 2:0.75:0.75 recorded in 0.5 M H <sub>2</sub> SO <sub>4</sub> at the scan rate of 50 mV·s <sup>-1</sup> .....	54
4.19	Mass activity vs. methanol concentration curves of PtRu/CNT/GC electrode with Pt to Ru mole ratio of 2:1.5 and PtRuMo/CNT/GC electrodes with Pt-to-Ru-to-Mo mole ratios of (a) 2:1:0.5, (b) 2:0.5:1, and (c) 2:0.75:0.75 recorded in 0.5 M H <sub>2</sub> SO <sub>4</sub> at the scan rate of 50 mV·s <sup>-1</sup> .....	55
4.20	Mass activity vs. methanol concentration curves of PtRu/CNT/GC electrode with Pt-to-Ru mole ratio of 2:1.5 and PtRuNi/CNT/GC electrodes with Pt-to-Ru-to-Mo mole ratios of (a) 2:1:0.5, (b) 2:0.5:1, and (c) 2:0.75:0.75 recorded in 0.5 M H <sub>2</sub> SO <sub>4</sub> at the scan rate of 50 mV·s <sup>-1</sup> .....	56
4.21	Mass activity vs. methanol concentration curves of the optimized PtRu/CNT/GC, PtRuCr/CNT/GC, PtRuMo/CNT/GC, and PtRuNi/CNT/GC electrodes recorded in 0.5 M H <sub>2</sub> SO <sub>4</sub> at the scan rate of 50 mV·s <sup>-1</sup> .....	57

<b>FIGURE</b>		<b>PAGE</b>
4.22	Mass activity <i>vs.</i> methanol concentration curves of the optimized PtRu/CNT/GC, PtRuCr/CNT/GC, and PtRuMo/CNT/GC electrodes recorded in 0.5 M H <sub>2</sub> SO <sub>4</sub> at the scan rate of 50 mV·s <sup>-1</sup> .....	58
4.23	Repetitive mass activity of the Pt/CNT/GC, 2:1.5 PtRu /CNT/GC, 2:0.5:1 PtRuCr/CNT/GC, and 2:1:0.5 PtRuMo/CNT /GC electrodes for the oxidation of 1.0 M methanol in 0.5 M H <sub>2</sub> SO <sub>4</sub> solution.....	60
4.24	Chronoamperograms of the Pt/CNT/GC, 2:1.5 PtRu/CNT/GC, 2:0.5:1 PtRuCr/CNT/GC, 2:1:0.5 PtRuMo/CNT/GC, and 2:1:0.5 PtRuNi/CNT/GC electrodes for the oxidation of 1.0 M methanol in 0.5 M H <sub>2</sub> SO <sub>4</sub> solution recorded at the potentials of (a) E <sub>1/2</sub> and (b) E <sub>1/4</sub> according to the information in Table 3.12.....	61
4.25	Percentage of mass activity <i>vs.</i> time for the oxidation of 1.0 M methanol in 0.5 M H <sub>2</sub> SO <sub>4</sub> recorded at the potential of E <sub>1/2</sub> by Pt/CNT/GC, 2:0.5:1 PtRuCr/CNT/GC, 2:1:0.5 PtRuMo/CNT /GC, and 2:1:0.5 PtRuNi/CNT/GC electrodes in chronoamperometric experiment.....	62
4.26	Percentage of mass activity <i>vs.</i> time for the oxidation of 1.0 M methanol in 0.5 M H <sub>2</sub> SO <sub>4</sub> recorded at the potential of E <sub>1/4</sub> by Pt/CNT/GC,2:0.5:1 PtRuCr/CNT/GC, 2:1:0.5 PtRuMo/CNT /GC, and 2:1:0.5 PtRuNi/CNT/GC electrodes in chronoamperometric experiment.....	62
1A	XRF-EDX spectrum of Pt/CNT catalyst.....	72
2A	XRF-EDX spectrum of PtRu/CNT catalyst with Pt-to-Ru mole ratio of 2:1.....	73
3A	XRF-EDX spectrum of PtRu/CNT catalyst with Pt-to-Ru mole ratio of 2:1.25.....	74
4A	XRF-EDX spectrum of PtRu/CNT catalyst with Pt-to-Ru mole ratio of 2:1.5.....	75
5A	XRF-EDX spectrum of PtRu/CNT catalyst with Pt-to-Ru mole ratio of 2:2.....	76

<b>FIGURE</b>		<b>PAGE</b>
6A	XRF-EDX spectrum of PtRu/CNT catalyst with Pt-to-Ru mole ratio of 2:4.....	77
7A	XRF-EDX spectrum of PtRuCr/CNT catalyst with Pt-to-Ru-to-Cr mole ratio of 2:0.5:1.....	78
8A	XRF-EDX spectrum of PtRuMo/CNT catalyst with Pt-to-Ru-to-Mo mole ratio of 2:1:0.5.....	79
9A	XRF-EDX spectrum of PtRuNi-CNT catalyst with Pt-to-Ru-to-Ni mole ratio of 2:1:0.5.....	80



## ABBREVIATIONS

A	Ampere
Å	Angstrom
BDD	Boron-Doped Dimond Thin Film
CO <sub>2</sub>	Carbon Dioxide
CO	Carbon Monoxide
CNT	Carbon Nanotube
CNF	Carbon Nanofiber
Cr	Chromium
Co	Cobalt
CE	Counter Electrode
°C	Degree Celsius
DMFC	Direct Methanol Fuel Cell
EAS	Electrochemical Active Surface
XRF-EDX	Energy Dispersive X-ray Fluorescence Spectroscopy
FTIR	Fourier transform infrared
GC	Glassy Carbon
Au	Gold
IUPAC	International Union for Pure and Applied Chemistry
Fe	Iron
Mn	Manganese
MCFC	Molten-Carbonate Fuel Cell
Mo	Molybdenum
MWNT	Multi-Walled Carbon Nanotube
Ni	Nickel
NO <sub>x</sub>	Nitrogen Oxides
OMC	Ordered Mesoporous Carbon
O <sub>2</sub>	Dioxygen
PAFC	Phosphoric Acid Fuel Cell
Pt	Platinum
PEMFC	Polymer Exchange Membrane Fuel Cell
E	Potential

RE	Reference Electrode
Ru	Ruthenium
s	Second
Ag/AgCl	Silver/Silver Chloride
SWNT	Single-Walled Carbon Nanotube
SOFC	Solid Oxide Fuel Cell
SO <sub>2</sub>	Sulfur Dioxide
TEM	Transmission Electron Microscopy
V	Volt
WE	Working Electrode
XRD	X-ray Diffraction
XPS	X-ray Photoelectron Spectroscopy

# CHAPTER I

## INTRODUCTION

### 1.1 Introduction

Recently, many signs of global warming have been detected. Considered as main cause of this phenomenon, air pollutants, for example, carbon dioxide ( $\text{CO}_2$ ), nitrogen oxides ( $\text{NO}_x$ ), sulfur dioxide ( $\text{SO}_2$ ), and many other volatile compounds, are discharged into the environment by incomplete burning of fossil fuels such as coal and oil using in machines and motor vehicles. In order to reduce the use of fossil fuels, modern electric machines and vehicles that release few numbers of detrimental pollutants are essential. Therefore, clean energy sources, especially fuel cells have been developed for uses in vehicles and power plant stations. Fuel cell is a device that directly converts chemical energy of a redox reaction into electrical energy and consists of anode, cathode, and electrolyte. Fuel cell produces electricity by supplying fuel on the anode side and oxidant on the cathode side. It can continuously operate as long as the necessary flows of reactants are maintained. About 150 years ago, the first fuel cell was built in England. Up to now, fuel cell technology has been used as an efficient and lightweight energy source for space exploration. Over the next few years, technological advances and cost reduction will likely lead to widespread use of fuel cell in several different applications. Fuel cell may someday be as common in residential households as a refrigerator or a dishwasher to produce clean and reliable electricity. In addition, it is likely that a new generation of clean automobile using electric-drive motor will rely on fuel cell as its source of power.

There are various types of fuel cells that can be classified by their chemistry, their operating temperatures, and their electrolyte types. Some fuel cells work well with stationary power generation plants whereas others may be useful for small portable applications or powering cars. The main types of fuel cells include:

### **Solid Oxide Fuel Cell (SOFC)**

SOFC has a solid oxide or ceramic electrolyte and operates at very high temperatures between 700-1,000°C. These high temperatures cause a dramatic problem because some parts of the fuel cell can break down after repeatedly cycling. However, SOFC is very stable for continuous use. In fact, SOFC has had the longest operating lifetime among most types of fuel cells under certain conditions. Its high operating temperatures also have an advantage that the steam produced during the operation can be channeled into turbines to generate more electricity. SOFC suits well large-scale stationary power generators that could provide electricity for factories or towns.

### **Molten Carbonate Fuel Cell (MCFC)**

The electrolytes of MCFC are molten mixtures of alkali metal carbonates ( $\text{Li}_2\text{CO}_3\text{-K}_2\text{CO}_3$  or  $\text{Li}_2\text{CO}_3\text{-Na}_2\text{CO}_3$ ), which are retained in a ceramic matrix of lithium aluminium oxide ( $\text{LiAlO}_2$ ). MCFC operates at 600°C so that it can generate steam which can be used for generating more power. Since MCFC has lower operating temperatures than SOFC, MCFC then does not need such exotic and durable materials, making its design be a little less expensive. Similar to SOFC, this fuel cell is also suitable for large stationary power generators.

### **Phosphoric Acid Fuel Cell (PAFC)**

PAFC typically operates at 180-220°C in an acid medium using liquid phosphoric acid as an electrolyte. Due to its high working temperatures, it has a long warm-up time. PAFC has potential for use in small stationary power generation system. Unfortunately, its cost is too high compared with other conventional power generating systems.

### **Polymer Exchange Membrane Fuel Cell (PEMFC)**

PEMFC uses a solid polymer membrane as an electrolyte. When this polymer is saturated with water, it allows proton to pervade through itself causing ionic conduction. PEMFC gives high power density and has a relatively low operating temperatures (ranging from 60-80°C), allowing fuel cell to have short warm-up time before generating electricity. This type of fuel cell has been worldwide developed as a high effective and environmentally-friendly energy conversion device for both mobile and stationary applications.

## Direct Methanol Fuel Cell (DMFC)

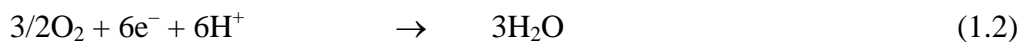
Using methanol as a liquid fuel, DMFC has many advantages over other fuel cell systems because of its high energy conversion efficiency, low pollutant emission, low operating temperature, low cost, and simplicity of handling and transporting liquid fuel. Therefore, methanol can be expanded in a consumer environment with little concern and portable power systems containing DMFCs have become favorable.

For the operation, DMFC oxidizes methanol with water to form CO<sub>2</sub>, protons, and electrons. As shown in equation 1.1, CO<sub>2</sub> is then released at the anode. Equation 1.2 shows the reaction at the cathode where the protons migrating through the electrolyte membrane, together with the electrons passing through the outer circuit combine with dioxygen (O<sub>2</sub>) to generate water [1].

Anode:



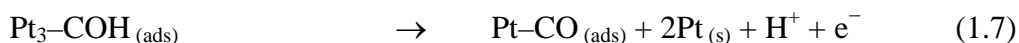
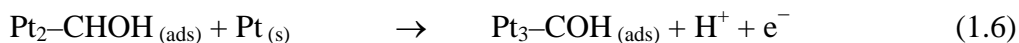
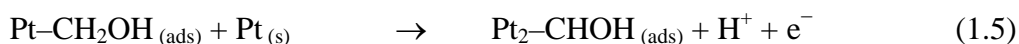
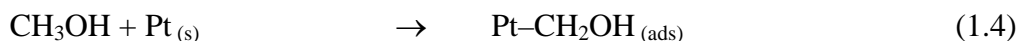
Cathode:



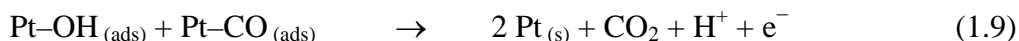
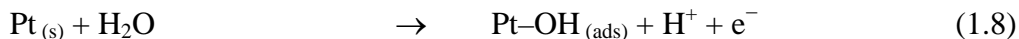
As displayed in equation 1.3, the overall reaction in DMFC is the catalytic conversion of methanol in the presence of O<sub>2</sub> into CO<sub>2</sub> and water. At 25°C, the maximum thermodynamic voltage of this reaction has a value of 1.18 V.



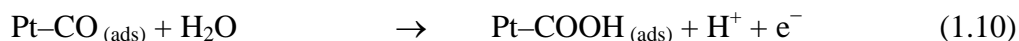
Despite of DMFC advantages, there are some difficulties to be overcome in terms of efficiency and power density. One of the reasons for poor efficiency of DMFC is the relatively slow kinetics of the methanol oxidation at the anode, leading to high over potential of the oxidation. Platinum (Pt) metal has high activity for methanol oxidation and has been used as anode electrocatalyst. Mechanism of methanol oxidation on Pt electrode in an acid medium involves parallel and consecutive oxidation reactions, as follows [2]:



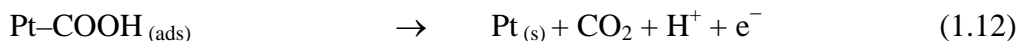
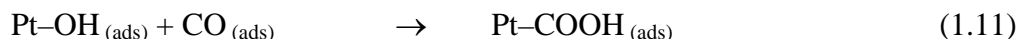
Equations 1.4-1.7 display a marked increase in the anodic current for the dehydrogenation of methanol followed by the oxidation of Pt surface-adsorbed intermediates. Arising from the equation 1.7, adsorbed Pt-carbon monoxide (Pt-CO<sub>(ads)</sub>) species might possibly poison the Pt catalyst. However, the extension of the potential might include the formation of Pt hydroxide (Pt-OH<sub>(ads)</sub>) and Pt carboxyl (Pt-COOH<sub>(ads)</sub>) as well as the oxidation of CO species to yield CO<sub>2</sub>. Possible reactions are demonstrated in equations 1.8-1.12.



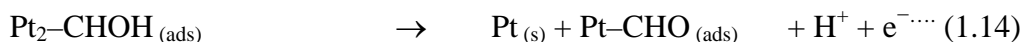
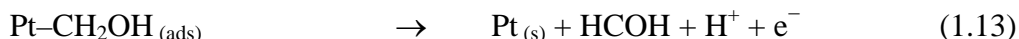
or



or



As described in equation 1.9, the adsorbed Pt-CO can mostly be removed by the oxygenated Pt-OH species. Since the dissociative adsorption of water in equation 1.10 occurs slowly at the normal operating potentials of DMFC. Additionally proposed reactions (equations 1.13-1.17) have been mentioned:



or



Although a great deal of effort has been made for research and development of DMFC, the problem of finding proper anode catalysts remains to be resolved. Since Pt is easy to be poisoned by CO-like species produced during the methanol oxidation and thus loses its continuously long-term catalytic activity, the metal co-catalysts such

as ruthenium (Ru) and rhodium (Rh) have been introduced to Pt-based binary and ternary catalytic systems.

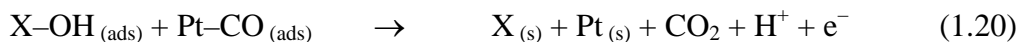
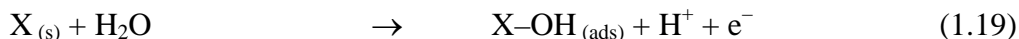
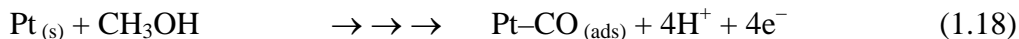
## 1.2 Literature Review: Development of Direct Methanol Fuel Cell (DMFC) Anode

Since Pt has high catalytic activity towards methanol oxidation, it has been used as an electrocatalyst for DMFC anode. M. Watanabe *et al.* [3] utilized Pt electrocatalyst for direct methanol oxidation. Using different carbon black supports, the influence of Pt crystallite dispersion on the electrocatalytic activity for methanol oxidation in acidic solution was examined. The mass activity increased proportionally with the specific surface area of the Pt crystallites.

M. Umeda *et al.* [4] investigated the electrochemical characterization of various Pt/carbon (Pt/C) catalysts and their electrocatalytic activity towards methanol oxidation by using the porous microelectrode (PME). Cyclic voltammograms revealed that 30 wt. % Pt/C exhibited the highest electroactivity whereas the 50 wt. % Pt/C showed extremely small current because of its small active-surface area. Anodic peak potential for methanol oxidation shifted towards positive direction as Pt-loading decreased, revealing the formation of Pt-oxide species. The activation energy for methanol oxidation was assessed at  $449 \pm 3 \text{ kJ} \cdot \text{mol}^{-1}$  for all Pt/C catalysts.

H. T. Kim *et al.* [5] reported the development of cathode catalyst layer based on Pt catalyst on ordered mesoporous carbon (Pt/OMC) for DMFC application. Pt nanoparticles were supported on OMC with Pt loading of 60 wt. %. The power density of the optimum cathode layer, which employed the Pt/OMC catalyst with Pt loading of  $2 \text{ mg} \cdot \text{cm}^{-2}$ , was greater than that of unsupported Pt.

However, during the methanol oxidation, Pt can be poisoned by CO-like species and, thus, continuously loses its catalytic activity. Therefore, Pt-based bimetal catalysts such as Pt–Ru [6] and Pt–gold (Pt–Au) [7] have been introduced to improve the CO-tolerance characteristics of Pt through the bi-metallic effect. Mechanistic studies for Pt–metal binary catalysts proposed that methanol can be electrochemically oxidized according to equations 1.18-1.20 [8]. Note that equation 1.18 combines equations 1.4-1.7 in single reaction and X represents any metal co-catalyst such as Ru or Au.



Metal co-catalyst usually transfers oxygen more effectively than Pt due to its ability to oxidatively absorb water at less positive potential. During the oxidation, surface Pt atoms oxidatively dehydrogenate the chemisorbed methyl moiety in consecutive steps (equation 1.18) to yield a residual adsorbed CO on Pt ( $\text{Pt-CO}_{(ads)}$ ) that is unlikely to be further oxidized to  $\text{CO}_2$  at DMFC potentials; however, the adsorbed  $\text{Pt-CO}$  can be removed via an oxygen transfer step with the electrogenerated hydroxide of co-catalyst ( $\text{X-OH}_{(ads)}$ ), as displayed in equation 1.20 [9].

J. Guo *et al.* [10] studied PtRu/C and PtRu black catalysts with nominal atomic Pt:Ru ratio of 1:1 as anode catalysts for DMFC. Indicated by X-ray diffraction (XRD) technique, both PtRu/C and PtRu black had almost the same alloy degree, but the PtRu supported on C could improve the influence of Ru on Pt towards methanol oxidation. Electrochemical activity of the catalysts for methanol oxidation was probed by cyclic voltammetry, showing that Ru was proved to have ability of reducing the potential for methanol oxidation on Pt.

W. Tokarz *et al.* [11] investigated the adsorption and electro-oxidation of methanol on different compositions of PtRh alloys as well as pure Pt and Rh metals. Current densities of methanol oxidation on Pt, Rh, and PtRh alloys were measured by means of cyclic voltammetry. Compared with Pt, PtRh alloys showed insufficient improvement of potential for continuous methanol oxidation due to the tendency of Rh to be strongly poisoned by the adsorption products. The poisoning phenomena switched off the bi-metallic system of methanol oxidation on these alloys.

I. S. Park *et al.* [12] prepared Pt modified with Au nanoparticles on carbon support (PtAu/C) as an electrocatalyst for methanol oxidation. Electrochemical results indicated that the PtAu/C showed higher electrocatalytic activity for methanol oxidation than the commercial electrocatalyst. The increase of electrocatalytic activity might be attributed to the PtAu/C surface structure that allowed high utilization of Pt for surface oxidation of methanol.

Typically, any catalyst with small and well-dispersed particles tends to have good catalytic activity. Therefore, the significance of the supporting material on



catalyst distribution has extensively been concerned. Many studies [3,4,13] used Pt on various supports such as carbon, graphite, and other alloys for methanol electro-oxidation. Those results showed that appropriate support could improve the activity of Pt for methanol oxidation and the activity of Pt also depended upon Pt loading on the support. In case of the bi-metallic systems, the effects of the following catalyst supports were studied.

J. Zhu *et al.* [14] prepared PtRu/C anode electrocatalysts for DMFC anode. The catalysts were composed of well-dispersed and homogeneous PtRu alloy nanoparticles. Electrochemical results demonstrated that the PtRu/C catalysts obtained via sensitizing and activating pretreatment exhibited 34% enhancement of peak current density for methanol electro-oxidation.

M. Carmo *et al.* [15] investigated PtRu electrocatalysts supported on functionalized carbon black. Electrochemical properties of both home-made and commercial PtRu electrocatalysts were compared to those of PtRu on the carbon black. Cyclic voltammetric curves demonstrated that PtRu supported on functionalized carbon black had the highest activity for the oxidation of methanol.

G. R. S. Banda *et al.* [16] prepared metal-based catalyst clusters on boron-doped diamond (BDD) powder formed by the agglomeration metal-based nanoparticles with the sizes varying between 500 nm and 5  $\mu\text{m}$ . Results showed that the deposited particles contained high purity and had a good electrical contact with the surface of BDD powder. However, the Pt–Ru oxides supported on BDD (PtRuO/BDD) showed lower activity for methanol oxidation than the PtRu/C commercial catalyst.

A. Bauer *et al.* [17] investigated pressed graphite felt with electrodeposited PtRu (43  $\text{g}\cdot\text{m}^{-2}$ , 1.4:1 atomic Pt:Ru ratio) or Pt–Ru–molybdenum (PtRuMo, 52  $\text{g}\cdot\text{m}^{-2}$ , 1:1:0.3 atomic Pt:Ru:Mo ratio) nanoparticle catalysts as an anodic material for DMFC. At the temperatures above 333K, the fuel cell performance of the PtRuMo catalyst was superior than that of the PtRu. Power density of the PtRuMo was 2,200  $\text{W}\cdot\text{m}^{-2}$  at 5,500  $\text{A}\cdot\text{m}^{-2}$  and 353 K while, under the same condition, PtRu yielded 1,925  $\text{W}\cdot\text{m}^{-2}$ .

Recently, carbon nanotube (CNT), which is allotrope of carbon, configurationally equivalent to two-dimensional graphite sheets rolled into a tube, has been proposed to be an alternative metal catalyst support due to its cylindrical nanostructure with high surface area as well as unique mechanical and electrical

properties. There has been recent work revealing that, compared with other carbon materials, CNT is a better support for electrocatalyst of methanol oxidation. Many researchers used Pt supported on CNT as a catalyst for methanol oxidation, for example:

D. J. Guo *et al.* [18] investigated the oxidation of methanol by Pt nanoparticles modified on single-walled carbon nanotubes (SWCNTs) using electrochemical method. The morphology of Pt nanoparticles on SWCNTs was studied by transmission electron microscopy (TEM) and XRD techniques, revealing that the mean diameter of Pt nanoparticles was about 5-8 nm. Cyclic voltammetric results showed excellent electrocatalytic activity of Pt nanoparticles on SWCNTs for methanol oxidation.

H. Tang *et al.* [19] used well-aligned CNT arrays as supporting materials for Pt electrocatalysts. The microstructure of the resulting Pt on aligned CNT (Pt/aligned-CNT) electrode was characterized by scanning electron microscopy (SEM) and its electrocatalytic properties for methanol oxidation were studied by using cyclic voltammetry. Results confirmed that the Pt/aligned-CNT electrode provided higher electrocatalytic activity for methanol oxidation than the Pt on tangled-CNT (Pt/tangled-CNT) and the Pt on graphite (Pt/graphite) electrodes.

C. C. Chen *et al.* [20] synthesized multi-walled carbon nanotube (MWCNT) from carbon cloth and modified it with Pt nanoparticles by using microwave digestion method in 5 M nitric acid ( $\text{HNO}_3$ ). The open-end and undamaged MWCNTs can provide a larger surface area for supporting more catalysts. The characterization of Pt modified MWCNT (Pt/MWCNT) was carried out by TEM, X-ray photoelectron spectroscopy (XPS), fourier transform infrared spectroscopy (FTIR), and Raman spectroscopy. Furthermore, the electrocatalytic oxidation of methanol with the microwave digestion-treated Pt/MWCNT electrode displayed higher anodic current than those with the pristine-/and nitric acid-treated Pt/MWCNT electrodes.

S. L. Knupp *et al.* [21] developed corrosion-resistant CNT and carbon nanofiber (CNF) modified with Pt catalysts for PEMFC application. Brunauer Emmer Teller (BET) surface area measurements, FTIR, XRD, TEM, thermal gravimetric analysis (TGA), and cyclic voltammetry were used to characterize all the Pt modified CNT and CNF. An increase of the Pt loading on a fixed surface area caused agglomeration. CNF with large diameter (100-200 nm), as compared to CNT (20-40 nm) had less

surface area and hence, larger Pt particles were formed under same synthetic conditions.

In addition, CNT has been utilized as a support for Pt-based bimetal catalysts in order to improve the electrocatalytic activity for methanol oxidation. J. Prabhuram *et al.* [22] compared the activity towards methanol oxidation of PtRu supported on MWCNT (PtRu/MWCNT) with that of PtRu on Vulcan XC-72 carbon (PtRu/C). Cyclic voltammetric results demonstrated that the PtRu/MWCNT catalyst exhibited higher mass activity for methanol oxidation than PtRu/C catalyst under the condition that both catalysts possessed more or less same PtRu loadings, particle sizes, dispersion, and electrochemical surface areas.

J. Xu *et al.* [23] reported electro-oxidation of methanol by Pt-iron supported on MWCNT (PtFe/MWCNT). Electrocatalytic activity of the PtFe/MWCNT electrodes for the oxidation of methanol was investigated by means of cyclic voltammetry and chronoamperometry. PtFe/MWCNT presented higher electrocatalytic activity and stability in comparison with the Pt/MWCNT. This result revealed that the addition of Fe might lead to small average particle size and high utilization of Pt in the PtFe/MWCNT catalyst, implying that the PtFe/MWCNT composite had high potential in fuel cell application.

Several synthetic methods, including electrodeposition [18], sodium borohydride ( $\text{NaBH}_4$ ) reduction [24], and polyol process [6], have been utilized to prepare metal supported on CNT (metal/CNT) catalysts for DMFC anode and other purposes. Polyol process, one of the simple syntheses, uses poly alcohol as a solvent and a reducing agent to produce metal nanoparticles deposited on CNT from the mixture of metallic cation precursor and CNT.

Earlier work [21,25] synthesized Pt supported on CNT (Pt/CNT) by polyol process and the uniform Pt particles deposited on CNT were obtained. Electrochemical measurements showed that the prepared Pt/CNT catalyst exhibited high performance for methanol electro-oxidization.

W. Chen *et al.* [26] prepared well-dispersed Pt nanoparticles with the average diameter of 3.0 nm on CNT by microwave-heated polyol process. TEM observations illustrated that microwave-synthesized Pt nanoparticles had a sharp size distribution and dispersed well on the surface of CNT. Cyclic voltammograms demonstrated that the synthesized Pt/CNT catalysts exhibited higher catalytic activity for methanol oxidation than the commercial Pt/C catalyst at room temperature, implying that the

significant improvement in electrocatalytic activity was due to that the size uniformity and well dispersion of the Pt nanoparticles on CNT prepared via microwave-heated polyol method.

Z. Liu *et al.* [27] synthesized Pt and PtRu supported on Vulcan XC-72 carbon and SWCNT by a microwave-assisted polyol process. The prepared catalysts were characterized by TEM, XRD, and XPS. PtRu nanoparticles, which were uniformly dispersed on carbon and SWCNT supports, had the diameters of 2-6 nm. Electro-oxidation of methanol was studied by means of cyclic voltammetry, linear sweep voltammetry, and chronoamperometry. Both catalysts on SWCNT had higher and more durable electrocatalytic activity for methanol oxidation than the Pt supported on carbon.

### 1.3 Objective and Scopes of The Thesis

The objective of this research is to develop metal nanoparticles supported on CNT catalysts (metal/CNT) for the oxidation of methanol. We have tried to co-deposit other metals with Pt and Ru on CNT to enhance its electrocatalytic activity for methanol oxidation and reduced the production cost by partially replacing expensive Pt and Ru with more affordable metals for commercializing purpose. The thesis is divided into four parts. For the first part, the preparation of metal nanoparticles supported on carbon nanotube (CNT) via the polyol process is demonstrated. The second part presents the electrochemical characterization of the metal/CNT catalysts by cyclic voltammetry and the morphological information of the catalysts by XRD, XRF-EDX, and TEM techniques. To gain better understanding of the mechanism for methanol oxidation, the third part, which is the main part of the thesis, involves with the optimization of the atomic ratios of Pt-to-metal co-catalyst used for the preparation of metal/CNT catalysts modified on glassy carbon (metal/CNT/GC) electrodes. Cyclic voltammetric experiment has been used to probe the activity of these metal/CNT modified electrodes for methanol oxidation in acidic media. Finally, using chronoamperometric technique, the stability of the metal/CNT/GC electrodes in methanol solution has been addressed.

## CHAPTER II

### THEORY

For the understanding of this thesis, the definitions and theories of the following terms will be described: carbon nanotube (CNT), polyol process, electrochemical techniques, real surface area, and characterization techniques.

#### 2.1 Carbon Nanotube (CNT) [28]

CNT is one allotrope of carbon, configurationally equivalent to hexagonal network of carbon atoms that has been rolled up to make a seamless cylinder. Its cylindrical carbon tubes generate novel properties that make CNTs be potentially useful in many applications in nanotechnology, electronics, optics, material science, and other fields. CNTs exhibit extraordinary strength, unique electrical properties, and efficient heat conducting characteristic. Their usage, however, may be possibly limited by their toxicity. The nature of the bonding of CNTs can be described by applied quantum chemistry, specifically, orbital hybridization. Similar to the chemical bonding of graphite, that of nanotubes is entirely composed of  $sp^2$  carbon bonds. CNTs can be classified into two main types: single-walled carbon nanotube (SWCNT) and multi-walled carbon nanotube (MWCNT).

##### 2.1.1 Single-Walled Carbon Nanotube (SWCNT)

The structure of SWCNT can be conceptualized by wrapping an one atom-thick-layer of graphite called graphene into a seamless cylinder. SWCNTs exhibit some important electric properties with that MWCNTs do not share, but they are still expensive to be produced.

##### 2.1.2 Multi-Walled Carbon Nanotube (MWCNT)

MWCNT consists of multiple layers of graphite rolled in on themselves to form a tubular shape. There are two models which can be used to describe the structure of MWCNT. In the Russian Doll model, the sheets of graphite are arranged

in concentric cylinders. In the Parchment model, a single sheet of graphite is rolled in around itself, resembling a rolled up newspaper. The interlayer distance in MWCNT is close to the distance between graphene layers in graphite, which is approximately 3.3 Å.

## 2.2 Polyol Process [29]

Metal nanoparticle catalysts have been prepared by various techniques, but most often by chemical reduction and precipitation from aqueous or organic solution. Chemical reduction of metal nanoparticles in ethylene glycol under different conditions is the basis of the so-called polyol process.

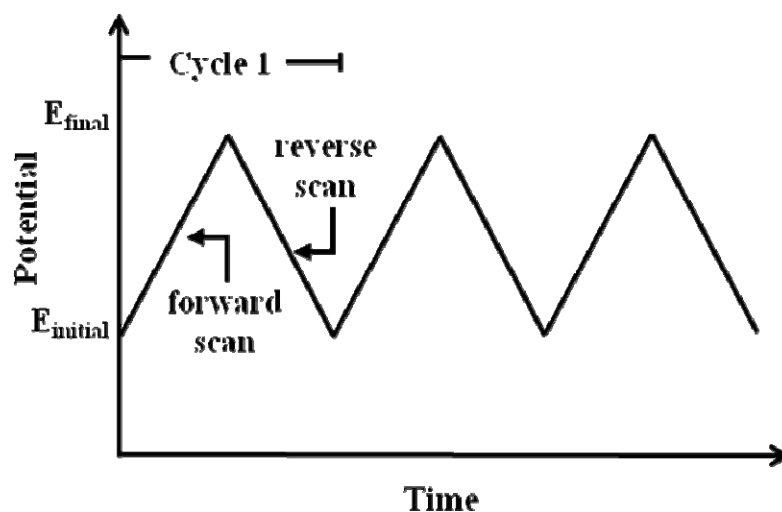
Since 1980s, polyol process has been largely used to prepare nanoparticles of various metals such as platinum (Pt), nickel (Ni), bismuth (Bi), cobalt (Co), silver (Ag), gold (Au), and palladium (Pd). The advantage of this method is that the formation of metal nanoparticles takes place in solution phase at the temperatures well below those temperatures used in typical solid state method. Synthesis of metal nanoparticles using the polyol process requires dissolution of the metal precursor in a liquid polyol, e.g., ethylene glycol, triethylene glycol, or tetraethylene glycol, which uses as both a solvent and a reducing agent. In addition, the liquid polyol often acts as a protecting agent that prevents interparticle sintering. The reaction rate is controlled by adjusting the temperature to acquire the reduction including the condensation of metal atoms from solution and finally the formation of metal nanoparticles. Rigorous adjustment of different parameters such as temperature, precursor type, precursor amount, and the order of reaction addition allows control of size, shape, and size distribution of the particles. Each metal synthesis is therefore a special case that requires optimization of reaction conditions.

## 2.3 Electrochemical Techniques [30]

Electrochemical techniques have been classified by International Union for Pure and Applied Chemistry (IUPAC) on the basis of their working principles. Although many electrochemical methods are available nowadays, only cyclic voltammetry and amperometry are used in this thesis.

### 2.3.1 Cyclic Voltammetry

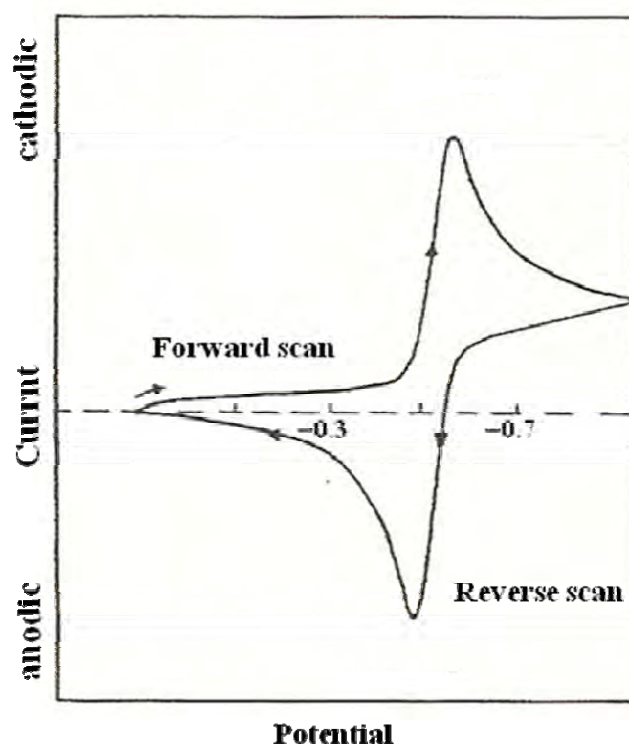
Cyclic voltammetry is the most widely used electrochemical technique for acquiring qualitative information about electrochemical reactions. The significance of cyclic voltammetry results from its ability to rapidly provide considerable information on the thermodynamic of redox processes, the kinetics of heterogeneous electron-transfer reactions, and the nature of coupled chemical reactions or adsorption processes. Thus, cyclic voltammetry is often the first experiment performed in any electroanalytical study. In particular, it offers a rapid location of redox potentials for electroactive species and convenient evaluation of medium effect upon the redox process.



**Figure 2.1** Potential-time excitation signal in cyclic voltammetry.

Cyclic voltammetry involves scanning linearly the potential of a stationary working electrode immersed in an unstirred solution using a triangular potential waveform showed in Fig. 2.1. Depending on the information sought, single

or multiple cycle(s) can be used. During the potential sweep, the potentiostat measures the current resulting from the applied potential. The plot of current versus applied potential is termed as a cyclic voltammogram, which represents characteristic features of a redox process depending on a large number of physical and chemical parameters.



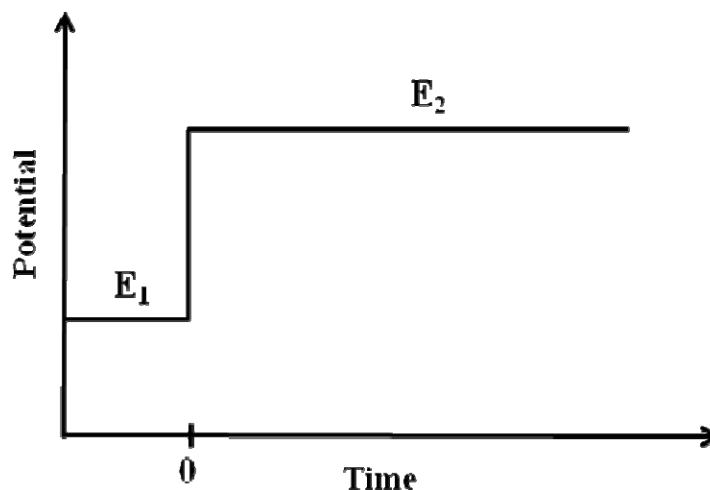
**Figure 2.2** Typical cyclic voltammogram for a reversible redox process.

Fig. 2.2 illustrates the expected response of a reversible redox couple during a single potential cycle. It is assumed that only the oxidized form, O, is present initially. Thus, a negative-going potential scan is chosen for the first half-cycle, starting from a potential value where no electrochemical reaction occurs. As the applied potential approaches the characteristic  $E^0$  of the redox process, a current for the reduction process begins to increase until the cathodic peak is reached. After traversing the potential region in which the reduction takes place, the direction of the potential sweep is reversed. During the reverse scan, the reduced form, R, (generated in the forward half cycle and accumulated near the electrode surface) re-oxidizes back to O, resulting in an anodic peak.



### 2.3.2 Chronoamperometry

Chronoamperometry deals with stepping the potential of the working electrode from a value at which no faradaic reaction of an electroactive species occurs to a potential at which the faradaic reaction occurs dramatically until the concentration of the electroactive species at the electrode surface is effectively zero. Fig. 2.3 reveals the applied potential-time waveform of this technique.



**Figure 2.3** Potential-time waveform of chronoamperometry.

Chronoamperometry is often used for the measurement of the diffusion coefficient of electroactive species and the surface area of working electrode. Analytical application of this method relies on pulsing of the working electrode potential repetitively at fixed time intervals. Additionally, this technique can be applied to study the mechanisms of electrode processes.

### 2.4 Real Surface Area [31,32]

One of the most important parameters in heterogeneous electrocatalysis is the real surface area of a working electrode or the catalyst at the electrode, which will determine the catalytic activity. To measure real surface area, we need to utilize a microscopic examination. One such examination is using the adsorption of gaseous atoms or molecules onto the solid surface. A gaseous molecule may be adsorbed on a solid surface by physisorption or chemisorption interaction. If physisorption takes

place, the gaseous particles carpet the electrode surface to form a monolayer on which successive gas layers may adsorb later (Fig. 2.4a). In this case, the real surface area can be evaluated by measuring the amount of adsorbed gas and the area occupied by each atom or molecule of gas. When the gas is absorbed by chemisorption, each atom or molecule of gas is attached by a real covalent bond to an adsorption site. In the case, the adsorption site is an atom (Fig. 2.4b). The evaluation of the real surface area then requires the determination of adsorbed gas amount.

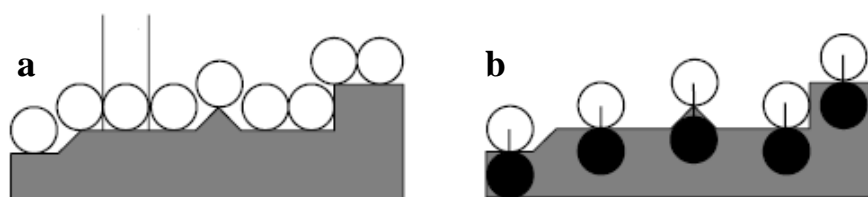


**Figure 2.4** Adsorbate particles packing with (a) physisorption and (b) chemisorption.

The determination of Pt surface area on the electrode using hydrogen adsorption has been one of the most widely used methods for determination of the real surface area of Pt-based catalysts used in fuel cell electrodes.

#### 2.4.1 Hydrogen Adsorption Method

Hydrogen adsorption on the Pt surface is achieved by applying sufficiently negative potentials to the electrode when in contact with an aqueous solution. Fig. 2.5 shows three regions distinguished in the cyclic voltammogram of a Pt electrode in an acid solution. The oxygen region is found at the positive potentials. During the positive sweep prior to dioxygen ( $O_2$ ) evolution, a hydrated Pt oxide monolayer is formed. Cyclic voltammogram revealed well Pt oxide (Pt–O) reduction process at 0.5 mV. In the center region, low cathodic and anodic currents can be found. This area is called as double-layer region since only capacitive processes take place. Finally, the hydrogen region can be observed at negative potentials.



When the electrode potential becomes more and more negative, until the formation of adsorbed H monolayer is achieved according to equation 2.1. Once the Pt surface is fully covered by hydrogen atoms, the adsorption of hydrogen (H<sub>2</sub>) molecules will take place:



These adsorbed H<sub>2</sub> molecules come together to form hydrogen bubbles that will leave the Pt electrode surface when they have grown large enough:



In the positive direction, the adsorbed hydrogen can desorb from the Pt surface (equation 2.4).



The integration of the anodic current in the hydrogen region can give the amount of desorbed hydrogen which indirectly represents Pt real surface area.

The experimentally obtained charge also contains a contribution from the double layer charge, which should be subtracted. Subtraction is usually made by assuming that double layer charge has the same value in all regions. Equation 2.5 represents actual charge from the hydrogen desorption

$$Q = \frac{1}{\nu} \int_{(V_0-V_i)/\nu}^{(V_0-V_f)/\nu} I dV - Q_{\text{dl}} \quad (2.5)$$

where Q is charge of hydrogen desorption, I is total current, Q<sub>dl</sub> is double layer charge, V<sub>0</sub> is initial potential of scan, V<sub>i</sub> is initial potential of the hydrogen desorption, V<sub>f</sub> is final potential of the hydrogen desorption, and ν is potential sweep rate.

When the catalytic powder consists of metal nanoparticles supported on carbon, it is useful to measure electrochemical active surface (EAS) area. EAS areas of the Pt-based catalysts can be estimated from cyclic voltammogram of the Pt-based catalyst modified electrodes in background solutions. Using coulombic charge associated with hydrogen desorption (Q<sub>H</sub>), EAS area of the catalyst can be written as equation 2.6

$$\text{EAS (m}^2 \cdot \text{g}^{-1}) = Q_{\text{H}} / (Q_{\text{Ho}} \times g_{\text{cat}}) \quad (2.6)$$

where the constant  $Q_{H_0}$  is the amount of charge per unit Pt surface area ( $210 \mu\text{C}\cdot\text{cm}^{-2}$ ), which represents the desorption of one-monolayer hydrogen, and  $g_{\text{cat}}$  is the actual weight of Pt-based catalyst.

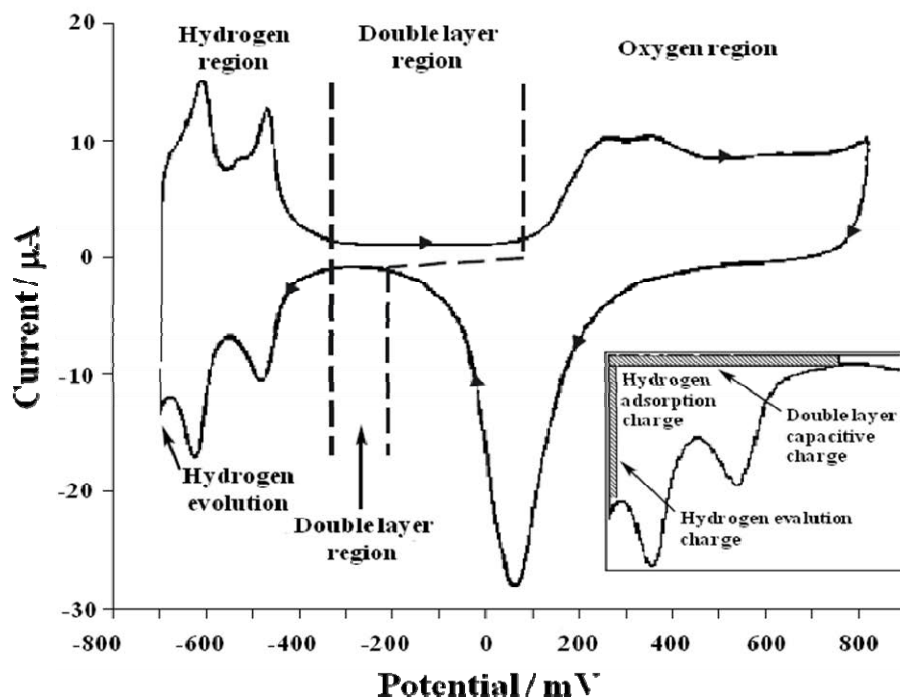


**Figure 2.5** Cyclic voltammetric current potential curve for a Pt electrode in contact with acid solution. The inset shows the different charge contributions in the hydrogen region.

## 2.5 Characterization Techniques

### 2.5.3 Infrared (IR) Spectroscopy [33]

IR spectroscopy is the study of the interaction of IR electromagnetic radiation with matter. Electromagnetic radiation is composed of electric and magnetic waves that are in planes perpendicular to each other. The radiation moves through space in a plane perpendicular to the planes containing the electric and magnetic waves. It is the electric part of the radiation, called the electric vector that interacts with matter. When IR radiation interacts with a molecule, it can be absorbed by the molecule causing the chemical bonds in the molecule to vibrate. Chemical structural fragment within a molecule, known as a functional group, tends to absorb IR radiation

in the same wavenumber range regardless of the structure of the rest of the molecule in which the functional group stays. This correlation between a functional group and the wavenumber of its absorbed IR allows the structure of an unknown molecule to be identified from the molecule's IR spectrum, making IR spectroscopy a useful chemical analysis tool.

### 2.5.2 X-ray Diffraction (XRD) Technique [34]

XRD is an efficient technique used for identification and characterization of unknown crystalline materials. When an X-ray beam hits an atom of a solid sample, the electrons around the atom start to oscillate with the same frequency as the incoming X-ray beam. Diffraction beam then occurs when a X-ray beam encounters the sample. It is described as the apparent bending of waves around small samples and the spreading out of waves past small openings. In almost all directions, destructive interference will occur because the combining waves are out of phase and there is no resultant energy leaving the solid sample. However, the atoms in a crystal are arranged in a regular pattern generating constructive interference in a few directions. The combining waves will be in phase causing well defined X-ray beams. Therefore, a diffracted beam may be described as a beam composed of a large number of scattered rays mutually reinforcing one another.

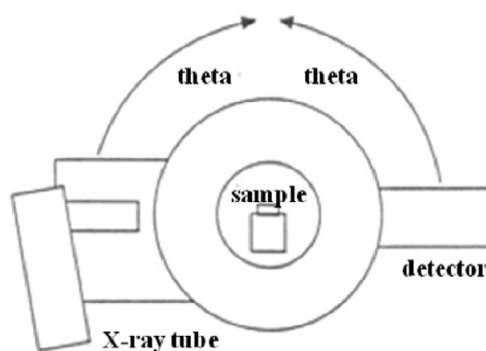


**Figure 2.6** Sketch of one possible configuration of the XRD instrument.

Fig. 2.6 displays simplified sketch of one possible configuration of XRD instrument. In this configuration, both X-ray tube and X-ray detector move through the angle theta whereas the sample remains stationary. A detector detects the X-ray

signal which is then proceeded and converted into a count rate either by a microprocessor or electronically.

### **2.5.3 Transmission Electron Microscopy (TEM) [35]**

TEM produces a transmitted electron image of a thin specimen, magnified from 100 to approximately 500,000 times and with a resolving power of approximately 0.2 nm. Thus, TEM has greater resolving capability as well as a wider and higher magnification range than the light microscope does. TEM finds applications in cancer research, virology, material science as well as semiconductor research. The quality of the image in TEM depends on not only the expertise of the microscopist, but also the quality of the specimen preparation.

The principle of TEM is to produce sample image by light source at the top of the microscope. This light source emits electrons that travel through vacuum in the microscope column. Instead of glass lenses in the light microscope, TEM uses electromagnetic lenses to focus the electrons into a very thin beam. The electron beam then travels through the interested specimen. Depending on the density of the specimen, some of the electrons are scattered and disappear from the beam. At the bottom of the microscope, the unscattered electrons hit a fluorescent screen and give rise to a shadow image of the specimen. Different parts of the image display in various darkness according to their density. The image can be directly studied by an operator or a photographer with a camera.

### **2.5.4 Energy Dispersive X-ray Fluorescence Spectroscopy (XRF-EDX) [34]**

XRF-EDX analysis separates characteristic X-ray on the basis of its photon energies rather than on its wavelengths. It is not only a powerful and versatile analysis method by its own, but sometimes used as an accessory to other instruments because of its compactness. XRF-EDX analysis is widely used for elemental analysis and chemical analysis, particularly in the investigation of metals, glass, ceramics and building materials, and for research in geochemistry, forensic science and archaeology. Fig. 2.7 shows schematic representation of an energy-dispersive spectrometer. Characteristic X-ray of a specimen irradiated with a primary X-ray beam enters a cooled Si(Li) detector which is connected to an amplifier system. It is necessary to cool the detector to liquid nitrogen temperatures in order to reduce

electronic noise and ensure optimum resolution. The fluorescent X-rays emitted by the sample are directed into the detector which produces a continuous distribution of pulses, the voltages of which are proportional to the incoming photon energies. This signal is processed by a multichannel analyzer (MCA) which produces an accumulating digital spectrum that can be processed to obtain analytical data. To be more precise, the detector converts the fluorescent X-ray into electron-hole pairs, which are then swept out of the detector by an applied voltage. In addition, the intensity of each characteristic radiation is directly related to the amount of each element in the material.

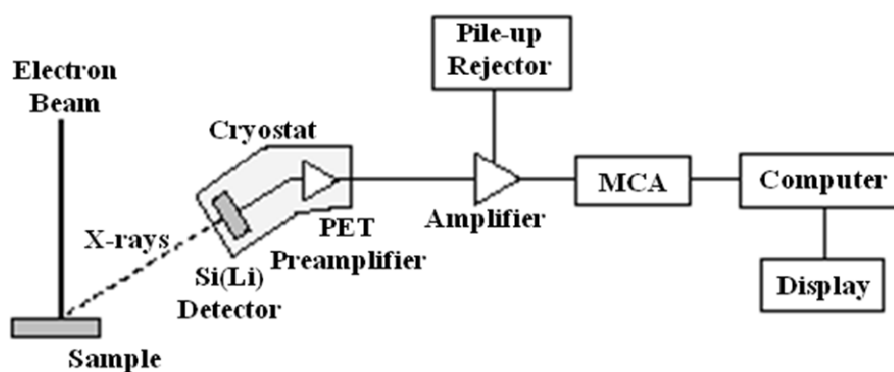


**Figure 2.7** Schematic representation of an energy-dispersive spectrometer.

## CHAPTER III

### EXPERIMENTAL

#### 3.1 Instruments and Apparatus

##### 3.1.1 Electrochemical Instruments

The employed electrochemical instruments and apparatus are summarized in Table 3.1.

**Table 3.1** Electrochemical instruments

Instrument	Model	Company (Country)
1. potentiostat/galvanostat	PG-30	Methrom (Switzerland)
2. working electrode		
2.1 glassy carbon (GC)		(China)
3. reference electrode		
3.1 silver/silver chloride (Ag/AgCl) electrode		BAS (Japan)
4. counter electrode		
4.1 home-made platinum (Pt) wire		
5. other apparatus		
5.1 home-made capcell		
5.2 home-made glass cell		
5.3 0.3 $\mu\text{m}$ -alumina powder polishing set	AM 0782	Alpha (USA)
5.4 1.0 $\mu\text{m}$ -alumina powder polishing set	AM 0786	Alpha (USA)
5.5 home-made salt-bridge		



### 3.1.2 Characterization Instruments

The characterization instruments are given in Table 3.2.

**Table 3.2** Characterization instruments

Instrument	Model	Company (Country)
1. Fourier transform infrared spectrometer	Spectrum One	Perkin Elmer (USA)
2. transmission electron microscopy	JEM-2100	JEOL (Japan)
3. X-ray diffraction instrument	DMAX 2200	Rigaku (USA)
4. energy dispersive X-ray fluorescence spectrometer	ED-2000	Oxford (Japan)

### 3.2 Chemicals

All chemicals employed in this research are AR grade. Milli-Q water was used for preparing all chemical solutions. Chemicals and their suppliers are summarized in Table 3.3.

**Table 3.3** Chemicals

Chemical	Manufacturer (Country)
1. carbon nanotube 99%, CNT	Chang Mai University (Thailand)
2. methanol, CH <sub>3</sub> OH	Merck (Germany)
3. ethanol, C <sub>2</sub> H <sub>5</sub> OH	Merck (Germany)
4. ethylene glycol, HO(CH <sub>2</sub> ) <sub>2</sub> OH	Merck (Germany)
5. sodium hydroxide, NaOH	Merck (Germany)
6. concentrated hydrochloric acid, HCl	Merck (Germany)
7. concentrated nitric acid, HNO <sub>3</sub>	Merck (Germany)
8. concentrated sulfuric acid, H <sub>2</sub> SO <sub>4</sub>	Merck (Germany)
9. chromium (III) nitrate nanohydrate, Cr(NO <sub>3</sub> ) <sub>3</sub> ·9H <sub>2</sub> O	Fluka (Switzerland)

Chemical	Manufacturer (Country)
10. cobalt (II) sulfate heptahydrate, $\text{CoSO}_4 \cdot 7\text{H}_2\text{O}$	Fluka (Germany)
11. hydrogen hexachloroplatinic acid (IV) hydrate, $\text{H}_2\text{PtCl}_6 \cdot 6\text{H}_2\text{O}$	Fluka (Italy)
12. hydrogen tetrachloroaurate (III) trihydrate; $\text{HAuCl}_4 \cdot 3\text{H}_2\text{O}$	Sigma Aldrich (Germany)
13. iron (III) chloride hexahydrate, $\text{FeCl}_3 \cdot 6\text{H}_2\text{O}$	Merck (Germany)
14. manganese (II) sulphate monohydrate, $\text{MnSO}_4 \cdot \text{H}_2\text{O}$	Fluka (USA)
15. molybdenum (V) chloride, $\text{MoCl}_5$	Sigma Aldrich (Germany)
16. nickel (II) nitrate hexahydrate, $\text{Ni}(\text{NO}_3)_2 \cdot 6\text{H}_2\text{O}$	Sigma Aldrich (Germany)
17. ruthenium (III) chloride hydrate, $\text{RuCl}_3 \cdot x\text{H}_2\text{O}$	Sigma Aldrich (Germany)

### 3.3 Preparation of Reagents

The following section explains procedures for preparing chemical solutions in this work.

#### 3.3.1 Solutions for pH Adjustment

##### 3.3.1.1 Sodium Hydroxide (1.0 M)

Accurate weight (1.0 g) of NaOH was dissolved in 50 mL of  $\text{HO}(\text{CH}_2)_2\text{OH}$  solution.

##### 3.3.1.2 Hydrochloric acid (2.0 M)

An aliquot of 3.06 mL of concentrated HCl was diluted with milli-Q water and made to the final volume of 50 mL.

### 3.3.2 Solutions of Catalyst Precursors

#### 3.3.2.1 Platinum and Platinum-Ruthenium Solutions

Pt and Pt-Ru composite solutions were prepared by dissolving accurate weight of  $\text{H}_2\text{PtCl}_6 \cdot 6\text{H}_2\text{O}$  and  $\text{RuCl}_3 \cdot x\text{H}_2\text{O}$  in 10 mL of  $\text{HO}(\text{CH}_2)_2\text{OH}$  solution. Weight of  $\text{H}_2\text{PtCl}_6 \cdot 6\text{H}_2\text{O}$  and  $\text{RuCl}_3 \cdot x\text{H}_2\text{O}$  in six composite solutions are listed in Table 3.4.

**Table 3.4** Platinum and platinum-ruthenium composite solutions

Pt:Ru Mole Ratio	$\text{H}_2\text{PtCl}_6 \cdot 6\text{H}_2\text{O}$ (mg)	$\text{RuCl}_3 \cdot x\text{H}_2\text{O}$ (mg)
2:0	40.0	-
2:1	40.0	10.0
2:1.25	40.0	12.5
2:1.5	40.0	15.0
2:2	40.0	20.0
2:4	40.0	40.0

#### 3.3.2.2 Platinum-Chromium, Platinum-Cobalt, Platinum-Gold, Platinum-Iron, Platinum-Manganese, Platinum-Molybdenum, and Platinum-Nickel Solutions at Mole Ratios of 2:1.5

Pt-Cr, Pt-Co, Pt-Au, Pt-Fe, Pt-Mn, Pt-Mo, and Pt-Ni composite solutions at the mole ratios of 2:1.5 were prepared using  $\text{HO}(\text{CH}_2)_2\text{OH}$  as a solvent. As shown in Table 3.5,  $\text{H}_2\text{PtCl}_6 \cdot 6\text{H}_2\text{O}$ ,  $\text{Cr}(\text{NO}_3)_3 \cdot 9\text{H}_2\text{O}$ ,  $\text{CoSO}_4 \cdot 7\text{H}_2\text{O}$ ,  $\text{HAuCl}_4 \cdot 3\text{H}_2\text{O}$ ,  $\text{FeCl}_3 \cdot 6\text{H}_2\text{O}$ ,  $\text{MnSO}_4 \cdot \text{H}_2\text{O}$ ,  $\text{MoCl}_5$ , and  $\text{Ni}(\text{NO}_3)_2 \cdot 6\text{H}_2\text{O}$  were accurately weighed to yield Pt-metal composite solutions.

**Table 3.5** Platinum-chromium, platinum-cobalt, platinum-gold, platinum-iron, platinum-manganese, platinum-molybdenum, and platinum-nickel solutions at mole ratios of 2:1.5

Pt:Metal at 2:1.5 Mole Ratio	H <sub>2</sub> PtCl <sub>6</sub> ·6H <sub>2</sub> O (mg)	Metal (mg)
Pt:Cr	40.0	28.8
Pt:Co	40.0	20.3
Pt:Au	40.0	28.5
Pt:Fe	40.0	19.4
Pt:Mn	40.0	12.2
Pt:Mo	40.0	19.8
Pt:Ni	40.0	21.0

### 3.3.2.3 Platinum-Chromium Solutions

Pt-Cr composite solutions were prepared by dissolving accurate weight of H<sub>2</sub>PtCl<sub>6</sub>·6H<sub>2</sub>O and Cr(NO<sub>3</sub>)<sub>3</sub>·9H<sub>2</sub>O in 10 mL of HO(CH<sub>2</sub>)<sub>2</sub>OH solution as displayed in Table 3.6.

**Table 3.6** Platinum-chromium composite solutions

Pt:Cr Mole Ratio	H <sub>2</sub> PtCl <sub>6</sub> ·6H <sub>2</sub> O (mg)	Cr(NO <sub>3</sub> ) <sub>3</sub> ·9H <sub>2</sub> O (mg)
2:1	40.0	19.2
2:1.25	40.0	24.0
2:2	40.0	38.4

### 3.3.2.4 Platinum-Molybdenum Solutions

Pt-Mo composite solutions were prepared by dissolving accurate weight of H<sub>2</sub>PtCl<sub>6</sub>·6H<sub>2</sub>O and MoCl<sub>5</sub> in 10 mL of HO(CH<sub>2</sub>)<sub>2</sub>OH solution as listed in Table 3.7.

**Table 3.7** Platinum-molybdenum composite solutions

Pt:Mo Mole Ratio	H <sub>2</sub> PtCl <sub>6</sub> ·6H <sub>2</sub> O (mg)	MoCl <sub>5</sub> (mg)
2:1	40.0	13.2
2:1.25	40.0	16.5
2:2	40.0	26.4

**3.3.2.5 Platinum-Nickel Solutions**

Pt-Ni composite solutions were prepared by dissolving accurate weight of H<sub>2</sub>PtCl<sub>6</sub>·6H<sub>2</sub>O and Ni(NO<sub>3</sub>)<sub>2</sub>·6H<sub>2</sub>O in 10 mL of HO(CH<sub>2</sub>)<sub>2</sub>OH solution as listed in Table 3.8.

**Table 3.8** Platinum-nickel composite solutions

Pt:Ni Mole Ratio	H <sub>2</sub> PtCl <sub>6</sub> ·6H <sub>2</sub> O (mg)	Ni(NO <sub>3</sub> ) <sub>2</sub> ·6H <sub>2</sub> O (mg)
2:1	40.0	14.0
2:1.25	40.0	17.5
2:2	40.0	28.0

### 3.3.2.6 Platinum-Ruthenium-Chromium Solutions

Pt-Ru-Cr composite solutions were prepared by dissolving accurate weight of  $\text{H}_2\text{PtCl}_6 \cdot 6\text{H}_2\text{O}$ ,  $\text{RuCl}_3 \cdot x\text{H}_2\text{O}$ , and  $\text{Cr}(\text{NO}_3)_3 \cdot 9\text{H}_2\text{O}$  in 10 mL of  $\text{HO}(\text{CH}_2)_2\text{OH}$  solution as listed in Table 3.9.

**Table 3.9** Platinum-ruthenium-chromium composite solutions

Pt:Ru:Cr Mole Ratio	$\text{H}_2\text{PtCl}_6 \cdot 6\text{H}_2\text{O}$ (mg)	$\text{RuCl}_3 \cdot x\text{H}_2\text{O}$ (mg)	$\text{Cr}(\text{NO}_3)_3 \cdot 9\text{H}_2\text{O}$ (mg)
2:1:0.5	40.0	10.0	9.6
2:0.5:1	40.0	5.0	19.2
2:0.75:0.75	40.0	7.5	14.4

### 3.3.2.7 Platinum-Ruthenium-Molybdenum Solutions

Pt-Ru-Mo composite solutions were prepared by accurately weighing  $\text{H}_2\text{PtCl}_6 \cdot 6\text{H}_2\text{O}$ ,  $\text{RuCl}_3 \cdot x\text{H}_2\text{O}$ , and  $\text{MoCl}_5$  according to Table 3.10 and dissolving the chemicals in 10 mL of  $\text{HO}(\text{CH}_2)_2\text{OH}$  solution.

**Table 3.10** Platinum-ruthenium-molybdenum composite solutions

Pt:Ru:Mo Mole Ratio	$\text{H}_2\text{PtCl}_6 \cdot 6\text{H}_2\text{O}$ (mg)	$\text{RuCl}_3 \cdot x\text{H}_2\text{O}$ (mg)	$\text{MoCl}_5$ (mg)
2:1:0.5	40.0	10.0	6.6
2:0.5:1	40.0	5.0	13.2
2:0.75:0.75	40.0	7.5	9.9

### 3.3.2.8 Platinum-Ruthenium-Nickel Solutions

Pt-Ru-Ni composite solutions were prepared by accurately weighing  $\text{H}_2\text{PtCl}_6 \cdot 6\text{H}_2\text{O}$ ,  $\text{RuCl}_3 \cdot x\text{H}_2\text{O}$ , and  $\text{Ni}(\text{NO}_3)_2 \cdot 6\text{H}_2\text{O}$  according to Table 3.11 and dissolving the chemicals in 10 mL of  $\text{HO}(\text{CH}_2)_2\text{OH}$  solution.

**Table 3.11** Platinum-ruthenium-nickel composite solutions

Pt:Ru:Ni Mole Ratio	$\text{H}_2\text{PtCl}_6 \cdot 6\text{H}_2\text{O}$ (mg)	$\text{RuCl}_3 \cdot x\text{H}_2\text{O}$ (mg)	$\text{Ni}(\text{NO}_3)_2 \cdot 6\text{H}_2\text{O}$ (mg)
2:1:0.5	40.0	10.0	7.0
2:0.5:1	40.0	5.0	14.0
2:0.75:0.75	40.0	7.5	10.5

### 3.3.3 Electrolyte Solution

#### 3.3.3.1 Sulfuric Acid Solution (0.5 M)

An aliquot of 1.33 mL of concentrated  $\text{H}_2\text{SO}_4$  was diluted with Milli-Q water and made to the final volume of 50 mL.

## 3.4 Experimental Procedures

In this section, it mainly consists of procedures for CNT modification, preparation of metal catalysts supported on CNT (metal/CNT catalysts), morphological studies of CNT and metal/CNT catalysts, electrode preparation, electrochemical characterization of the modified electrodes, investigation of methanol oxidation by the modified electrodes, and stability studies of the modified electrodes.

#### 3.4.1 Modification of Carbon Nanotube (CNT) [36]

In order to functionalize CNT with active groups such as carboxylic acid, 1.0 g of CNT was dispersed in 60 mL of 1:3 v/v mixed concentrated  $\text{HNO}_3$  and  $\text{H}_2\text{SO}_4$  and the mixture was agitated by ultrasonic wave. Then, the CNT mixture was washed with milli-Q water until the pH of the mixture approached 7. After that, the mixture was filtered and finally dried at  $50^\circ\text{C}$ . The information of functional groups attached on modified CNT was provided by Fourier transform infrared (FTIR) spectrometer.

### **3.4.2 Preparation of Metal Catalysts Supported on Carbon Nanotube (Metal/CNT Catalysts) [10]**

Metal/CNT catalysts were prepared via the following procedure. Required amounts of metal precursors (Table 3.4-3.11) were added into HO(CH<sub>2</sub>)<sub>2</sub>OH solution to form a brown solution. The pH of the solution was adjusted to above 7 with 2.0 M NaOH solution, followed by the addition of the modified CNT. The mixture was ultrasonically treated to ensure that the modified CNT was uniformly dispersed in the solution mixture. Then, the mixture was heated to 160-180°C in an oil bath and maintained at this temperature range for several hours to complete the reduction of metal precursors. When the mixture was cooled, its pH was adjusted with 2.0 M HCl solution. After that, the mixture was refluxed at 80-100°C to settle the metal/CNT catalyst which was subsequently filtered, washed, and dried.

### **3.4.3 Morphology of CNT and Metal/CNT Catalysts**

The morphological and structural information of CNT and metal/CNT catalysts were obtained by transmission electron microscope (TEM), X-ray diffraction (XRD) instrument, and energy dispersive X-ray fluorescence spectrometer (XRF-EDX).

### **3.4.4 Electrode Preparation**

#### **3.4.4.1 Glassy Carbon Electrode**

Served as a working electrode, GC electrode was polished with 1.0 and 0.3 μm alumina slurries until a mirror-like electrode surface was obtained. Then, the electrode was rinsed with milli-Q water prior to use.

#### **3.4.4.2 CNT Modified Glassy Carbon Electrodes**

Accurate weight (3.0 mg) of CNT was sonicated in ethanol to form slurry. Then, 30 μL of the slurry was cast on the surface of GC electrode and allowed to dry at room temperature to generate the GC electrode modified with CNT (CNT/GC).



#### 3.4.4.3 Metal/CNT Catalysts Modified Glassy Carbon Electrodes

Accurate weight (3.0 mg) of metal/CNT catalyst was sonicated in ethanol to form slurry. Then, 30  $\mu\text{L}$  of the slurry was cast on the surface of GC electrode and allowed to dry at room temperature to generate the GC electrode modified with metal/CNT catalyst (metal/CNT/GC).

### 3.4.5 Electrochemical Characterization of CNT and Metal/CNT Catalyst Modified Glassy Carbon Electrodes

#### 3.4.5.1 Electrochemical Set-up

Electrochemical cell for cyclic voltammetric experiment is shown in Fig. 3.1. Working electrodes (WEs) were CNT and the metal/CNT catalyst modified GC (CNT/GC and metal/CNT/GC) electrodes. Counter electrode (CE) and reference electrode (RE) were Pt wire and Ag/AgCl, respectively. WE, CE, and RE were contained in a glass cell and connected with a PG-30 potentiostatic system.

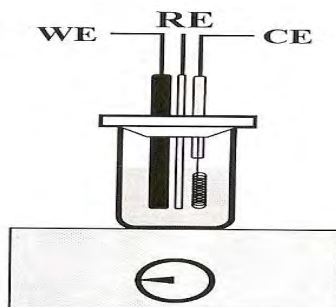


**Figure 3.1** Electrochemical cell for cyclic voltammetry.

#### 3.4.5.2 Background Current

Cyclic voltammograms of the modified electrodes were obtained in the solution of 0.5 M  $\text{H}_2\text{SO}_4$  which served as a supporting electrolyte. These cyclic voltammograms were used as background voltammograms as well as electrochemical characterization of the modified electrodes. In addition, all cyclic voltammograms were performed at the scan rate  $50 \text{ mV} \cdot \text{s}^{-1}$ .

### 3.4.6 Catalytic Activity of Metal/CNT Catalyst Modified Glassy Carbon Electrodes

Catalytic activity of the metal/CNT/GC electrodes towards methanol oxidation was investigated by obtaining their cyclic voltammograms in 0.5-2.5 M methanol solution containing 0.5 M H<sub>2</sub>SO<sub>4</sub> at room temperature.

### 3.4.7 Stability of Metal/CNT Catalyst Modified Glassy Carbon Electrodes

The stability of the metal/CNT/GC electrodes was probed by collecting current vs. time curve for the oxidation of 1.0 M methanol containing 0.5 M H<sub>2</sub>SO<sub>4</sub>. Using chronoamperometric technique, the potential of the metal/CNT/GC electrodes was constantly hold at the values corresponding to a half and a quarter of the cyclic voltammetric peak current for methanol oxidation to allow the oxidation existence. The potential values of each modified electrodes are shown in Table 3.12.

**Table 3.12** Potentials for the metal/CNT/GC electrodes in chronoamperometric measurement

Metal/CNT Catalyst	Mole Ratio of Metals	Potential (E <sub>1/2</sub> ,V)	Potential (E <sub>1/4</sub> ,V)
Pt/CNT	-	0.567	0.482
PtRu/CNT	2:1.5	0.573	0.455
PtRuCr/CNT	2:0.5:1	0.708	0.543
PtRuMo/CNT	2:1:0.5	0.586	0.451
PtRuNi/CNT	2:1:0.5	0.475	0.267

## CHAPTER IV

### RESULTS AND DISCUSSION

This chapter describes experimental results related to the glassy carbon electrodes modified with metals supported on carbon nanotube (metal/CNT/GC electrodes). Morphological information of CNT, metal/CNT catalysts and metal/CNT/GC electrodes were obtained. Furthermore, all metal/CNT/GC electrodes were discussed in terms of their current density and mass activity for methanol oxidation.

#### 4.1 Modification of Carbon Nanotube (CNT)

After CNT was functionalized with carboxylic acid groups, fourier transform infrared (FTIR) spectroscopy, X-ray diffraction (XRD) technique, and transmission electron microscopy (TEM) were introduced to obtain the information about the functional groups attached on the modified CNT, in comparison with the unmodified CNT.

##### 4.1.1 Fourier Transform Infrared Spectroscopic Analysis

Since, the surface of raw CNT is chemically inert and hydrophobic, CNT is unfavorable for supporting catalyst. Therefore, the modification of CNT surface with functional groups is essential. FTIR spectra of unmodified and modified CNT are presented in Fig. 4.1. In both cases, the peak at about  $3,400\text{ cm}^{-1}$  can be attributed to OH symmetrical stretching whereas the peak at about  $1,630\text{ cm}^{-1}$  is suggested to be C=C stretching [21]. For the unmodified CNT (Fig. 4.1a), the peak at  $1,130\text{ cm}^{-1}$  can be attributed to C-H bending. After CNT modification with the acid treatment, FTIR spectrum of the modified CNT (Fig. 4.1b) shows the peaks at  $1,550$  and  $1,720\text{ cm}^{-1}$  representing  $\text{COO}^-$  and C=O stretching of carboxyl group as well as the peak at  $1,200\text{ cm}^{-1}$  corresponding to C-O stretching [36,37]. FTIR result revealed that oxygen-containing functional groups can be introduced to CNT by the oxidative

treatment with by mixed strong acids, making CNT favor high loading of well-dispersed metal nanoparticles.

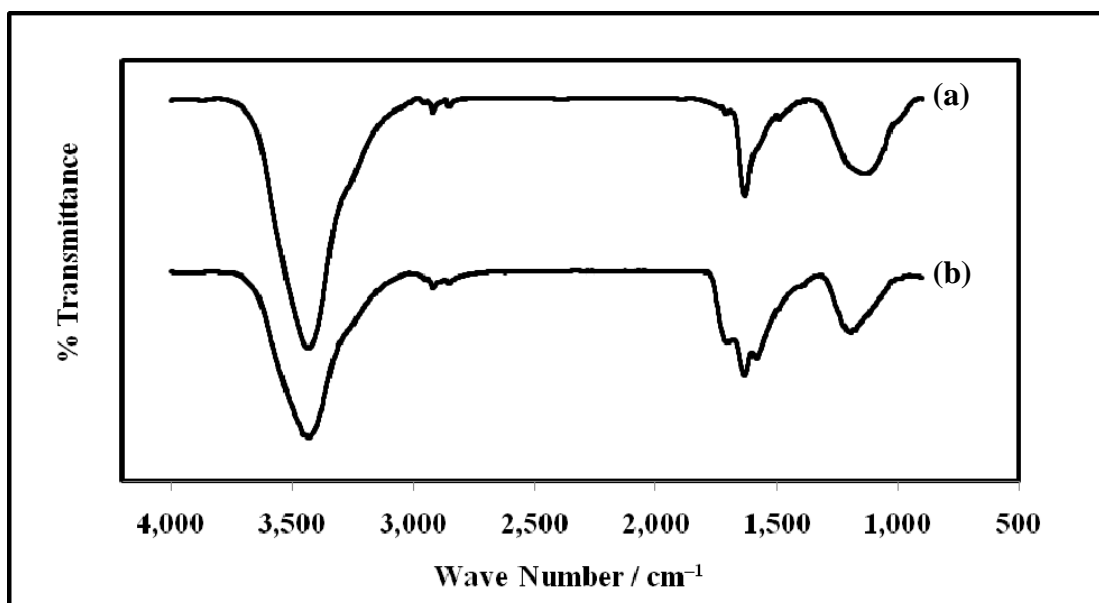


**Figure 4.1** FTIR spectra of (a) unmodified and (b) modified CNT.

#### 4.1.2 X-ray Diffraction Analysis

Fig. 4.2 shows XRD patterns of the unmodified and modified CNT observed at room temperature.

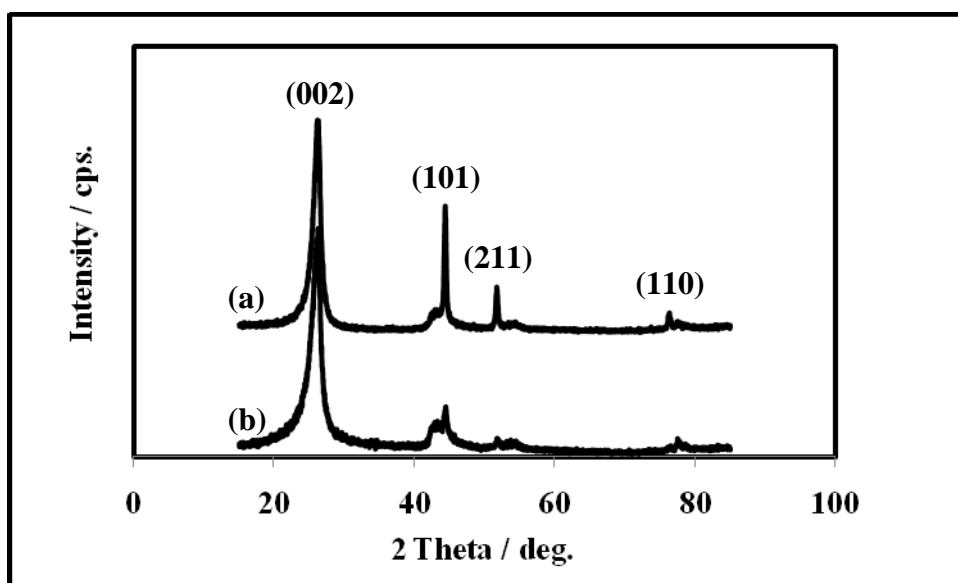


**Figure 4.2** XRD patterns of (a) unmodified and (b) modified CNT.

The XRD peaks at 25.87 degrees of unmodified and modified CNT can be attributed to CNT (002). For the unmodified CNT (Fig. 4.2a), the (101) peak near 43.95 degrees reflects the diffraction peak of residual Ni whereas the (221) and (110) peaks reveal the diffraction peaks of graphite at 52.35 and 77.50 degrees, respectively [38]. After the acid treatment, XRD pattern of the modified CNT (Fig. 4.2b) shows peaks at 43.95, 52.35, and 77.50 degrees, but with less intensities, demonstrating that the quantity of graphite and Ni residue can be reduced by the strong acid treatment.

#### 4.1.3 Transmission Electron Microscopic Analysis

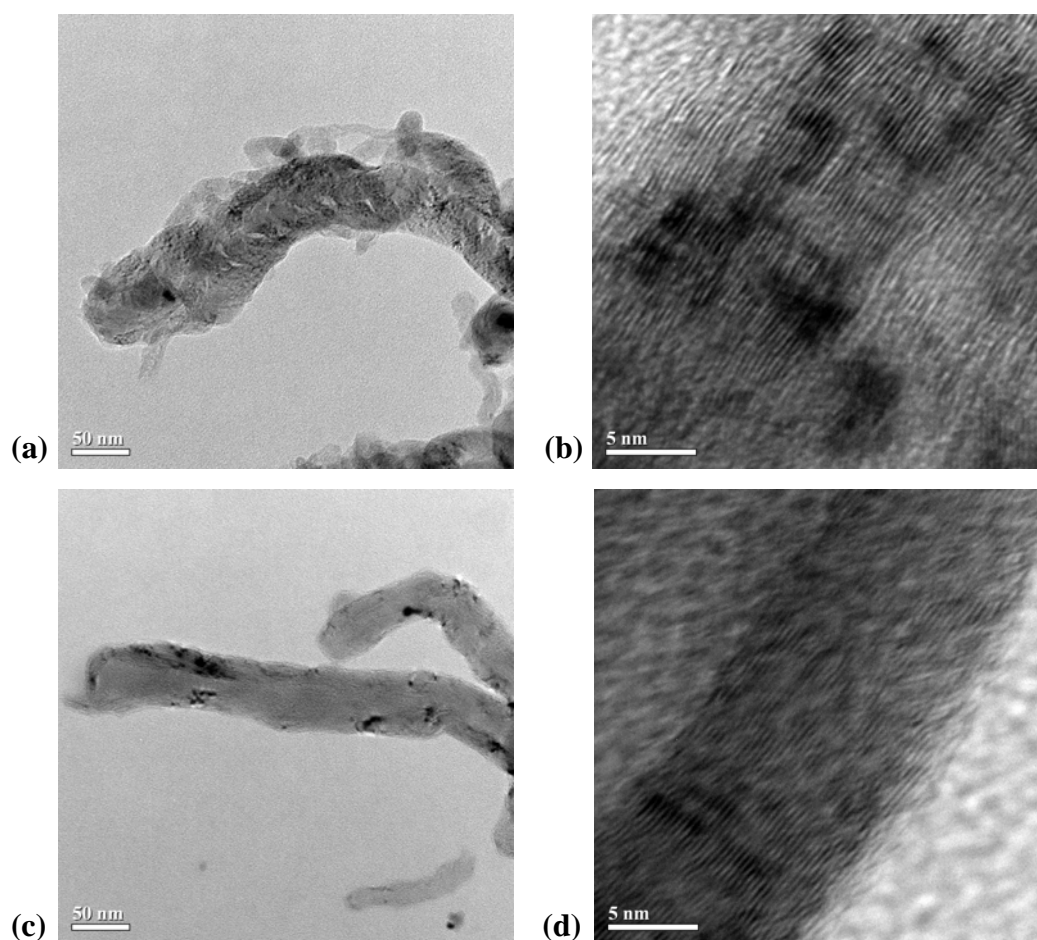


**Figure 4.3** TEM images of unmodified CNT ((a) and (b)) and modified CNT ((c) and (d)) with the magnification power of 50,000 ((a) and (c)) and 800,000 ((b) and (d)).

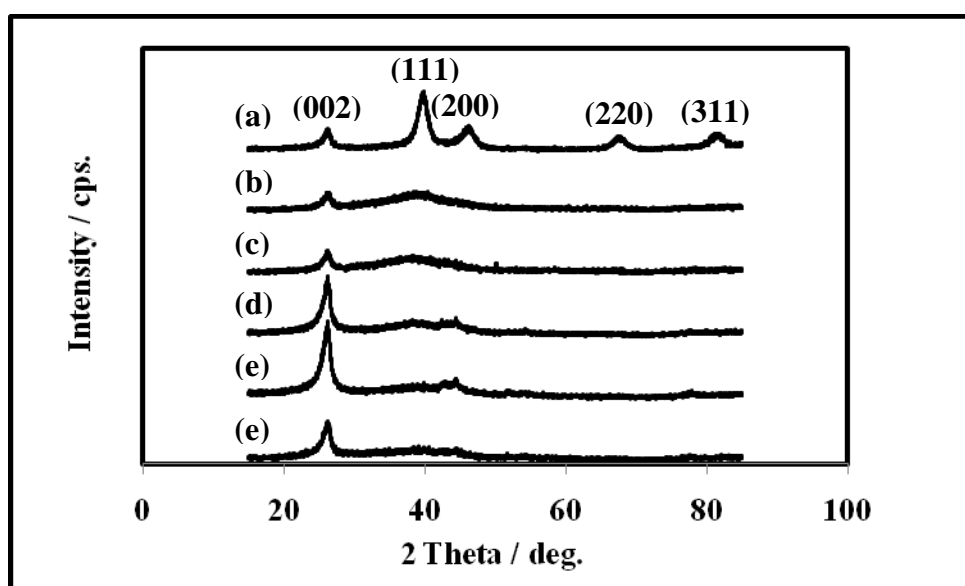
TEM images of the unmodified and modified CNT are shown in Fig. 4.3. It can be seen from Fig. 4.3a and 4.3b that the unmodified CNT contained impurities on its outer walls. These impurities could be amorphous carbon formed as

a side product along with the CNT formation and the trace amount of Ni coming from the Ni nanoparticles used as the catalyst for CNT synthesis. After the acid treatment, these impurities were removed from the outer walls of the CNT (Fig. 4.3c and 4.3d). However, a few metal nanoparticles presented inside the nanotubes could not be removed because of the inaccessibility of acid solution inside the tubes during the acid treatment.

## 4.2 Morphological Information of Metal/CNT Catalysts

Synthesized metal/CNT catalysts were also characterized by XRD technique, TEM and energy dispersive X-ray fluorescence spectrometry (XRF-EDX)

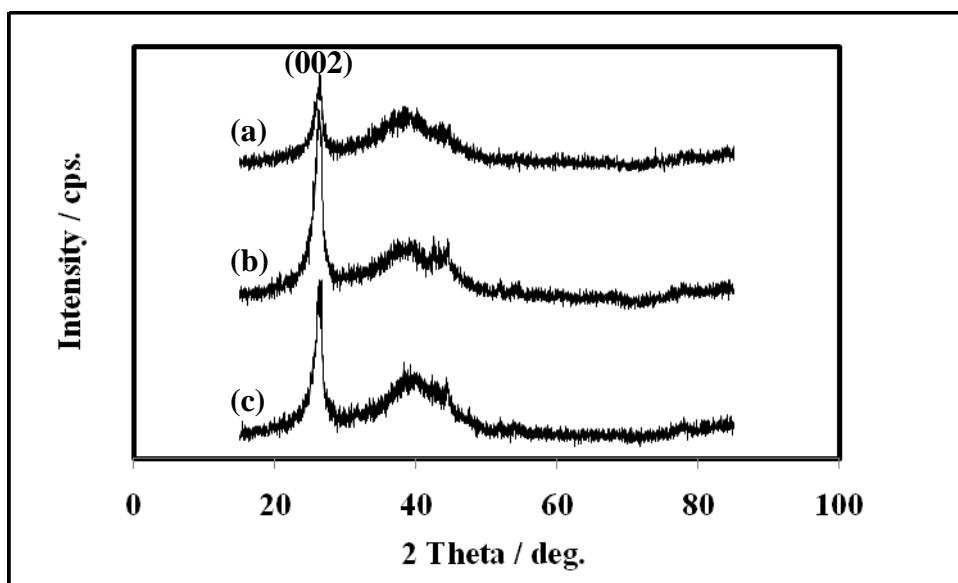
### 4.2.1 X-Ray Diffraction Analysis



**Figure 4.4** XRD patterns of (a) Pt/CNT, (b) PtRu/CNT (2:1), (c) PtRu/CNT (2:1.25), (d) PtRu/CNT (2:1.5), (e) PtRu/CNT (2:2), and (f) PtRu/CNT (2:4).

Fig. 4.4 shows XRD patterns of Pt/CNT and PtRu/CNT catalysts with various Pt:Ru mole ratios. For Pt/CNT and all PtRu/CNTs, the typical peak for (002) plane of CNT was observed. The XRD peaks at 39.7, 46.2, 67.4, and 81.2 degrees correspond to (111), (200), (220), and (311) crystalline planes of the face-centered cubic (fcc) structure of Pt, confirming the successful deposition of Pt on CNT. Similar to previous literatures [6,41], all of the PtRu/CNT catalysts displayed no

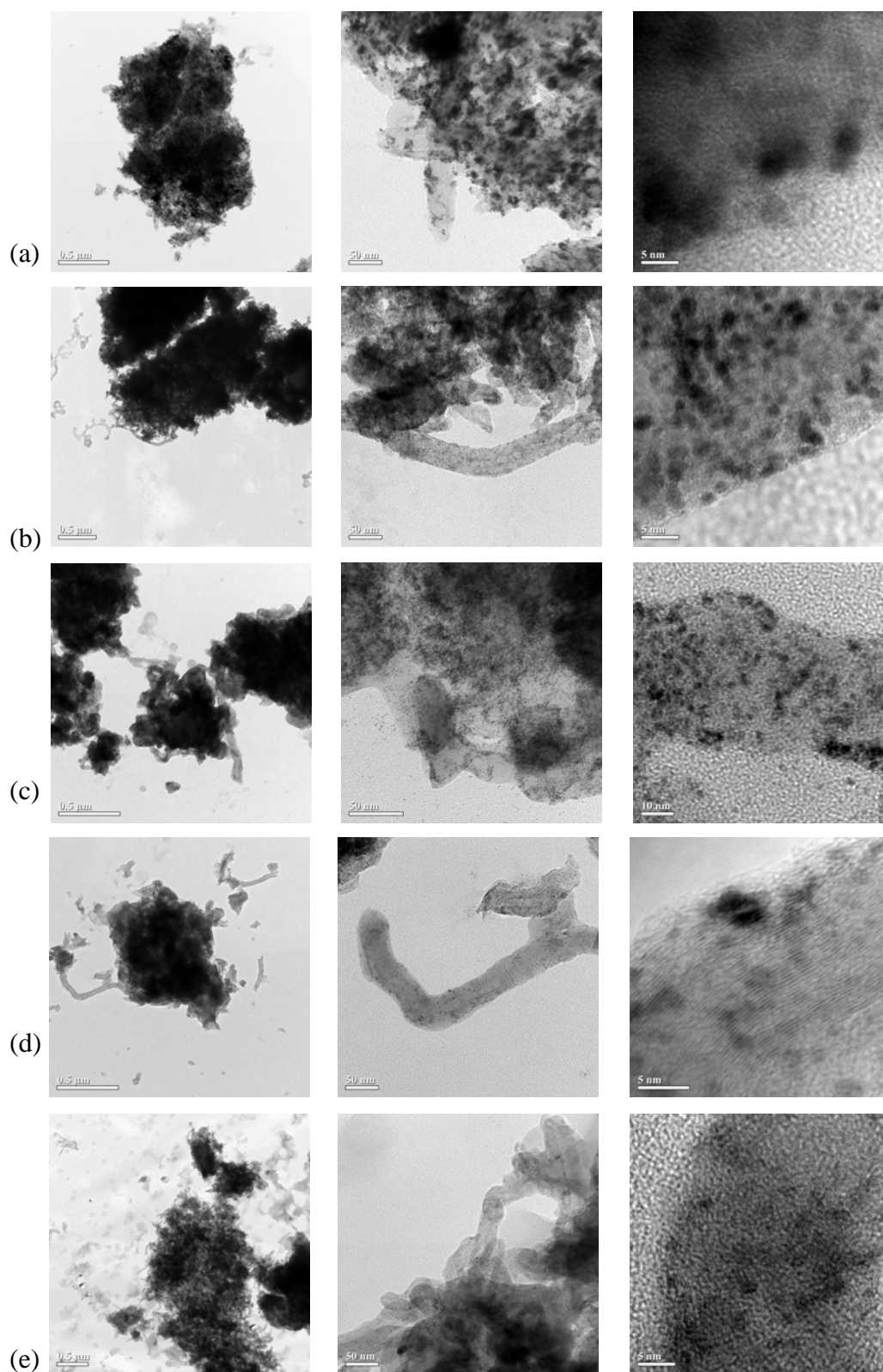
diffraction peak of Ru. The broadening diffraction peak suggests that catalysts had small crystal size [6].



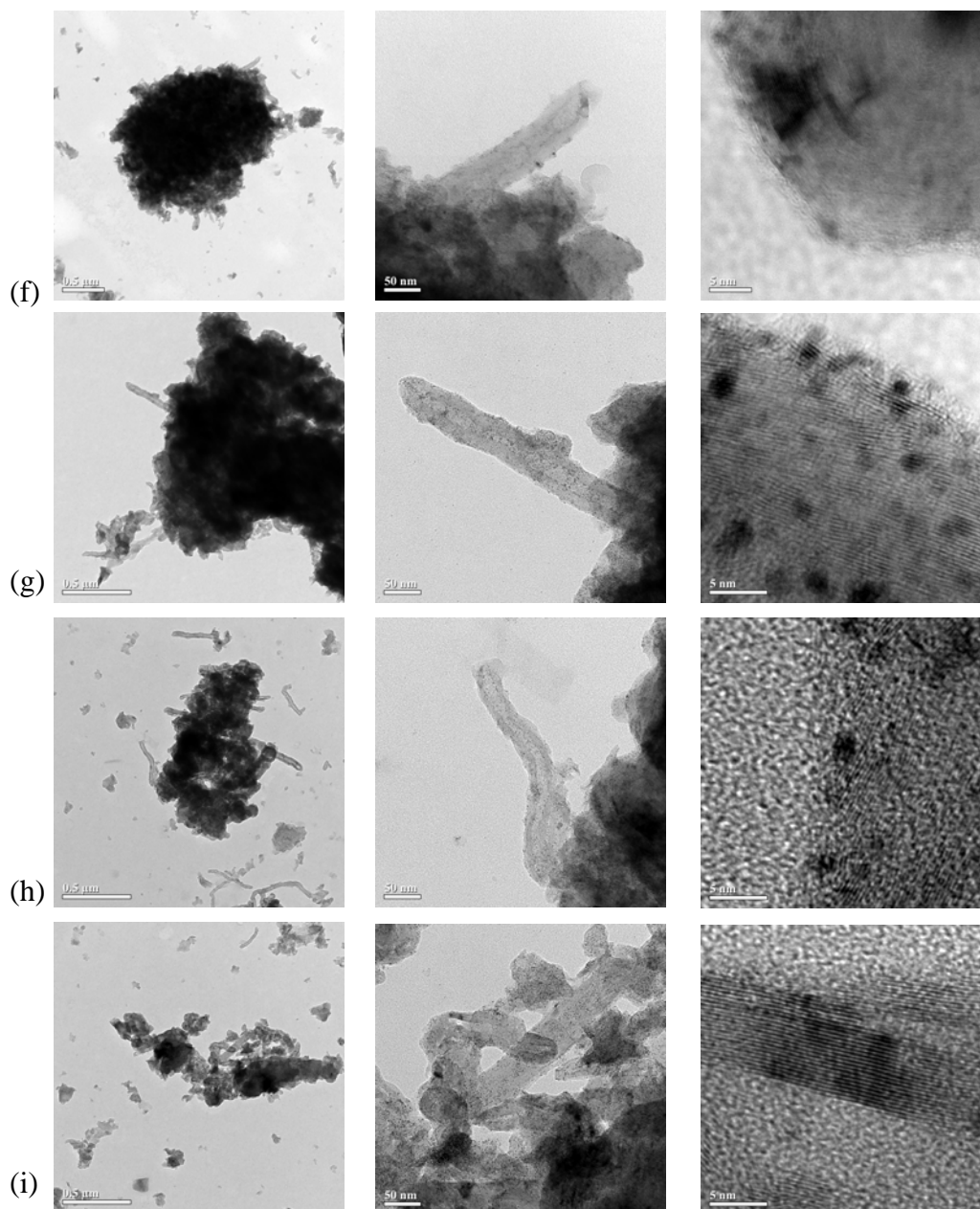
**Figure 4.5** XRD patterns of (a) PtRuCr/CNT (2:0.5:1), (b) PtRuMo/CNT (2:1:0.5), and (c) PtRuNi/CNT (2:1:0.5).

Fig. 4.5 shows the XRD patterns of PtRuCr/CNT (2:0.5:1), PtRuMo/CNT (2:1:0.5), and PtRuNi/CNT (2:1:0.5) catalysts. No diffraction peak for Ru or the third metal (Cr, Mo, or Ni) was observed, indicating that well-mixed PtRuCr, PtRuMo, and PtRuNi alloy catalysts were formed [38] with the small particles beyond the detection limit of XRD.

## 4.2.2 Transmission Electron Microscopic Analysis







**Figure 4.6** TEM images of (a) Pt/CNT, (b) PtRu/CNT (2:1), (c) PtRu/CNT (2:1.25), (d) PtRu/CNT (2:1.5), (e) PtRu/CNT (2:2), (f) PtRu/CNT (2:4), (g) PtRuCr/CNT (2:0.5:1), (h) PtRuMo/CNT (2:1:0.5), and (i) PtRuNi/CNT (2:1:0.5) with the magnification power of 6,000, 50,000, and 800,000.

TEM images of Pt/CNT, PtRu/CNT (2:1), PtRu/CNT (2:1.25), PtRu/CNT (2:1.5), PtRu/CNT (2:2), PtRu/CNT (2:4), PtRuCr/CNT (2:0.5:1), PtRuMo/CNT (2:1:0.5), and PtRuNi/CNT (2:1:0.5) catalysts are displayed in Fig. 4.6. It can be seen that small metal particles distributed uniformly on the surface of CNT despite the high metal loading. Well dispersion of the metal/CNT catalysts without

further agglomeration was observed for all catalysts. The average size of the metal/CNT catalysts is approximately 2.5 nm.

### 4.2.3 Energy Dispersive X-ray Fluorescence Spectrometric Analysis

XRF-EDX measurement was used to analyze the actual composition of the catalysts. Table 4.1 displays chemical composition of Pt/CNT and PtRu/CNT catalysts. It is evident that both Pt and Ru are presented on the CNT support, indicating that the  $\text{H}_2\text{PtCl}_6 \cdot 6\text{H}_2\text{O}$  and  $\text{RuCl}_3 \cdot x\text{H}_2\text{O}$  precursors can be reduced to their respective metal phases by  $\text{HO}(\text{CH}_2)_2\text{OH}$ . Moreover, the amount of Pt on CNT was decreased when the moles of Ru were increased. This might be because CNT had limited active sites so that the increasing Ru blocked Pt from the CNT active sites. It is likely that, due to the limited active sites of CNT, the percentage of weight (wt. %) of Pt/CNT and PtRu/CNT catalysts were unequal with the real amount adding in synthesis.

**Table 4.1** Percentage of weight (wt. %) for Pt/CNT and PtRu/CNT catalysts

Mole Ratio of PtRu/CNT	wt. % of Pt	wt. % of Ru	wt. % of CNT
2:0	23.09	-	76.91
2:1	35.19	6.95	57.86
2:1.25	19.33	4.54	76.13
2:1.5	16.67	2.78	80.55
2:2	10.50	3.90	85.60
2:4	9.58	8.13	82.29

Shown in Table 4.2, the chemical composition of PtRuCr/CNT, PtRuMoCNT, and PtRuNi/CNT confirmed the presence of corresponding metals on the CNT support, indicating that the  $\text{H}_2\text{PtCl}_6 \cdot 6\text{H}_2\text{O}$ ,  $\text{RuCl}_3 \cdot x\text{H}_2\text{O}$ ,  $\text{Cr}(\text{NO}_3)_3 \cdot 9\text{H}_2\text{O}$ ,  $\text{MoCl}_5$ , and  $\text{Ni}(\text{NO}_3)_2 \cdot 6\text{H}_2\text{O}$  precursors can be reduced to their respective metals by  $\text{HO}(\text{CH}_2)_2\text{OH}$ . In addition, wt. % for PtRuCr/CNT, PtRuMoCNT, and PtRuNi/CNT

catalysts were unequal with actual amount added in the synthesis since each metal had different ability of reduction and deposition.

**Table 4.2** Percentage of weight (wt. %) for PtRuM/CNT (M = Cr, Mo, and Ni)

Mole Ratio of PtRuM/CNT	wt. % of Pt	wt. % of Ru	wt. % of M	wt. % of CNT
2:0.5:1(Cr)	22.31	3.08	1.22	73.39
2:1:0.5 (Mo)	20.06	3.44	0.29	76.21
2:1:0.5(Ni)	32.41	4.95	1.22	61.42

### 4.3 CNT Modified Glassy Carbon (CNT/GC) Electrode

#### 4.3.1 Background Current

Background current for the CNT/GC electrode was studied by using cyclic voltammetry. Cyclic voltammograms of the bare GC electrode and the CNT/GC electrode in 0.5 M H<sub>2</sub>SO<sub>4</sub> solution scanned from -0.1 to 1.2 V at the sweep rate 50 mV·s<sup>-1</sup> are displayed in Fig. 4.7. It can be observed that the CNT/GC electrode exhibited higher background current than the bare GC electrode implying that the modified CNT can change the electrical properties of the GC electrode. Note that all the potentials in the thesis correspond to Ag/AgCl reference electrode and all cyclic voltammogram were firstly scanned in the positive direction.

#### 4.3.2 Methanol Oxidation by CNT Modified Glassy Carbon Electrode

CNT/GC electrode was used to record the methanol oxidation. Fig. 4.8 shows cyclic voltammogram for 1.0 M methanol in H<sub>2</sub>SO<sub>4</sub> solution recorded with CNT/GC electrode from -0.1 to 1.2 V at the scan rate 50 mV·s<sup>-1</sup>. No anodic peak for methanol oxidation was observed. In addition, there was a pair of broad redox peaks present at +0.30 and +0.38 V correlating with surface-oxygen containing groups such as carboxyl and carbonyl groups on the CNT defect sites [37]. Since cyclic voltammetric result revealed that CNT cannot be used to catalyze methanol oxidation, CNT was only used as a supporting material for metal catalysts in order to improve the catalyst performance for methanol oxidation.

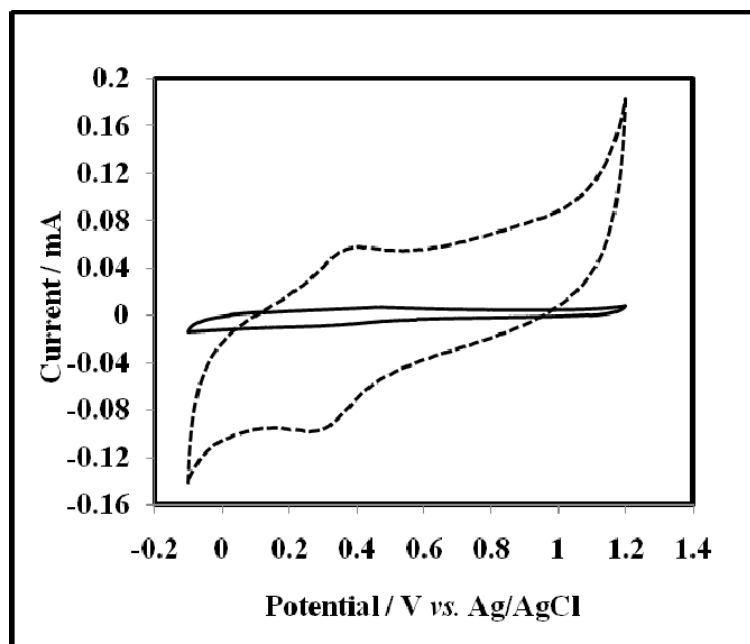


**Figure 4.7** Cyclic voltammograms for 0.5 M  $\text{H}_2\text{SO}_4$  recorded with GC electrode (solid line) and CNT/GC electrode (dash line) at the scan rate of  $50 \text{ mV}\cdot\text{s}^{-1}$ .

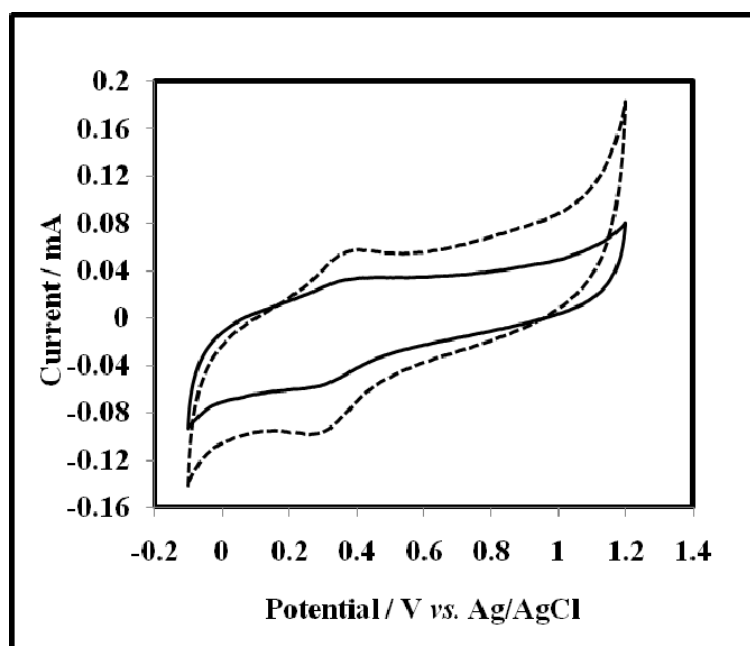


**Figure 4.8** Cyclic voltammograms for in 0.5 M  $\text{H}_2\text{SO}_4$  solution recorded with CNT/GC electrode in absence (solid line) and presence (dash line) of 1.0 M methanol at the scan rate of  $50 \text{ mV}\cdot\text{s}^{-1}$ .

#### 4.4 Pt/CNT Modified Glassy Carbon Electrode

Since it is well known that Pt has high activity for methanol oxidation and has been used as an anode catalyst for DMFC. We firstly synthesized Pt supported on CNT by polyol process as a reference catalyst for methanol oxidation.

##### 4.4.1 Background Current

Background cyclic voltammogram for the Pt/CNT modified GC electrode (Pt/CNT/GC) is presented in Fig. 4.9. Cyclic voltammogram was obtained in 0.5 M H<sub>2</sub>SO<sub>4</sub> solution from -0.35 to 1.2 V and 1.2 to -0.35 V at the sweep rate of 50 mV·s<sup>-1</sup>. Cyclic voltammogram exhibits the cathodic peak for the Pt–O reduction at +0.38 V, which is the characteristic feather of Pt, and the hydrogen adsorption–desorption peaks between -0.35 and 0 V. By using the charge passed for H desorption (Q<sub>H</sub>), the surface area of Pt can be estimated from the equations below 2.4-2.5 in Chapter 2. Since the charge per unit surface area of Pt (Q<sub>H0</sub>) is 210 μC·cm<sup>-2</sup> [40], the calculated electrochemical active surface (EAS) area of Pt is 6.88 m<sup>2</sup>·(g catalyst)<sup>-1</sup> for the Pt/CNT/GC electrode.

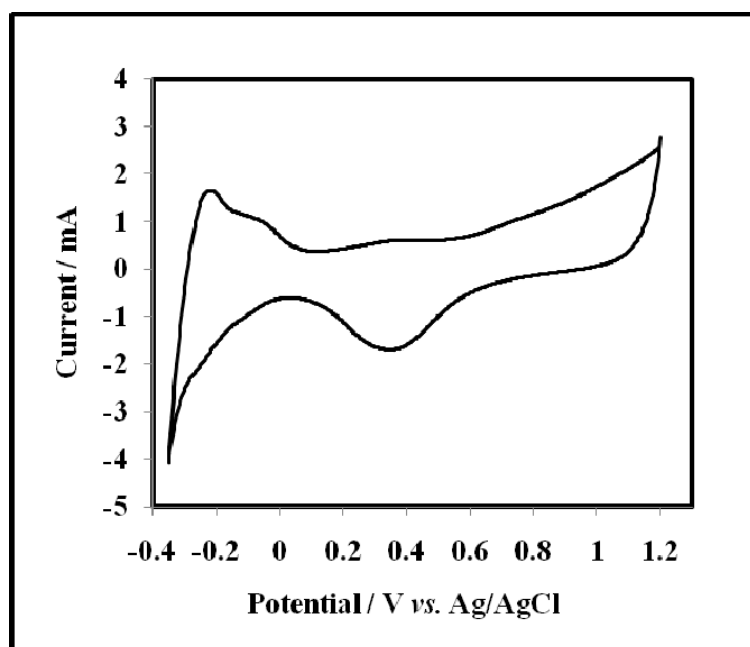


**Figure 4.9** Cyclic voltammogram for 0.5 M H<sub>2</sub>SO<sub>4</sub> solution recorded with Pt/CNT/GC electrode at the scan rate of 50 mV·s<sup>-1</sup>.

#### 4.4.2 Catalytic Activity of Pt/CNT Modified Glassy Carbon Electrode

Using cyclic voltammetry, the electrocatalytic activity of Pt/CNT/GC electrode towards methanol solution at the potential range from  $-0.1$  to  $1.2$  V was studied. The electrocatalytic activity was estimated from the anodic peak current for methanol oxidation obtained from the forward scan ( $-0.1$  to  $1.2$  V) of the third cycle where the anodic current became constant. Fig. 4.10 displays two anodic peaks, which are related to the oxidation of methanol at  $+0.68$  V in the forward scan and the oxidation of its intermediate at  $+0.37$  V in the backward scan.

The first anodic peak at  $+0.68$  V in the cyclic voltammogram represents methanol oxidation according to equations 1.4-1.7 in Chapter 1.

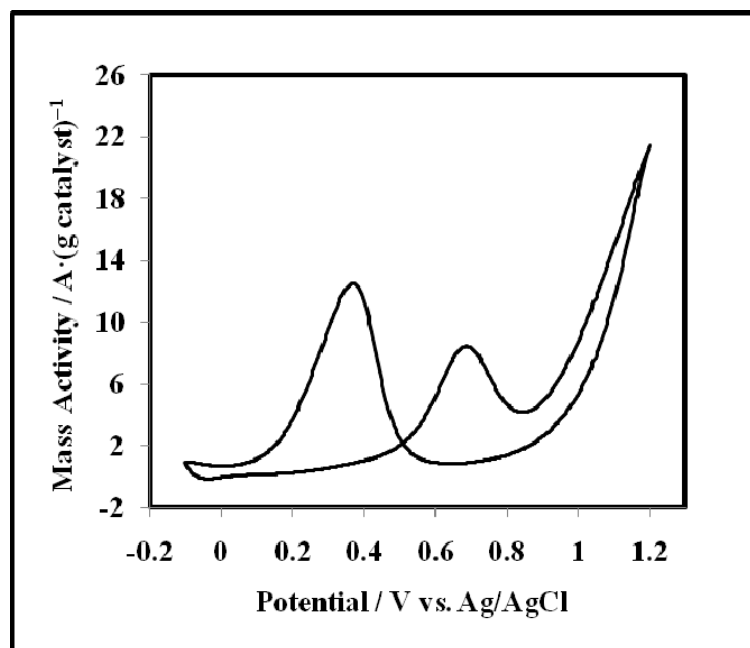
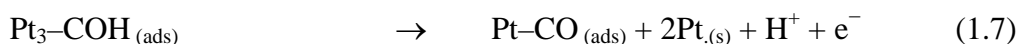
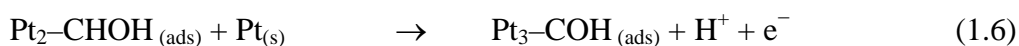
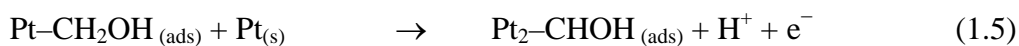
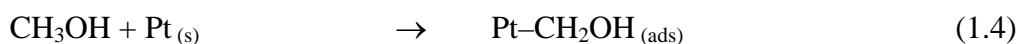


**Figure 4.10** Cyclic voltammogram for 1.0 M methanol in 0.5 M  $\text{H}_2\text{SO}_4$  solution recorded with Pt/CNT/GC electrode at the scan rate of  $50 \text{ mV}\cdot\text{s}^{-1}$ .

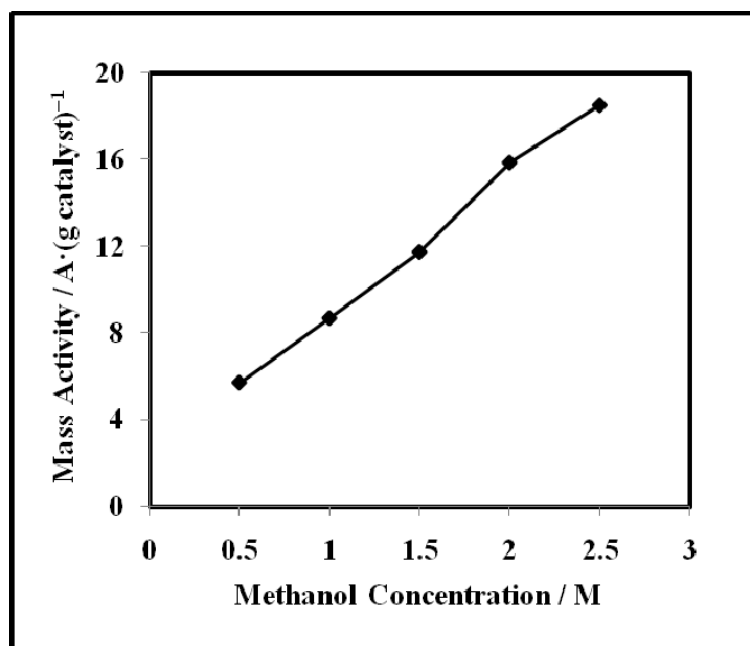


**Figure 4.11** Mass activity vs. methanol concentration curve of Pt/CNT/GC electrode recorded in 0.5 M H<sub>2</sub>SO<sub>4</sub> solution at the scan rate of 50 mV·s<sup>-1</sup>.

The second anodic peak at +0.37 V in the backward scan illustrates the re-oxidation process as shown in equation 1.9.

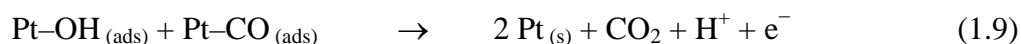


Fig. 4.11 shows mass activity of Pt/CNT/GC electrode for the oxidation of 0.5-2.5 M methanol, indicating that the Pt/CNT catalytic activity was found to be directly proportional to methanol concentration. Note that the range of methanol concentration was selected to be in the similar range with other researches [18] for comparison.

#### 4.5 Pt-Based Di-metal/CNT Modified Glassy Carbon Electrodes

Normally, Pt has high activity for methanol oxidation. However, Pt catalyst can be poisoned by the intermediate of methanol oxidation such as adsorbed Pt-CO. To minimize this poisoning, alloying Pt with oxophilic metals had been introduced. In preliminary research, eight metals, Ru, Cr, Co, Au, Fe, Mn, Mo, and Ni, were selected as Pt co-catalysts.

### 4.5.1 Background Current

Background cyclic voltammograms for the PtRu/CNT, PtCr/CNT, PtCo/CNT, PtAu/CNT, PtFe/CNT, PtMn/CNT, PtMo/CNT, and PtNi/CNT modified electrodes with Pt to metal co-catalyst ratio of 2:1.5 are shown in Fig. 4.12. The voltammogram of Pt/CNT electrode is also displayed for comparison. All voltammograms were obtained in 0.5 M H<sub>2</sub>SO<sub>4</sub> from -0.1 to 1.2 V and 1.2 to -0.1 at the sweep rate 50 mV·s<sup>-1</sup>. Fig. 4.12a displays that the cathodic peak of PtRu/CNT/GC electrode shifts positively in comparison with that of Pt/CNT electrode, due to the overlapping signals of Pt-O and Ru-O reduction. Fig. 4.11b-4.11h display the characteristic features of PtCr/CNT/GC, PtCo/CNT/GC, PtAu/CNT/GC, PtFe/CNT/GC, PtMn/CNT/GC, PtMo/CNT/GC, and PtNi/CNT/GC electrodes, respectively. The cathodic peaks of all these modified electrodes shift positively due to the potential overlapping for Pt-O reduction and the reduction of these metal oxides. Note that the PtCr/CNT/GC, PtCo/CNT/GC, PtAu/CNT/GC, PtFe/CNT/GC, PtMn/CNT/GC, PtMo/CNT/GC, and PtNi/CNT/GC electrodes show cathodic peaks at 0.15, 0.24, 0.35, 0.23, 0.23, 0.33, and 0.23 V, respectively.



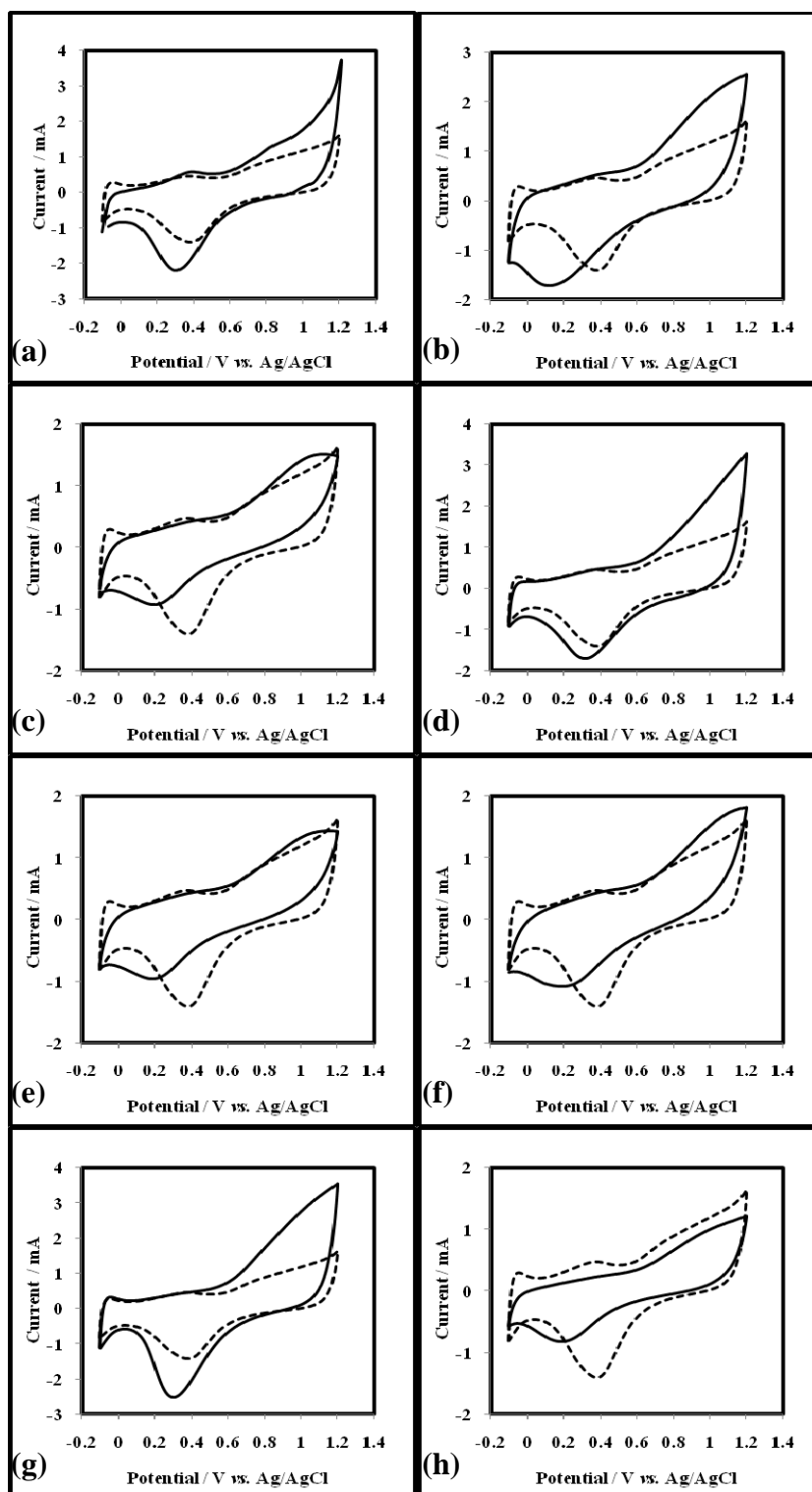


**Figure 4.12** Cyclic voltammograms for 0.5 M  $\text{H}_2\text{SO}_4$  solution recorded by Pt/CNT/GC electrode (solid lines) in comparison with (a) PtRu/CNT/GC, (b) PtCr/CNT/GC, (c) PtCo/CNT/GC, (d) PtAu/CNT/GC, (e) PtFe/CNT/GC, (f) PtMn/CNT/GC, (g) PtMo/CNT/GC, and (h) PtNi/CNT/GC electrodes (dash lines) with Pt-to-co-catalyst ratio of 2:1.5 at the scan rate of  $50 \text{ mV}\cdot\text{s}^{-1}$ .

#### 4.5.2 Catalytic Activity of Pt-based Di-metal/CNT Modified Glassy Carbon Electrodes

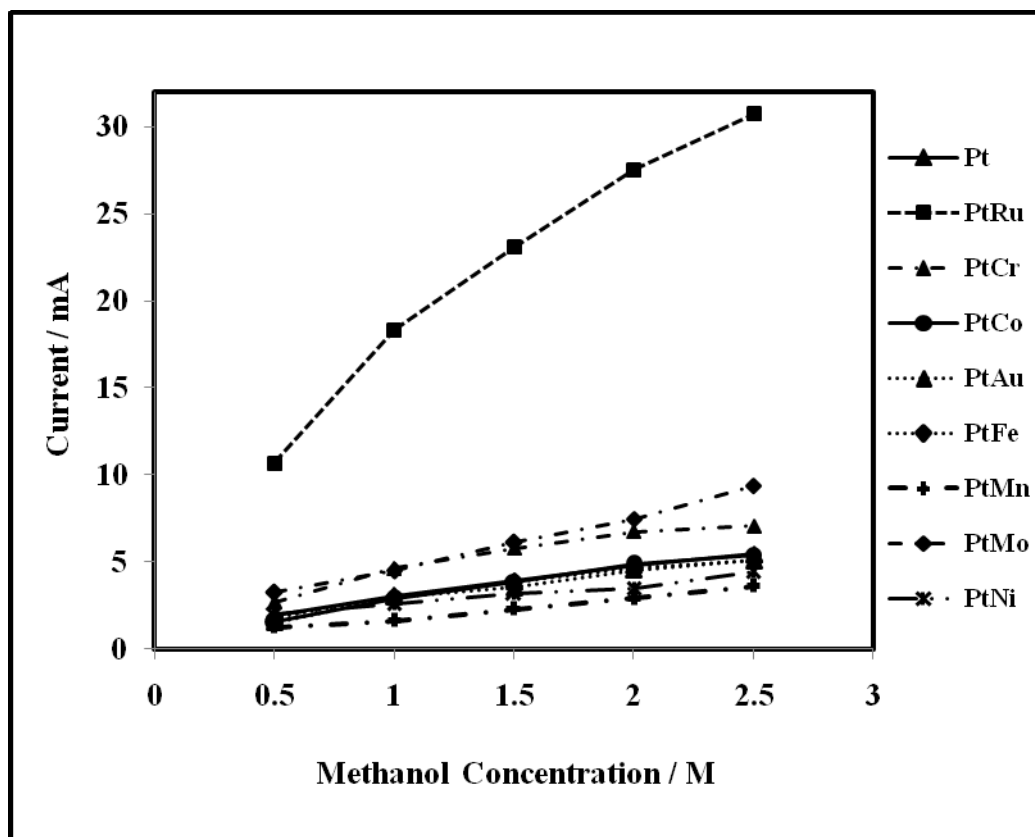


**Figure 4.13** Current vs. methanol concentration curves of Pt/CNT/GC, PtRu/CNT/GC, PtCr/CNT/GC, PtCo/CNT/GC, PtAu/CNT/GC, PtFe/CNT/GC, PtMn/CNT/GC, PtMo/CNT/GC, and PtNi/CNT/GC electrodes recorded in 0.5 M  $\text{H}_2\text{SO}_4$  at the scan rate of  $50 \text{ mV}\cdot\text{s}^{-1}$ .

Fig. 4.13 shows current for the oxidation of 0.5-2.5 M methanol recorded with Pt/CNT/GC, PtRu/CNT/GC, PtCr/CNT/GC, PtCo/CNT/GC, PtAu/CNT/GC, PtFe/CNT/GC, PtMn/CNT/GC, PtMo/CNT/GC, and PtNi/CNT/GC electrodes at the scan rate of  $50 \text{ mV}\cdot\text{s}^{-1}$ . The results demonstrate that the PtRu/CNT/GC, PtCr/CNT/GC, and PtMo/CNT/GC electrodes give higher anodic current for methanol oxidation than the remaining electrodes. For this reason, PtRu/CNT, PtCr/CNT, and PtMo/CNT catalysts were then prepared with the following Pt to co-catalyst ratios: 2:1, 2:1.25, and 2:2. Note that only PtRu/CNT catalyst with 2:4 Pt-to-Ru was also prepared to see the effects of excess amount of co-catalyst on the Pt catalytic activity.

#### 4.5.2.1 PtRu/CNT Modified Glassy Carbon Electrodes

In the order to optimize the mole ratio between Pt and Ru, the PtRu/CNT/GC electrodes with 2:1, 2:1.25, 2:1.5, 2:2, and 2:4 Pt-to-Ru ratios were used as working electrodes for methanol oxidation in cyclic voltammetric measurement. Using the potential range from  $-0.1$  to  $1.2$  V at the scan rate of  $50 \text{ mV}\cdot\text{s}^{-1}$ , the mass activity of PtRu/CNT/GC electrodes for methanol oxidation are shown in Fig. 4.14. The best Pt-to-Ru mole ratio for PtRu/CNT/GC electrodes was 2:1.5. The electrode with 2:1.5 Pt-to-Ru ratio gave the anodic mass activity of  $62.1 \text{ A}\cdot(\text{g catalyst})^{-1}$  for  $1.0 \text{ M}$  methanol in  $0.5 \text{ M H}_2\text{SO}_4$  solution (curve c). The value is 5.74 times higher than the mass activity of the Pt/CNT/GC electrode for  $1.0 \text{ M}$  methanol. In case of curves a, b, and d, adding Ru in the catalyst improved the performance of Pt/CNT catalyst, causing except when Ru was added more than Pt (curve e), the catalytic activity for methanol oxidation decreased quickly to be lower than that of Pt/CNT/GC electrode.

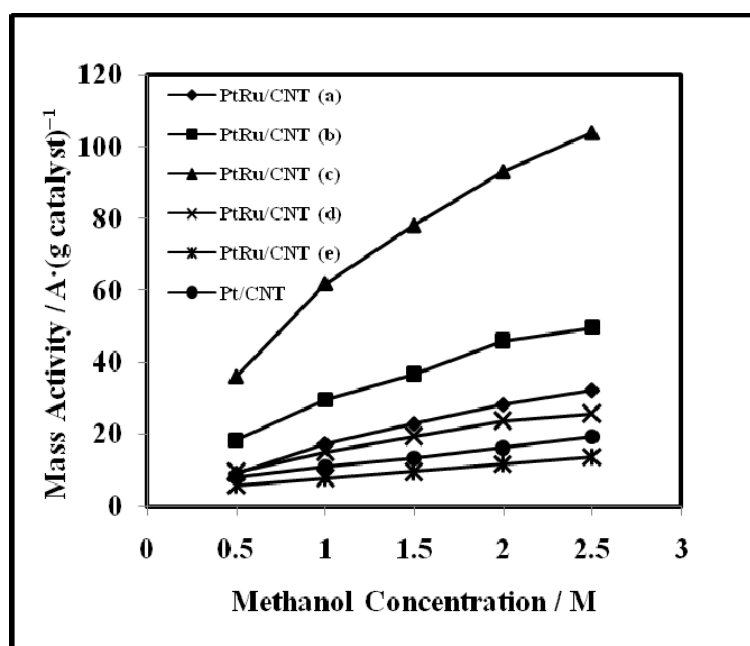


**Figure 4.14** Mass activity vs. methanol concentration curves of Pt/CNT/GC and PtRu/CNT/GC electrodes with (a) 2:1, (b) 2:1.25, (c) 2:1.5, (d) 2:2, and (e) 2:4 Pt-to-Ru mole ratios recorded in  $0.5 \text{ M H}_2\text{SO}_4$  at the scan rate of  $50 \text{ mV}\cdot\text{s}^{-1}$ .

#### 4.5.2.2 PtCr/CNT Modified Glassy Carbon Electrodes

Fig. 4.15 compares the mass activity of PtCr/CNT/GC electrodes at different Pt-to-Cr ratios for the oxidation of 0.5-2.5 M methanol. These results were obtained from cyclic voltammetric experiment scanned from  $-0.1$  to  $1.2$  V at the scan rate of  $50 \text{ mV}\cdot\text{s}^{-1}$ . Among the PtCr/CNT/GC electrodes, the optimal Pt-to-Cr mole ratio was 2:1, giving the PtCr/CNT/GC electrode with the anodic current of  $7.13 \text{ mA}$  for  $1.0 \text{ M}$  methanol (curve a). This value is 2.3 times higher than that of the Pt/CNT/GC electrode. In addition, the PtCr/CNT/GC electrodes with 2:1 (curve a) and 2:1.25 (curve b) Pt-to-Cr ratios had similar activity for methanol oxidation. Curves c and d reveal that too much Cr in the PtCr/CNT catalyst, can dramatically decrease the activity of the electrodes towards methanol oxidation. However, all of the PtCr/CNT/GC electrodes exhibited higher activity for the oxidation than the Pt/CNT/GC electrode.

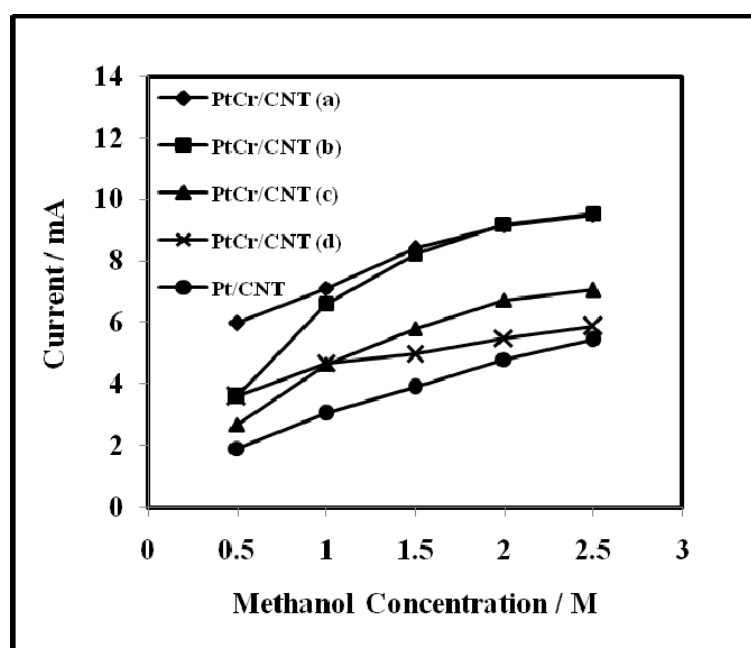


**Figure 4.15** Current vs. methanol concentration curves of Pt/CNT/GC and PtCr/CNT/GC electrodes with (a) 2:1, (b) 2:1.25, (c) 2:1.5, and (d) 2:2 Pt-to-Cr mole ratios recorded in  $0.5 \text{ M H}_2\text{SO}_4$  at the scan rate of  $50 \text{ mV}\cdot\text{s}^{-1}$ .

### 4.5.2.3 PtMo/CNT Modified Glassy Carbon Electrodes

To find the best Pt-to-Mo mole ratio, the PtMo/CNT/GC electrodes with 2:1, 2:1.25, 2:1.5, and 2:2 Pt-to-Mo ratios were used as working electrodes to probe the methanol oxidation by means of cyclic voltammetry. Using the potential range from  $-0.1$  to  $1.2$  V at the scan rate  $50 \text{ mV}\cdot\text{s}^{-1}$ , the mass activity of PtMo/CNT/GC electrodes at various Pt-to-Mo mole ratios for  $0.5$ - $2.5$  M methanol is displayed in Fig. 4.16. It was found that 2:1.5 was the best Pt-to-Mo mole ratio for PtMo/CNT/GC electrode. This electrode gave the anodic current of  $4.5$  mA for the oxidation of  $1.0$  M methanol in  $0.5$  M  $\text{H}_2\text{SO}_4$  solution (curve c). Compared with the Pt/CNT/GC electrode, all of the Pt/Mo/CNT/GC electrodes except the PtMo/CNT/GC with 2:1 Pt-to-Mo ratio (curve a) gave higher current for methanol oxidation.

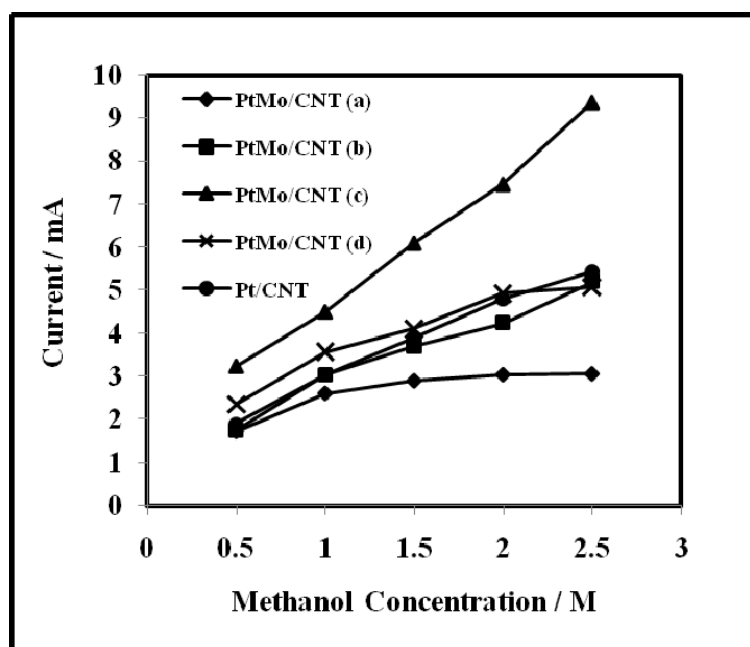


**Figure 4.16** Current vs. methanol concentration curves of Pt/CNT/GC electrode and PtMo/CNT/GC electrodes with (a) 2:1, (b) 2:1.25, (c) 2:1.5, and (d) 2:2 Pt-to-Mo mole ratios recorded in  $0.5$  M  $\text{H}_2\text{SO}_4$  at the scan rate of  $50 \text{ mV}\cdot\text{s}^{-1}$ .

The results of di-metallic electrodes displayed that the 2:1.5 PtRu/CNT catalyst had the highest catalytic activity than the optimized PtCr/CNT and PtMo/CNT catalysts. In addition, under similar conditions, our PtRu/CNT/GC electrode provided 5 times higher current density for methanol oxidation than the PtRu/MWNT/GC electrode prepared by pyrolysis process [41]. Moreover, the prepared PtRu/CNT/GC electrode exhibited 19.6, 15.3, and 12.2 times higher mass activity than the PtFe/CNT, PtNi/CNT, and PtCo/CNT electrodes reported in the literatures elsewhere [42].

#### 4.6 Pt-based Tri-Metal/CNT Modified Glassy Carbon Electrodes

Results from the previous section have shown that proper di-metallic catalysts supported on CNT could efficiently be able to catalyze the oxidation of methanol. To improve the electrocatalytic activity of the Pt-based di-metal catalysts supported on CNT, the third metal was added. The PtRu/CNT catalyst had the highest catalytic activity than other Pt-based di-metal catalysts; therefore, Ru was selected as the first co-catalyst. In this section, three metals, Cr, Mo, and Ni were selected as the second co-catalysts because Cr and Mo gave comparatively high anodic current for methanol oxidation. Although PtNi/CNT showed poor catalytic performance for methanol oxidation, Ni was yet chosen to be one of the second co-catalysts to see whether it might be able to promote the activity of PtRu/CNT system.

##### 4.6.1 Background Current

Background cyclic voltammograms for the PtRuCr/CNT, PtRuMo/CNT, and PtRuNi/CNT modified GC electrodes with Pt-to-Ru-to-third metal mole ratio of 2:1:0.5 are shown in Fig. 4.17. Cyclic voltammograms were obtained in 0.5 M H<sub>2</sub>SO<sub>4</sub> from -0.1 to 1.2 V and 1.2 to -0.1 at the sweep rate 50 mV·s<sup>-1</sup>. The PtRuCr/CNT/GC electrode exhibited the cathodic peak at 0.27 V corresponding to the overlapping of Pt-O, Ru-O, and Cr-O reduction, as shown in Fig. 4.17a (solid line). Fig. 4.17b shows cyclic voltammogram of PtRuMo/CNT/GC electrode (solid line) having the cathodic peak at 0.29 V for the overlapping signals of Pt-O, Ru-O, and Mo-O reduction. The background current of PtRuCr/CNT/GC and PtRuMo/CNT/GC electrodes demonstrate higher current than that of the PtRu/CNT/GC electrode (dash lines). Fig. 4.17c displays the reduction peak of PtRuNi/CNT/GC electrode at 0.29 V.

The peak consists of Pt–O, Ru–O, and Ni–O reduction. Characteristic features of the background current of PtRuCr/CNT/GC, PtRuMo/CNT/GC, and PtRuNi/CNT/GC electrodes seem to be similar to that of PtRu/CNT/GC electrode.

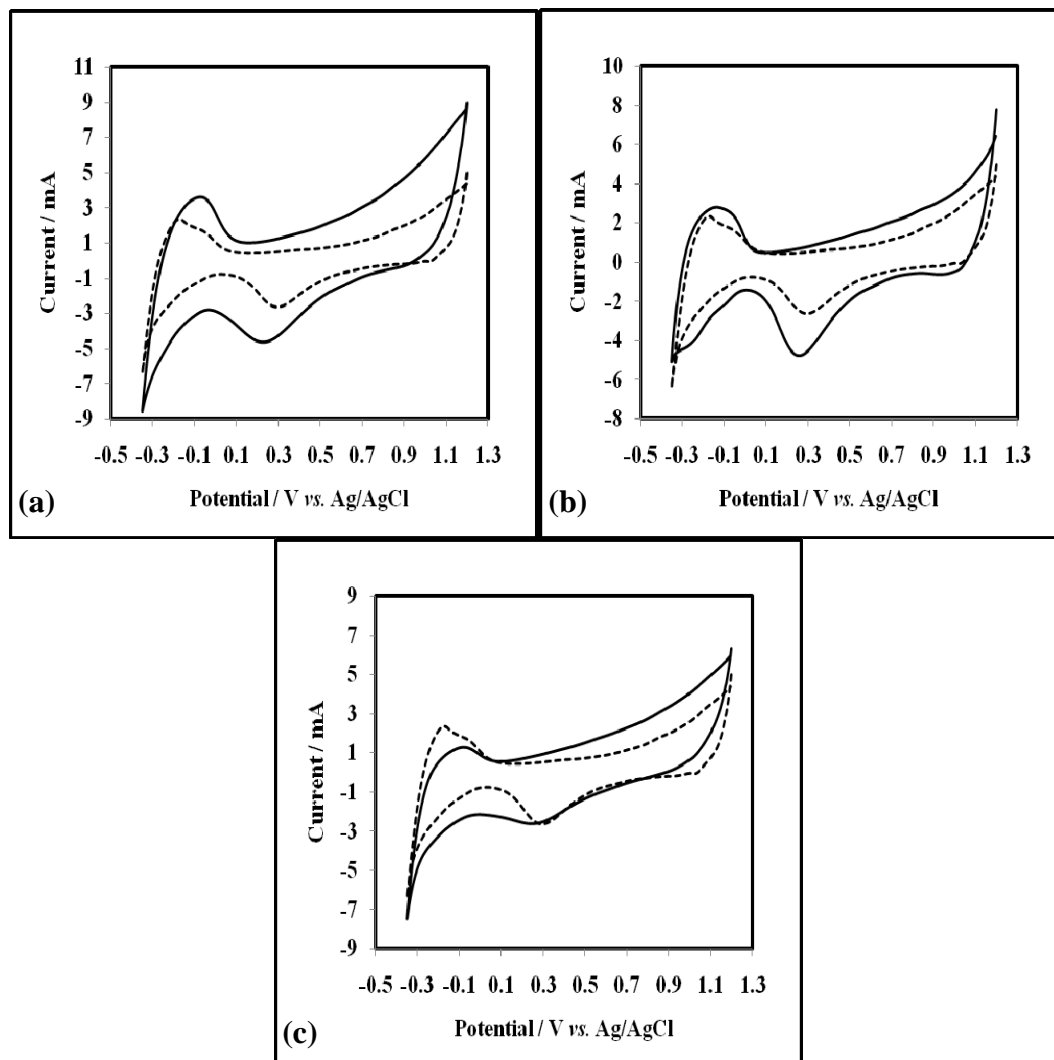


**Figure 4.17** Cyclic voltammograms for 0.5 M H<sub>2</sub>SO<sub>4</sub> solution recorded at the scan rate of 50 mV·s<sup>-1</sup> by PtRu/CNT/GC electrode (dash lines) and (a) PtRuCr/CNT/GC, (b) PtRuMo/CNT/GC, and (c) PtRuNi/CNT/GC electrodes with Pt-to-Ru-to-the third metal mole ratio of 2:1:0.5 (solid lines).

## 4.6.2 Catalytic Activity of Tri-metal/CNT Modified Glassy Carbon Electrodes

### 4.6.2.1 PtRuCr/CNT Modified Glassy Carbon Electrodes

Shown in Fig. 4.18, the mass activity for methanol oxidation of PtRuCr/CNT/GC electrodes with the following Pt-to-Ru-to-Cr mole ratios: 2:1:0.5, 2:0.5:1, and 2:0.75:0.75 are displayed in comparison with that of PtRu/CNT/GC. Only PtRuCr/CNT/GC electrode with 2:0.5:1 Pt-to-Ru-to-Cr ratio (curve b) gave higher mass activity than the optimized PtRu/CNT/GC electrode and this electrode produced  $71.1 \text{ A}\cdot(\text{g catalyst})^{-1}$  for 1.0 M methanol. The activity for methanol oxidation of the PtRuCr/CNT/GC electrode was 1.15 times higher than that of the optimized PtRu/CNT/GC electrode.

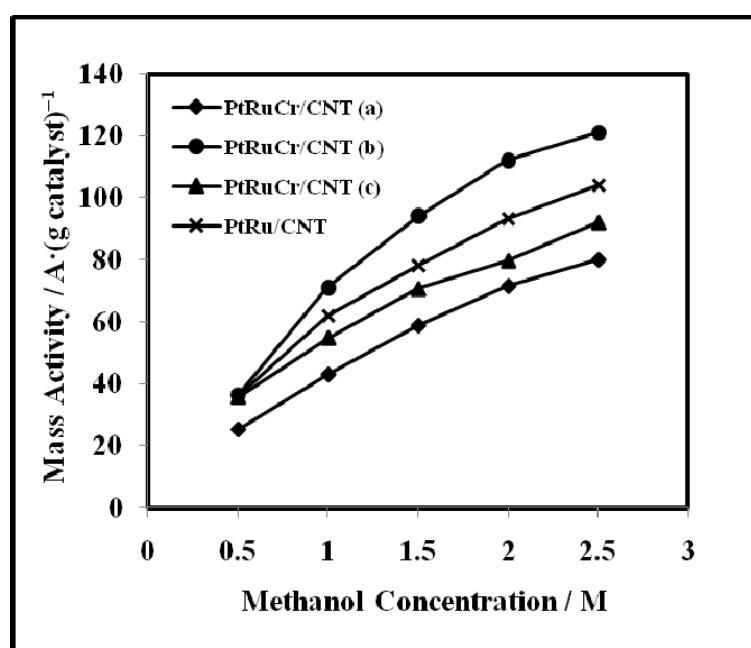


**Figure 4.18** Mass activity vs. methanol concentration curves of PtRu/CNT/GC electrode with Pt-to-Ru mole ratio of 2:1.5 and PtRuCr/CNT/GC electrodes with Pt-to-Ru-to-Cr mole ratios of (a) 2:1:0.5, (b) 2:0.5:1, and (c) 2:0.75:0.75 recorded in 0.5 M  $\text{H}_2\text{SO}_4$  at the scan rate of  $50 \text{ mV}\cdot\text{s}^{-1}$ .



#### 4.6.2.2 PtRuMo/CNT Modified Glassy Carbon Electrodes

Fig. 4.19 shows mass activity for methanol oxidation recorded with PtRuMo/CNT/GC electrodes in comparison with that of PtRu/CNT/GC (2:1.5) electrode. The PtRuMo/CNT/GC electrode with 2:1:0.5 Pt-to-Ru-to-Mo ratio (curve a) showed the best performance for methanol oxidation. The mass activity for 1.0 M methanol in 0.5 M H<sub>2</sub>SO<sub>4</sub> solution were 77.5, 53.3, and 59.6 A·(g catalyst)<sup>-1</sup> for the PtRuMo/CNT/GC electrodes with 2:1:0.5, 2:0.5:1, and 2:0.75:0.75 Pt-to-Ru-to-Mo mole ratios, respectively. In addition, the 2:0.5:1 and 2:0.75:0.75 PtRuMo/CNT/GC electrodes (curves b and c) gave similar mass activity as the 2:1.5 PtRu/CNT electrode.

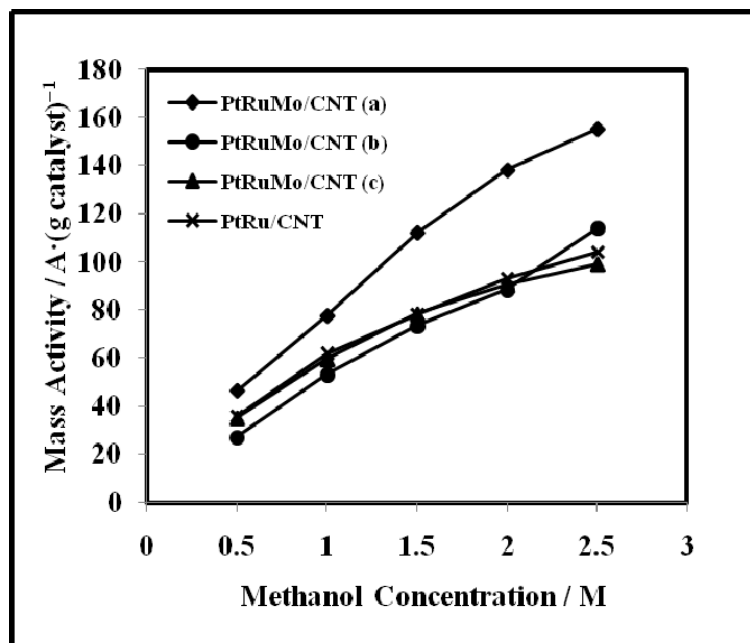


**Figure 4.19** Mass activity vs. methanol concentration curves of PtRu/CNT/GC electrode with Pt-to-Ru mole ratio of 2:1.5 and PtRuMo/CNT/GC electrodes with Pt-to-Ru-to-Mo mole ratios of (a) 2:1:0.5, (b) 2:0.5:1, and (c) 2:0.75:0.75 recorded in 0.5 M H<sub>2</sub>SO<sub>4</sub> at the scan rate of 50 mV·s<sup>-1</sup>.

#### 4.6.2.3 PtRuNi/CNT Modified Glassy Carbon Electrodes

Fig. 4.20 displays results from PtRuNi/CNT/GC electrodes. Unfortunately, the activity of PtRuNi/CNT/GC electrodes for methanol oxidation was worse than the PtRu/CNT/GC electrode, suggesting that Ni cannot improve the performance of PtRu/CNT/GC electrode because Ni stays typically at lower positive oxidation states such as +1 and +2, making Ni–OH, an intermediate that promotes CO desorption, less preferable. Therefore, Ni is not suitable to serve as a co-metal of PtRu catalyst for methanol oxidation.

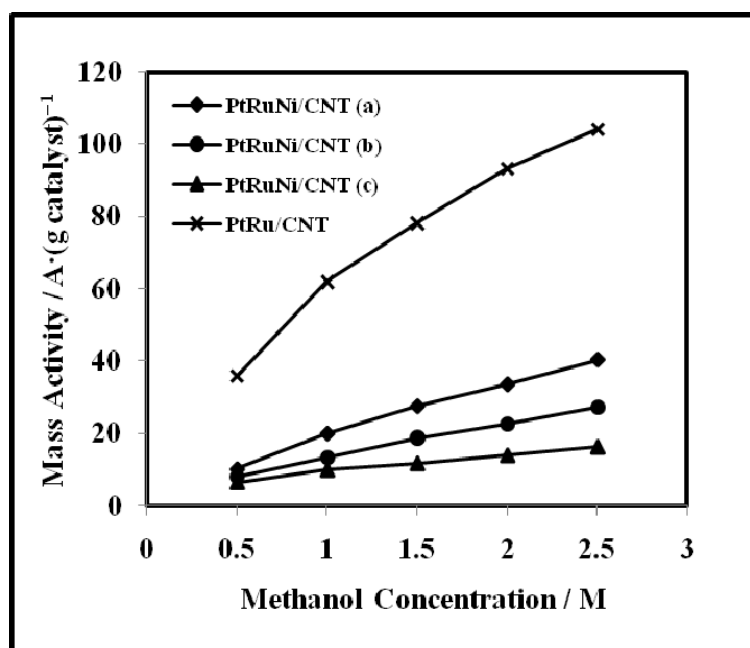


**Figure 4.20** Mass activity vs. methanol concentration curves of PtRu/CNT/GC electrode with Pt-to-Ru mole ratio of 2:1.5 and PtRuNi/CNT/GC electrodes with Pt-to-Ru-to-Mo mole ratios of (a) 2:1:0.5, (b) 2:0.5:1, and (c) 2:0.75:0.75 recorded in 0.5 M H<sub>2</sub>SO<sub>4</sub> at the scan rate of 50 mV·s<sup>-1</sup>.

In summary, the mass activity for methanol oxidation of each optimized tri-metallic electrodes are listed in Fig. 4.21. The 2:1:0.5 PtRuMo/CNT/GC electrode gave the best electroactivity, followed by the 2:0.5:1 PtRuCr/CNT/GC and the 2:1:0.5 PtRuNi/CNT/GC electrodes in the second and third catalytic activity ranking. Moreover, it has been found that the PtRuCr/CNT/GC, PtRuMo/CNT/GC, and PtRuNi/CNT/GC electrodes prepared by our method provided 29.3, 31.9, and 8.2 times higher mass activity for methanol oxidation, respectively, than the ternary

metal/C/GC electrodes prepared by the reduction of  $\text{NaBH}_4$  [39]. Furthermore, the 2:1:0.5 PtRuMo/CNT catalyst gave 5.5 times higher mass activity than the thin porous layer of PtRuMo nano-catalyst supported on carbon black [43].

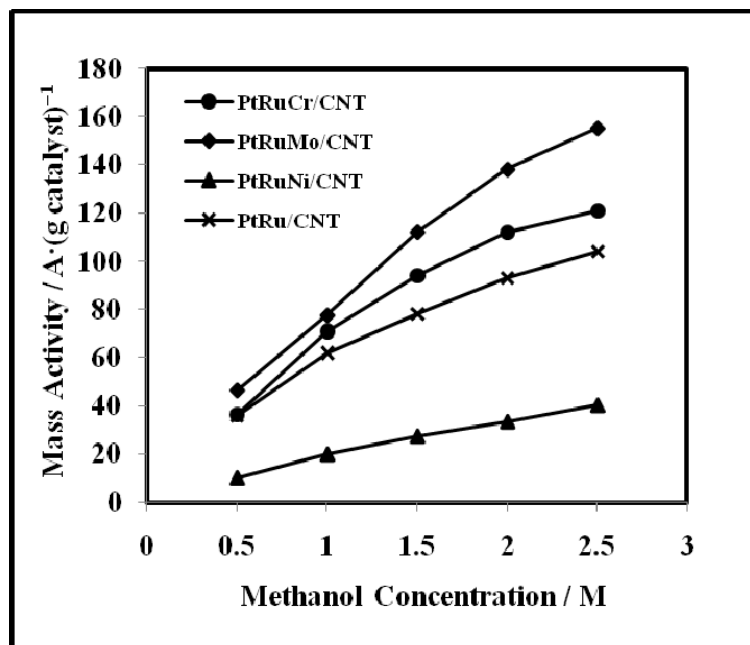


**Figure 4.21** Mass activity vs. methanol concentration curves of the optimized PtRu/CNT/GC, PtRuCr/CNT/GC, PtRuMo/CNT/GC, and PtRuNi/CNT/GC electrodes recorded in 0.5 M  $\text{H}_2\text{SO}_4$  at the scan rate of  $50 \text{ mV} \cdot \text{s}^{-1}$ .

#### 4.7 Effect of Methanol Concentration

Using PtRu/CNT/GC, PtRuCr/CNT/GC, and PtRuMo/CNT/GC as promising candidates of the metal/CNT modified electrodes, cyclic voltammetry was used to study the influence of methanol concentration towards the electrocatalytic activity of the metal/CNT catalysts for methanol oxidation. At first, methanol was gradually added into 0.5 M  $\text{H}_2\text{SO}_4$  solution while the mass activity of the chosen electrode for methanol oxidation was tested. Fig. 4.22 displays the mass activity of the optimized PtRu/CNT/GC, PtRuCr/CNT/GC, and PtRuMo/CNT/GC electrodes at various concentration of methanol. At 4.0 M methanol, all the modified GC electrodes reached the maximum activity towards methanol. After that, the activity of the modified electrodes held down and decayed. The optimized PtRu/CNT/GC, PtRuCr/CNT/GC, and PtRuMo/CNT/GC electrodes gave mass activity of 123.99,

150.62, and 170.17  $\text{A}\cdot(\text{g catalyst})^{-1}$  respectively, for 4.0 M methanol. Possibly, the excess quantity of methanol in the system might inhibit the catalyst active site on the electrode surface for methanol oxidation, causing the decrease in the mass activity with methanol concentration more than 4.0 M.

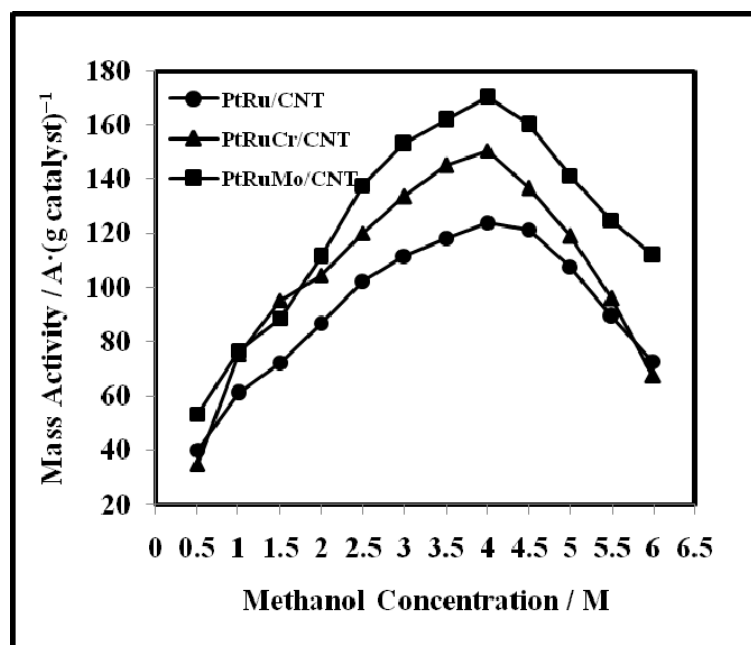


**Figure 4.22** Mass activity vs. methanol concentration curves of the optimized PtRu/CNT/GC, PtRuCr/CNT/GC, and PtRuMo/CNT/GC electrodes recorded in 0.5 M  $\text{H}_2\text{SO}_4$  at the scan rate of  $50 \text{ mV}\cdot\text{s}^{-1}$ .

Next, we tried to all at once add 4.0 M methanol in 0.5 M  $\text{H}_2\text{SO}_4$  and measured the mass activity for methanol oxidation by the PtRu/CNT/GC, PtRuCr/CNT/GC, and PtRuMo/CNT/GC electrodes at the scan rate  $50 \text{ mV}\cdot\text{s}^{-1}$ . As shown in Table 4.3, the obtained mass activity for all of the modified electrodes was in good agreement with the results from Fig. 4.22, indicating the reproducibility of these electrodes. Moreover, it can be concluded that 0.5-4.0 M methanol is the optimized range of methanol concentration for the PtRu/CNT/GC, PtRuCr/CNT/GC, and PtRuMo/CNT/GC electrodes.

**Table 4.3** Mass activity of the optimized PtRu/CNT/GC, PtRuCr/CNT/GC, and PtRuMo/CNT/GC electrodes for 4.0 M methanol in 0.5 M H<sub>2</sub>SO<sub>4</sub> recorded at the scan rate of 50 mV·s<sup>-1</sup>

Catalyst	Mass Activity / A·(g catalyst) <sup>-1</sup>
PtRu/CNT (2:1.5)	122.76
PtRuCr/CNT (2:0.5:1)	148.98
PtRuMo/CNT (2:1:0.5)	170.57

#### 4.8 Repeatability of Metal/CNT Modified Glassy Carbon Electrodes

Repeatability of the optimal metal/CNT/GC electrodes has been investigated by using cyclic voltammetry. Fig. 4.23 demonstrates repetitive mass activity of the Pt/CNT/GC, 2:1.5 PtRu/CNT/GC, 2:0.5:1 PtRuCr/CNT/GC, 2:1:0.5 PtRuMo/CNT/GC, and 2:1:0.5 PtRuNi/CNT/GC electrodes obtained for the oxidation of 1.0 M methanol in 0.5 M H<sub>2</sub>SO<sub>4</sub>. The results revealed that the Pt/CNT/GC, 2:1.5 PtRu/CNT/GC, 2:0.5:1 PtRuCr/CNT/GC, and 2:1:0.5 PtRuNi/CNT/GC electrodes can be used to oxidize 1.0 M methanol at least four times before slowly decreasing its activity for methanol oxidation. For the 2:1:0.5 PtRuMo/CNT/GC electrode, it can be fully used to oxidize 1.0 M methanol for seven times without any significant activity change. It is clear that the repeatability of each modified electrode was not equal, depending on the catalyst components and the results of repeatability test indicated that the PtRuMo/CNT/GC electrode had better performance for methanol oxidation than the others.

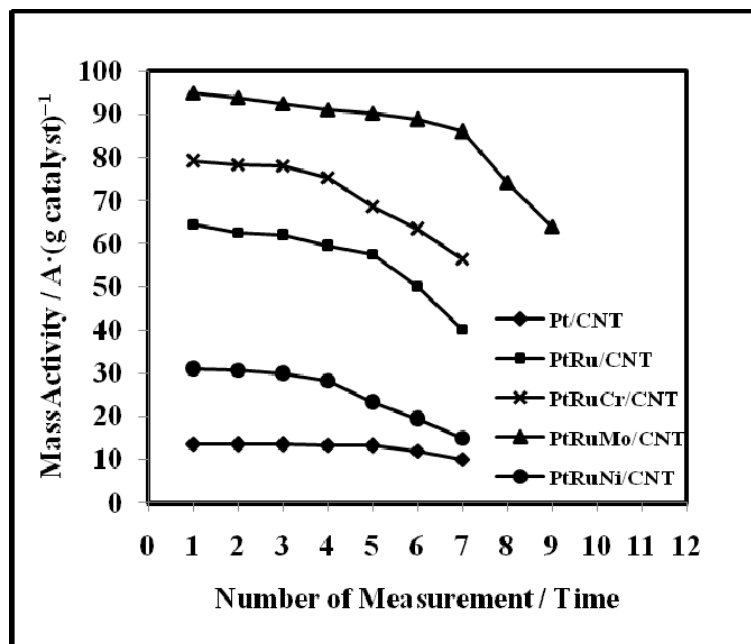


**Figure 4.23** Repetitive mass activity of the Pt/CNT/GC, 2:1.5 PtRu/CNT/GC, 2:0.5:1 PtRuCr/CNT/GC, and 2:1:0.5 PtRuMo/CNT/GC electrodes for the oxidation of 1.0 M methanol in 0.5 M H<sub>2</sub>SO<sub>4</sub> solution.

#### 4.9 Stability of Metal/CNT Modified Glassy Carbon Electrodes

The stability of the metal/CNT/GC electrodes has been studied by chronoamperometry. Fig. 4.24 shows the mass activity obtained from the oxidation of 1.0 M methanol for 1,800 s at the potentials of (a)  $E_{1/2}$  and (b)  $E_{1/4}$  (Table 3.12, p.32) for the Pt/CNT/GC, 2:1.5 PtRu/CNT/GC, 2:0.5:1 PtRuCr/CNT/GC, 2:1:0.5 PtRuMo/CNT/GC, and 2:1:0.5 PtRuNi/CNT/GC electrodes. Initially, the mass activity of methanol oxidation decreased rapidly for the Pt/CNT/GC, PtRu/CNT/GC, and PtRuNi/CNT/GC electrodes, but the mass activity increased rapidly for the PtRuCr/CNT/GC and PtRuMo/CNT/GC electrodes. These results may be due to the formation of intermediate species during the oxidation of methanol [41]. After that, the mass activity was gradually perished for all of the modified electrodes. One reason for the long time decay can be attributed to the adsorbed species (e.g., Pt-O<sub>(ads)</sub> and SO<sub>4</sub><sup>2-</sup>) on the Pt surface, which can restrict methanol oxidation reaction [24].

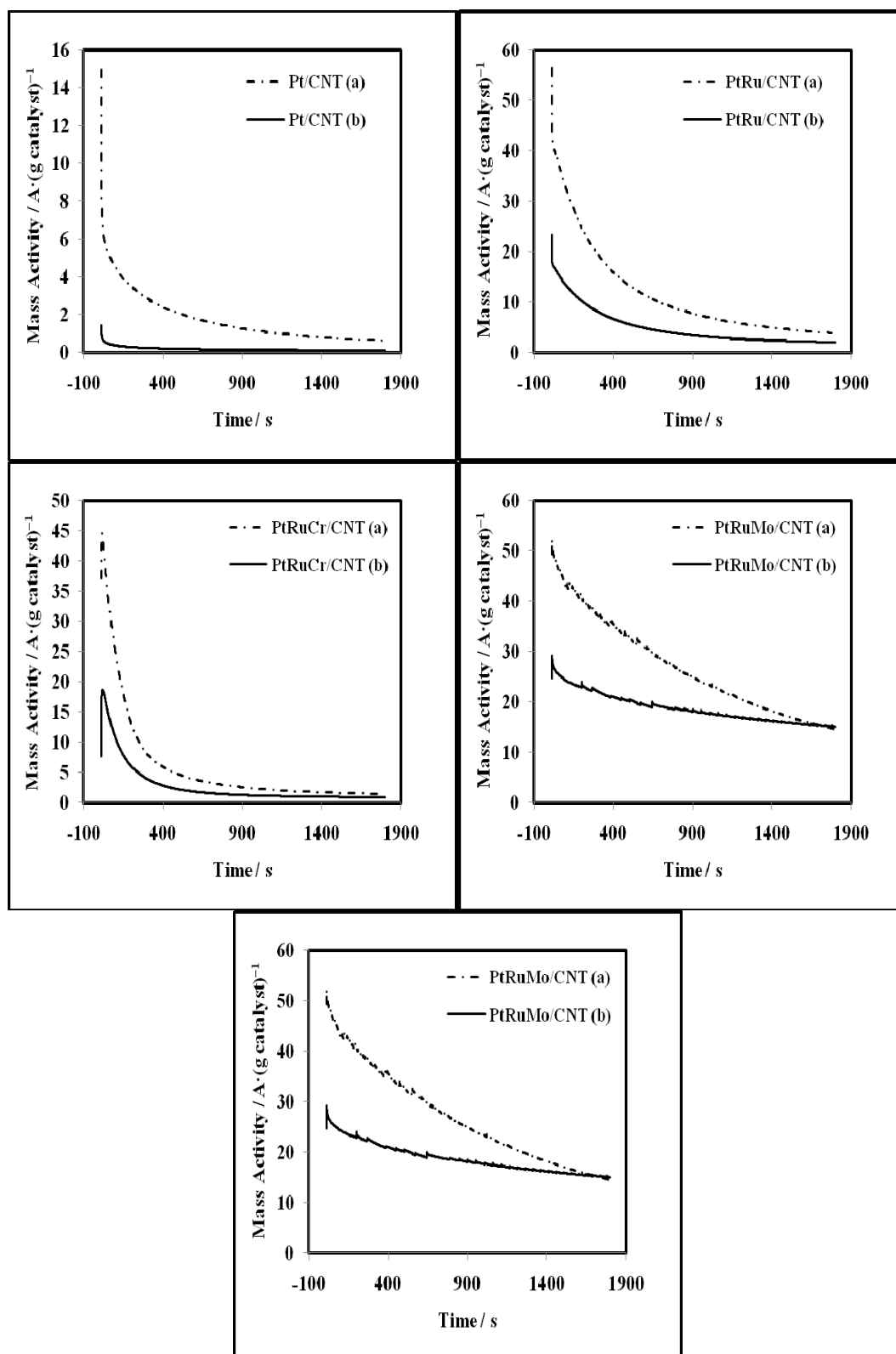


**Figure 4.24** Chronoamperograms of the Pt/CNT/GC, 2:1.5 PtRu/CNT/GC, 2:5:1 PtRuCr/CNT/GC, 2:1:0.5 PtRuMo/CNT/GC, and 2:1:0.5 PtRuNi/CNT/GC electrodes for the oxidation of 1.0 M methanol in 0.5 M H<sub>2</sub>SO<sub>4</sub> solution recorded at the potentials of (a)  $E_{1/2}$  and (b)  $E_{1/4}$  according to the information in Table 3.12.

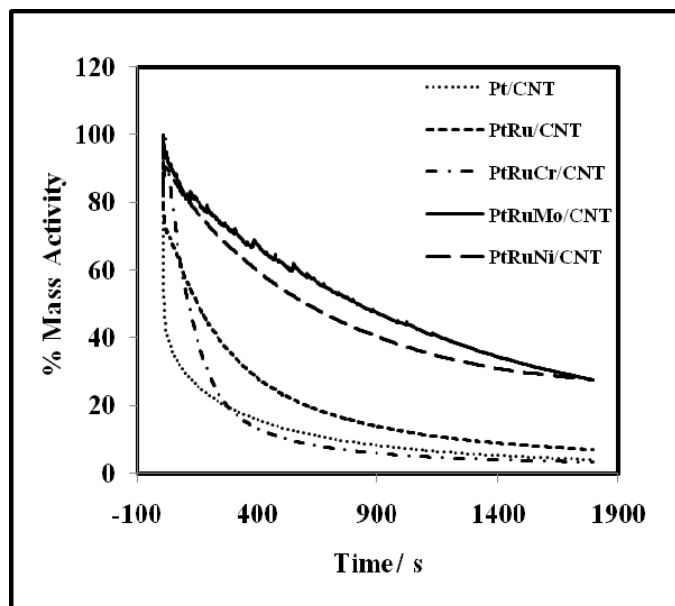


**Figure 4.25** Percentage of mass activity vs. time for the oxidation of 1.0 M methanol in 0.5 M H<sub>2</sub>SO<sub>4</sub> recorded at the potential of  $E_{1/2}$  by Pt/CNT/GC, 2:0.5:1 PtRuCr/CNT/GC, 2:1:0.5 PtRuMo/CNT/GC, and 2:1:0.5 PtRuNi/CNT/GC electrodes in chronoamperometric experiment.

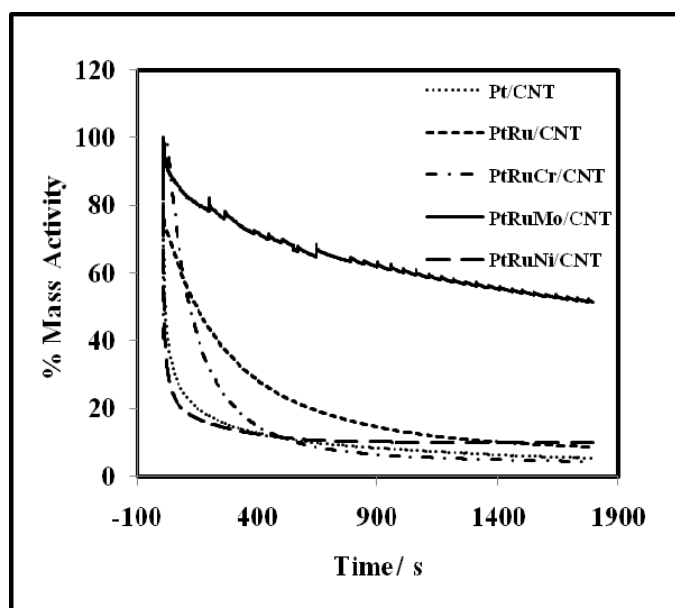


**Figure 4.26** Percentage of mass activity vs. time for the oxidation of 1.0 M methanol in 0.5 M H<sub>2</sub>SO<sub>4</sub> recorded at the potential of  $E_{1/4}$  by Pt/CNT/GC, 2:0.5:1 PtRuCr/CNT/GC, 2:1:0.5 PtRuMo/CNT/GC, and 2:1:0.5 PtRuNi/CNT/GC electrodes in chronoamperometric experiment.



To compare the chronoamperometric results of all electrodes directly, Fig. 4.25 and 4.26 display percentage of mass activity at the potentials of  $E_{1/2}$  and  $E_{1/4}$  vs. time for the oxidation of 1.0 M methanol. The results at these potentials were studied to mimic the real usage situation. Besides the  $E_{1/4}$  and  $E_{1/2}$  potentials might cause different degrees of methanol oxidation and re-oxidation processes, making the investigation at these two potentials be worthwhile. Results from Fig. 4.25 showed that the mass activity for methanol oxidation decreased slowly for the PtRuMo/CNT/GC and PtRuNi/CNT/GC electrodes. Although the PtRuNi/CNT/GC electrode had poor activity for methanol oxidation, it had good stability for long time usage. The Pt/CNT/GC, PtRu/CNT/GC, and PtRuCr/CNT/GC electrodes displayed poor stability for methanol oxidation at this  $E_{1/2}$  potential. As shown in Fig. 4.26, only the percentage of the mass activity of PtRuMo/CNT/GC electrode decreased gradually. Thus, it can be concluded from Fig.4.25 and 4.26 that the PtRuMo/CNT/GC electrode had the highest stability. Furthermore, although the PtRuNi/CNT/GC electrode had excellent stability at  $E_{1/2}$ , it showed low stability at  $E_{1/4}$ .

## CHAPTER V

### CONCLUSIONS AND SUGGESTIONS

#### 5.1 Conclusions

Pt-based bi-metallic and tri-metallic catalysts supported on CNT have been prepared by polyol process for the oxidation of methanol. XRD, TEM, and XRF-EDX results confirmed the successful formation of Pt/CNT, PtRu/CNT, PtRuCr/CNT, PtRuMo/CNT, PtRuNi/CNT and other Pt-based catalysts. TEM images showed that well-dispersed metal nanoparticles with the approximate size of 2.5 nm were deposited on the CNT. Catalytic activity of the synthesized catalysts for methanol oxidation in 0.5 M H<sub>2</sub>SO<sub>4</sub> were investigated by means of cyclic voltammetry at the scan rate of 50 mV.s<sup>-1</sup>. Our results indicated that the addition of the second metal to Pt distinctly improved its catalytic activity for methanol oxidation. It was found that Ru, Cr, and Mo greatly enhanced the catalytic performance of Pt. For the bi-metallic system, the PtRu/CNT/GC electrode with 2:1.5 Pt-to-Ru mole ratio was the optimal modified electrode for methanol oxidation.

Using PtRu/CNT as a base catalyst, the addition of Cr or Mo to PtRu/CNT could improve the electrocatalytic activity for methanol oxidation whereas Ni could not improve this property. Among various ratios of metal components, the 2:1:0.5 PtRuMo/CNT/GC showed the highest catalytic activity. Although the PtRuCr/CNT/GC electrode with the optimal Pt-to-Ru-to-Cr mole ratio (2:0.5:1) had lower activity for methanol oxidation, it exhibited higher catalytic activity than the optimized PtRu/CNT/GC electrode.

Moreover, good electrode candidates including 2:1.5 PtRu/CNT/GC, 2:0.5:1 PtRuCr/CNT/GC, and 2:1:0.5 PtRuMo/CNT/GC electrodes produced highest mass activity for methanol oxidation at the methanol concentration of 4.0 M. In terms of electrode repeatability, the PtRuMo/CNT can be reproducibly used to oxidize 1.0 M methanol for seven times, showing the best repeatability for methanol oxidation among other modified electrodes. In addition, the PtRuMo/CNT/GC electrode had the highest stability. Therefore, considering from the criteria of the mass activity for

methanol oxidation, the reproducibility, and the stability, the PtRuMo/CNT/GC electrode with the 2:1:0.5 Pt-to-Ru-to-Mo mole ratio seems likely to be the best candidate for methanol oxidation. Note that although the 2:1:0.5 PtRuNi/CNT/GC electrode had excellent stability, it showed poor catalytic activity for methanol oxidation.

## 5.2 Suggestion

It is known that the activity of the metal/CNT catalysts is greatly dependent on the catalyst loading on CNT. Various amount of metals used in the preparation of metal/CNT catalysts will be investigated to obtain the optimized metal loading on CNT. In addition, the optimal catalysts such as 2:0.5:1 PtRuCr/CNT and 2:1:0.5 PtRuMo/CNT will be tested in single cell measurements to check the catalyst performance towards DMFC application.

## REFERENCES

- [1] Samant, P.V.; Rangel, C.M.; Romero, M.H.; Fernandes, J.B.; and Figueiredo, J.L. Carbon supports for methanol oxidation catalyst. J. Power Sources 151 (2005): 79–84.
- [2] Hamnett, A. Mechanism and electrocatalysis in the direct methanol fuel cell. Catal. Today 38 (1997): 445–457.
- [3] Watanabe, M.; Saegusa, S.; and Stonehart, P. High platinum electrocatalyst utilizations for direct methanol oxidation. J. Electroanal. Chem. 271 (1989): 213–220.
- [4] Umeda, M.; Kokubo, M.; Mohamedi, M.; and Uchida, I. Porous-microelectrode study on Pt/C catalysts for methanol electrooxidation. Electrochim. Acta 48 (2003): 1367–1374.
- [5] Kim H.T.; You, D.J.; Yoon, H.K.; Joo, S.H.; Pak, C.; Chang, H.; and Song, I.S. Cathode catalyst layer using supported Pt catalyst on ordered mesoporous carbon for direct methanol fuel cell. J. Power Sources 180 (2008): 724–732.
- [6] Yan, S.; Sun, G.; Tian, J.; Jiang, L.; Qi, J.; and Xin, Q. Polyol synthesis of highly active PtRu/C catalyst with high metal loading. Electrochim. Acta 52 (2006): 1692–1696.
- [7] Fernández, P.H.; Rojas, S.; Ocón, P.; de Frutos, A.; Figueroa, J.M.; Terreros, P.; Peña, M.A.; and Fierro, J.L.G. Relevance of the nature of bimetallic PtAu nanoparticles as electrocatalysts for the oxygen reduction reaction in the presence of methanol. J. Power Sources 177 (2008): 9–16.
- [8] Gasteiger, H.A.; Markovic, N.; Ross Jr., P.N.; and Cairns, E.J. Methanol electrooxidation on well-characterized platinum-ruthenium bulk alloys. J. Phys. Chem. 97 (1993): 12020–12029.
- [9] He, Z.; Chen, J.; Liu, D.; Zhou, H.; and Kuang, Y. Electrodeposition of Pt–Ru nanoparticles on carbon nanotubes and their electrocatalytic properties for methanol electrooxidation. Diamond Relat. Mater. 13 (2004): 1764–1770.

- [10] Guo, J.; Sun, G.; Sun, S.; Yan, S.; Yang, W.; Qi, J.; Yan, Y.; and Xin, Q. Polyol-synthesized PtRu/C and PtRu black for direct methanol fuel cells. J. Power Sources 168 (2007): 299–306.
- [11] Tokarz, W.; Siwek, H.; Piela, P.; and Czerwiński, A. Electro-oxidation of methanol on Pt-Rh alloys. Electrochim Acta 52 (2007): 5565–5573.
- [12] Park, I.S.; Lee, K.S.; Jung, D.S.; Park, H.Y.; and Sung, Y.E. Electrocatalytic activity of carbon-supported Pt–Au nanoparticles for methanol electro-oxidation. Electrochim. Acta 52 (2007): 5599–5605.
- [13] Wang, Z.H.; Zhang, L.L.; and Qiu, K.Y. Electrocatalytic oxidation of methanol by platinum nanoparticles on nickel–chromium alloys. J. Power Sources 161 (2006): 133–137.
- [14] Zhu, J.; Su, Y.; Cheng, F.; and Chen, J. Improving the performance of PtRu/C catalysts for methanol oxidation by sensitization and activation treatment. J. Power Sources 166 (2007): 331–336.
- [15] Carmo, M.; Linardi, M.; and Poco, J.G.R. Characterization of nitric acid functionalized carbon black and its evaluation as electrocatalyst support for direct methanol fuel cell applications. Appl. Catal. A: General 355 (2009): 132–138.
- [16] Salazar-Banda, G.R.; Eguiluz, K.I.B.; and Avaca, L.A. Boron-doped diamond powder as catalyst support for fuel cell applications. Electrochem. Commun. 9 (2007): 59–64.
- [17] Bauer, A.; Gyenge, E.L.; and Oloman, C.W. Direct methanol fuel cell with extended reaction zone anode: PtRu and PtRuMo supported on graphite felt. J. Power Sources 167 (2007): 281–287.
- [18] Guo, D.J. and Li, H.L. Electrocatalytic oxidation of methanol on Pt modified single-walled carbon nanotubes. J. Power Sources 160 (2006): 44–49.
- [19] Tang, H.; Chen, J.; Yao, S.; Nie, L.; Kuang, Y.; Huang, Z.; Wang, D.; and Ren, Z. Deposition and electrocatalytic properties of platinum on well-aligned carbon nanotube (CNT) arrays for methanol oxidation. Mater. Chem. Phys. 92 (2005): 548–553.
- [20] Chen, C.C.; Chen, C.F.; Chen, C.M.; and Chuang, F.T. Modification of multi-walled carbon nanotubes by microwave digestion method as electrocatalyst supports for direct methanol fuel cell applications. Electrochem. Commun. 9 (2007): 159–163.

- [21] Knupp, S.L.; Li, W.; Paschos, O.; Murray, T.M.; Snyder, J.; and Haldar, P. The effect of experimental parameters on the synthesis of carbon nanotube/nanofiber supported platinum by polyol processing techniques. Carbon 46 (2008) 1276–1284.
- [22] Prabhuram, J.; Zhao, T.S.; Tang, Z.K.; Chen, R.; and Liang, Z.X. Multiwalled carbon nanotube supported PtRu for the anode of direct methanol fuel cells. J. Phys. Chem. B 110 (2006): 5245–5252.
- [23] Xu, J.; Hua, K.; Sun, G.; Wang, C.; Lv, X.; and Wang, Y. Electrooxidation of methanol on carbon nanotubes supported Pt–Fe alloy electrode. Electrochem. Commun. 8 (2006): 982–986.
- [24] Prabhuram, J.; Zhao, T.S.; Liang, Z.X.; and Chen R.A. A simple method for the synthesis of PtRu nanoparticles on the multi-walled carbon nanotube for the anode of a DMFC. Electrochim. Acta 52 (2007): 2649–2656.
- [25] Li, X.; Chen, W.X.; Zhao, J.; Xing, W.; and Xu, Z.D. Microwave polyol synthesis of Pt/CNTs catalysts: effects of pH on particle size and electrocatalytic activity for methanol electrooxidation. Carbon 43 (2005): 2168–2174.
- [26] Chen, W.; Zhao, J.; Lee, J.Y.; and Liu, Z. Microwave heated polyol synthesis of carbon nanotubes supported Pt nanoparticles for methanol electro-oxidation. Mater. Chem. Phys. 91(2005): 124–129.
- [27] Liu, Z.; Ling, X.Y.; Guo, B.; Hong, L.; and Lee, J.Y. Pt and PtRu nanoparticles deposited on single-wall carbon nanotubes for methanol electro-oxidation. J. Power Sources 167 (2007): 272–280.
- [28] Saito, R., Dresselhaus, G., and Dresselhaus, M.S. Physical properties of carbon nanotubes. London: Imperial College Press, 1998.
- [29] Roychowdhury, C.; Matsumoto, F.; Mutolo, P.F.; Abrua, H.D.; and DiSalvo, F.J. Synthesis, characterization, and electrocatalytic activity of PtBi nanoparticles prepared by the polyol process. Chem. Mater. 17 (2005): 5871–5876.
- [30] Wang, J. Analytical Electrochemistry. 2<sup>nd</sup> ed. USA: John Wiley & Sons, Inc., Publication, 1976.
- [31] Rodríguez, J.M.D.; Melián, J.A.H.; and Peña, J.P. Determination of the real surface area of Pt electrodes by hydrogen adsorption using cyclic voltammetry. J. Chem. Educ. 77 (2000): 1195–1197.

- [32] Grigoriev, S.A.; Millet, P.; and Fateev, V.N. Evaluation of carbon-supported Pt and Pd nanoparticles for the hydrogen evolution reaction in PEM water electrolyzers. J. Power Sources 177 (2008): 281–285.
- [33] Smith, B.C. Fundamentals of Fourier Transform Infrared Spectroscopy. USA: CRC Press, 1996.
- [34] Whiston, C. X-ray Methods: Analytical Chemistry by Open Learning. Singapore: John Wiley & Sons, Inc., Publication, 1991.
- [35] Flegler, S.L.; Heckman Jr., J.W.; and Klomparens, K.L. Scanning and Transmission Electron Microscopy An Introduction. USA: Oxford University Press, 1993.
- [36] Wang, Z.; Liu, J.; Liang, Q.; Wang, Y.; and Luo, G. Carbon nanotube-modified electrodes for the simultaneous determination of dopamine and ascorbic acid. The Analyst 127 (2002): 653–658.
- [37] Chen, J.; Wang, M.; Liu, B.; Fan, Z.; Cui, K.; and Kuang, Y. Platinum catalysts prepared with functional carbon nanotube defects and its improved catalytic performance for methanol oxidation. J. Phys. Chem. B 110 (2006): 11775–11779.
- [38] Yuan, P.S.; Wu, H.Q.; Xu, H.Y.; Xu, D.M.; Cao, Y.J.; and Wei, X.W. Synthesis, characterization and electrocatalytic properties of FeCo alloy nanoparticles supported on carbon nanotubes. Mater. Chem. Phys. 105 (2007): 391–394.
- [39] Jeon, M.K.; Lee, K.R.; Daimon, H.; Nakahara, A.; and Woo, S.I. Pt<sub>45</sub>Ru<sub>45</sub>M<sub>10</sub>/C (M = Fe, Co, and Ni) catalysts for methanol electro-oxidation. Catal. Today 132 (2008): 123–126.
- [40] Nart, F.C.; and Vielstich, W. Wang, Handbook of Fuel Cells: Fundamental, Technology and Applications. Vol.2. USA: John Wiley & Sons, 2003.
- [41] Gu, Y.J. and Wong, W.T. Nanostructure PtRu/MWNTs as anode catalysts prepared in a vacuum for direct methanol oxidation. Langmuir 22 (2006): 11447–11452.
- [42] Hsieh, C.T.; and Lin, J.Y. Fabrication of bimetallic Pt–M (M= Fe, Co, and Ni) nanoparticle/carbon nanotube electrocatalysts for direct methanol fuel cells. J. Power Sources 188 (2009): 347–352.

- [43] Franco, E.G.; Neto, A.O.; Linardi, M.; and Aricó, E. Synthesis of electrocatalysts by the Bönemann method for the oxidation of methanol and the mixture H<sub>2</sub>/CO in a proton exchange membrane fuel cell. J. Braz. Chem. Soc. 13 (2002) 516–521.



## **APPENDIX**

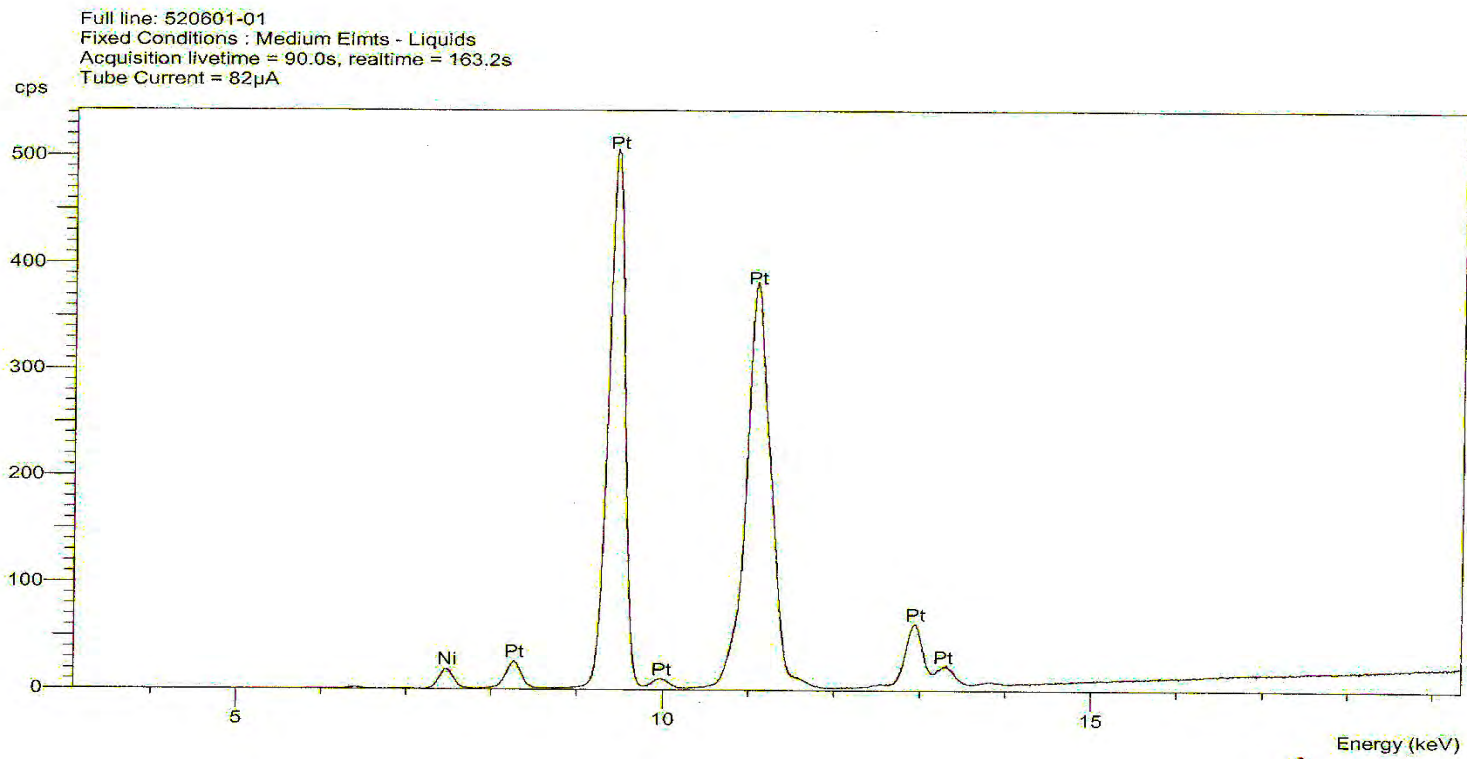


**Figure 1A** XRF-EDX spectrum of Pt/CNT catalyst

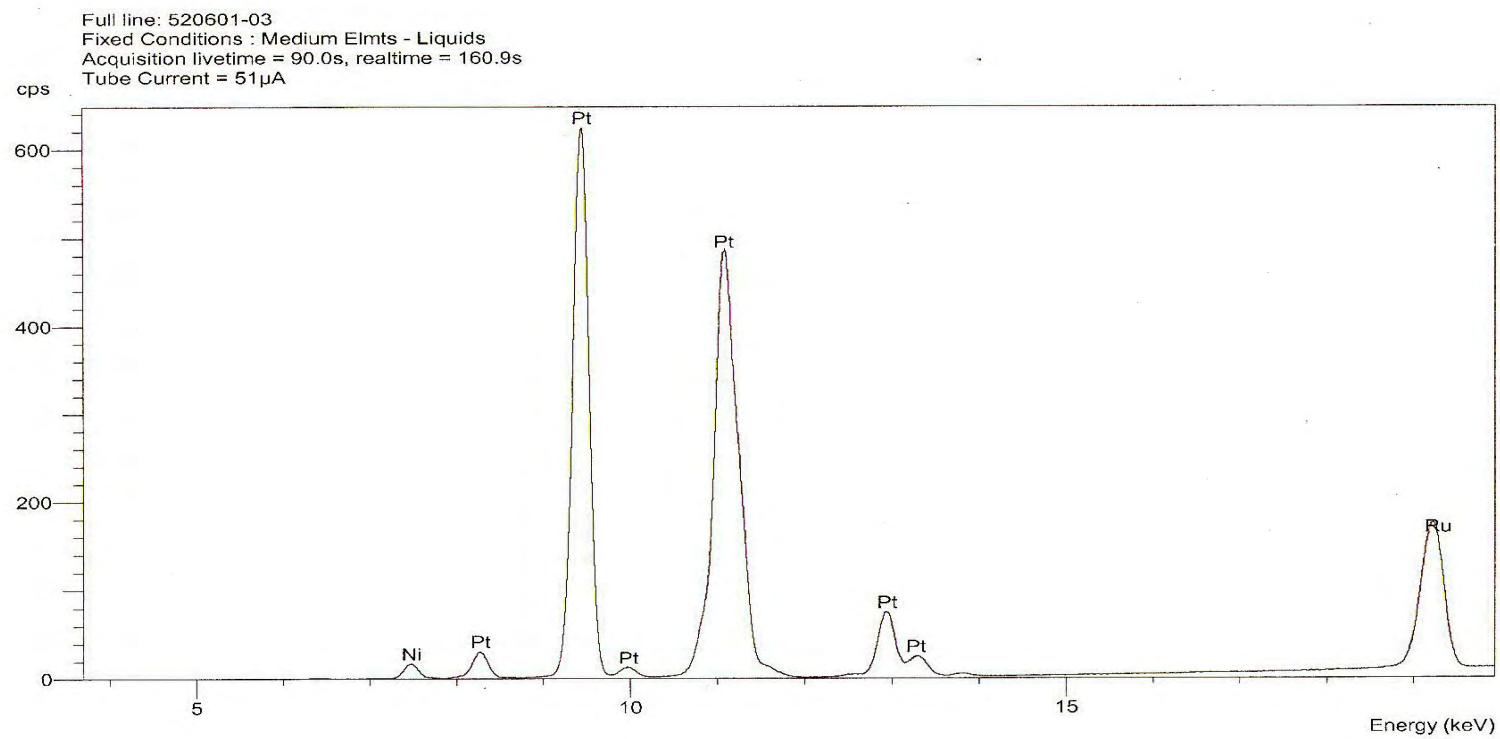


**Figure 2A** XRF-EDX spectrum of PtRu/CNT catalyst with Pt-to-Ru mole ratio 2:1

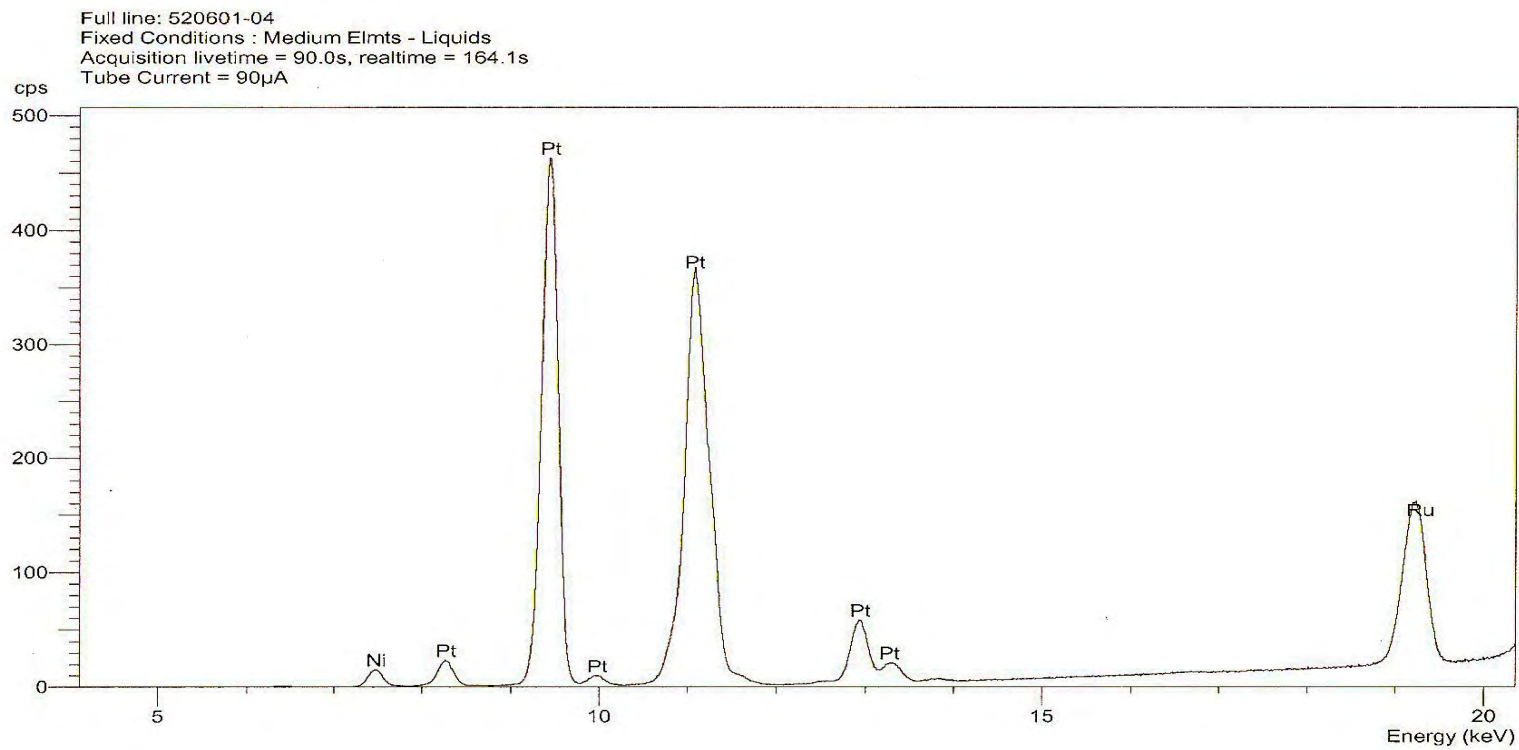


**Figure 3A** XRF-EDX spectrum of PtRu/CNT catalyst with Pt-to-Ru mole ratio 2:1.25

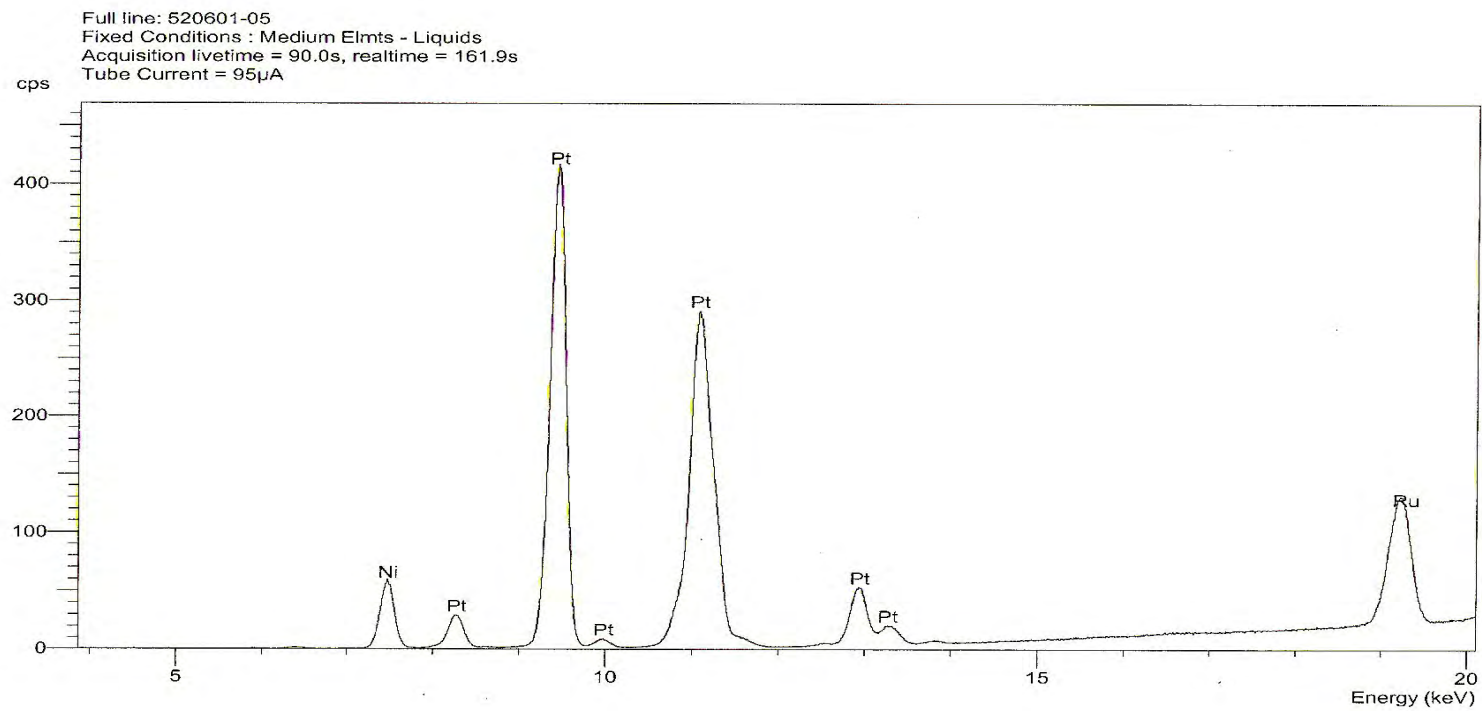


**Figure 4A** XRF-EDX spectrum of PtRu/CNT catalyst with Pt-to-Ru mole ratio 2:1.5

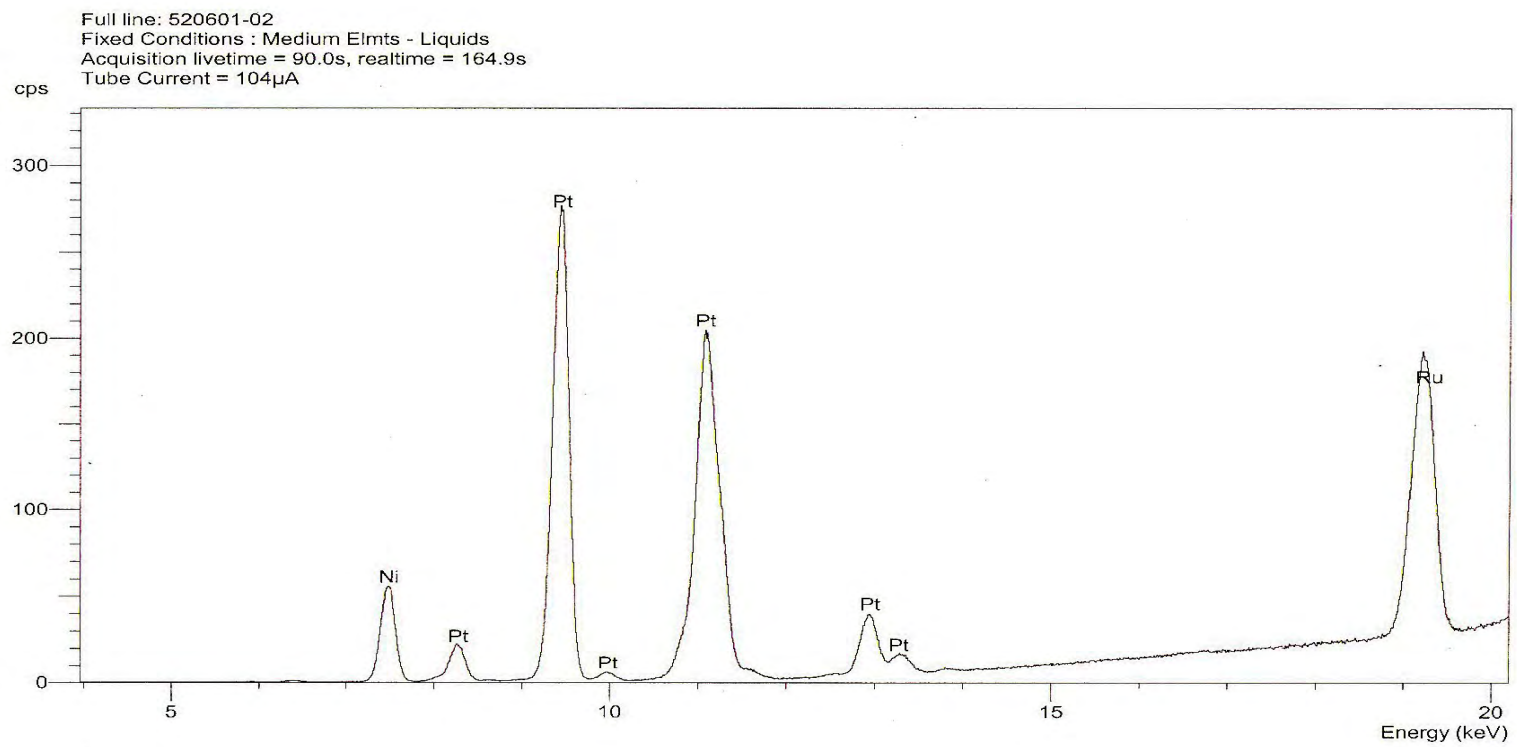


**Figure 5A** XRF-EDX spectrum of PtRu/CNT catalyst with Pt-to-Ru mole ratio 2:2

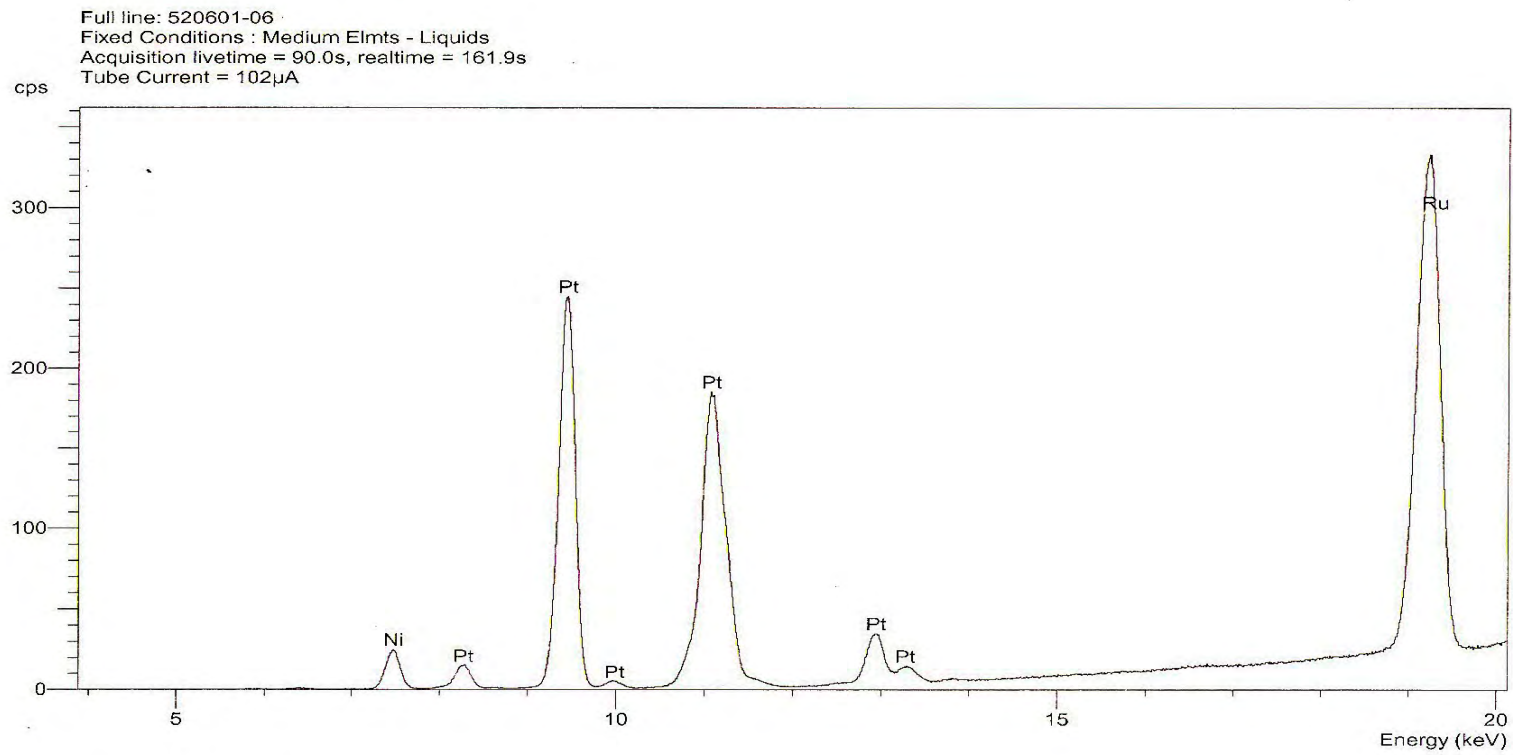


**Figure 6A** XRF-EDX spectrum of PtRu/CNT catalyst with Pt-to-Ru mole ratio 2:4

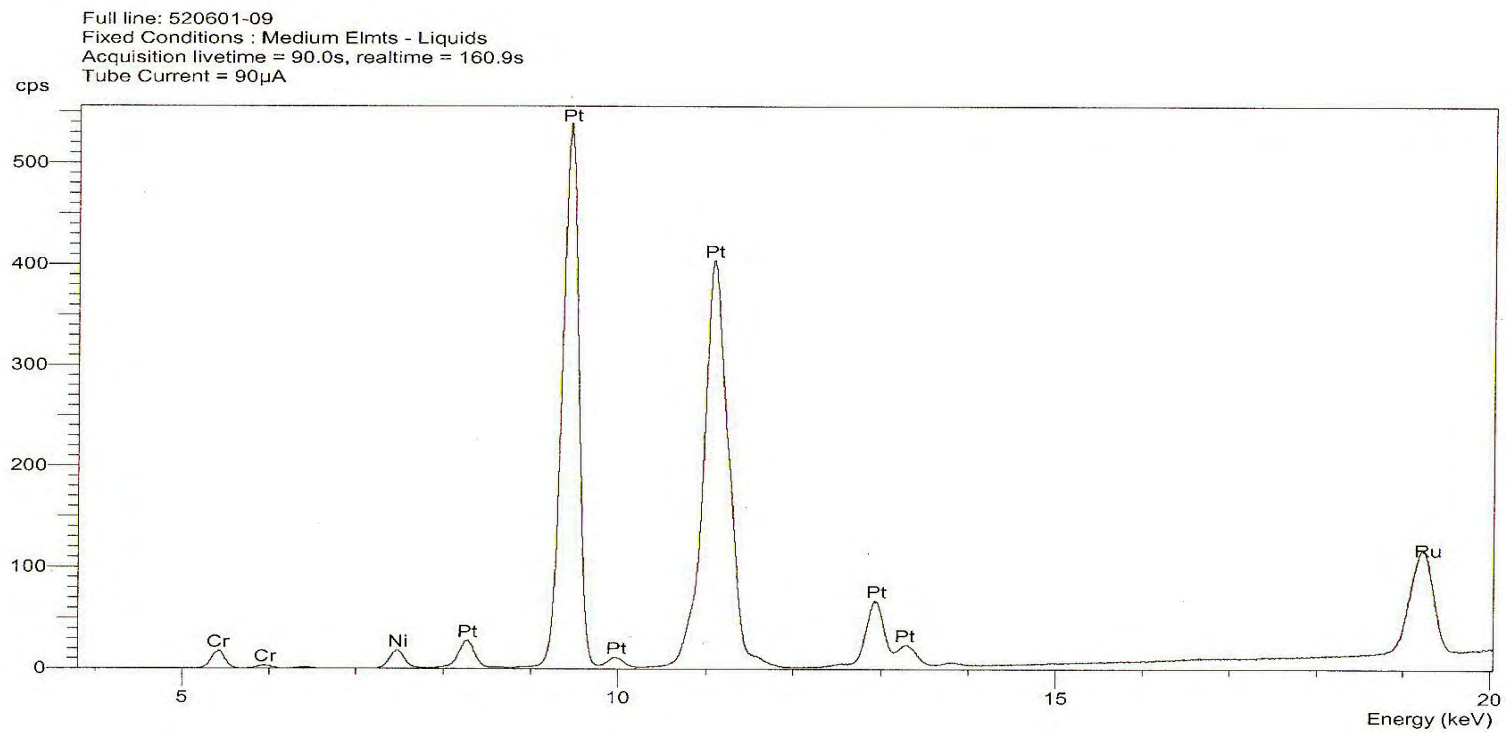


**Figure 7A** XRF-EDX spectrum of PtRuCr/CNT catalyst with Pt-to-Ru-to-Cr mole ratio 2:0.5:1



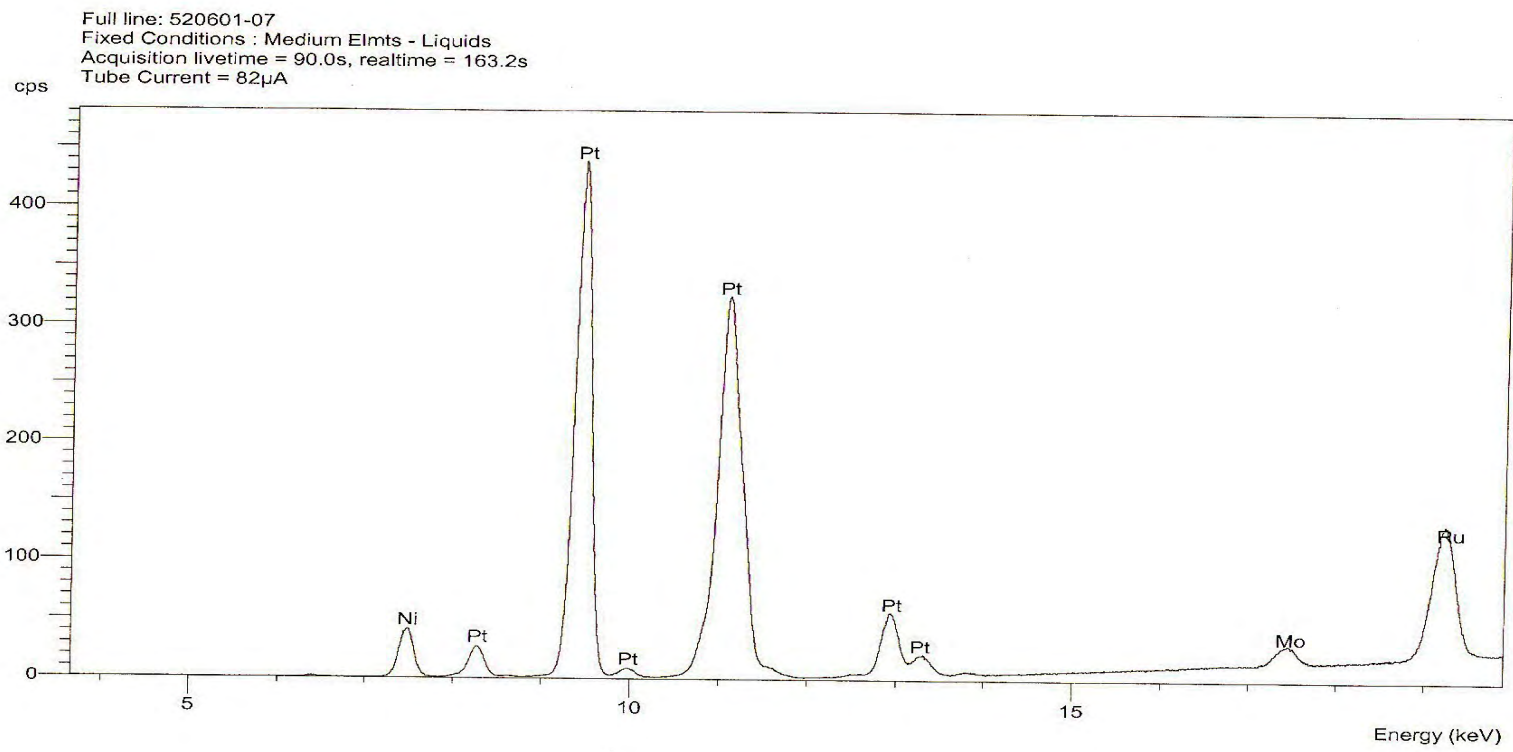


**Figure 8A** XRF-EDX spectrum of PtRuMo/CNT catalyst with Pt-to-Ru-to-Mo mole ratio 2:1:0.5

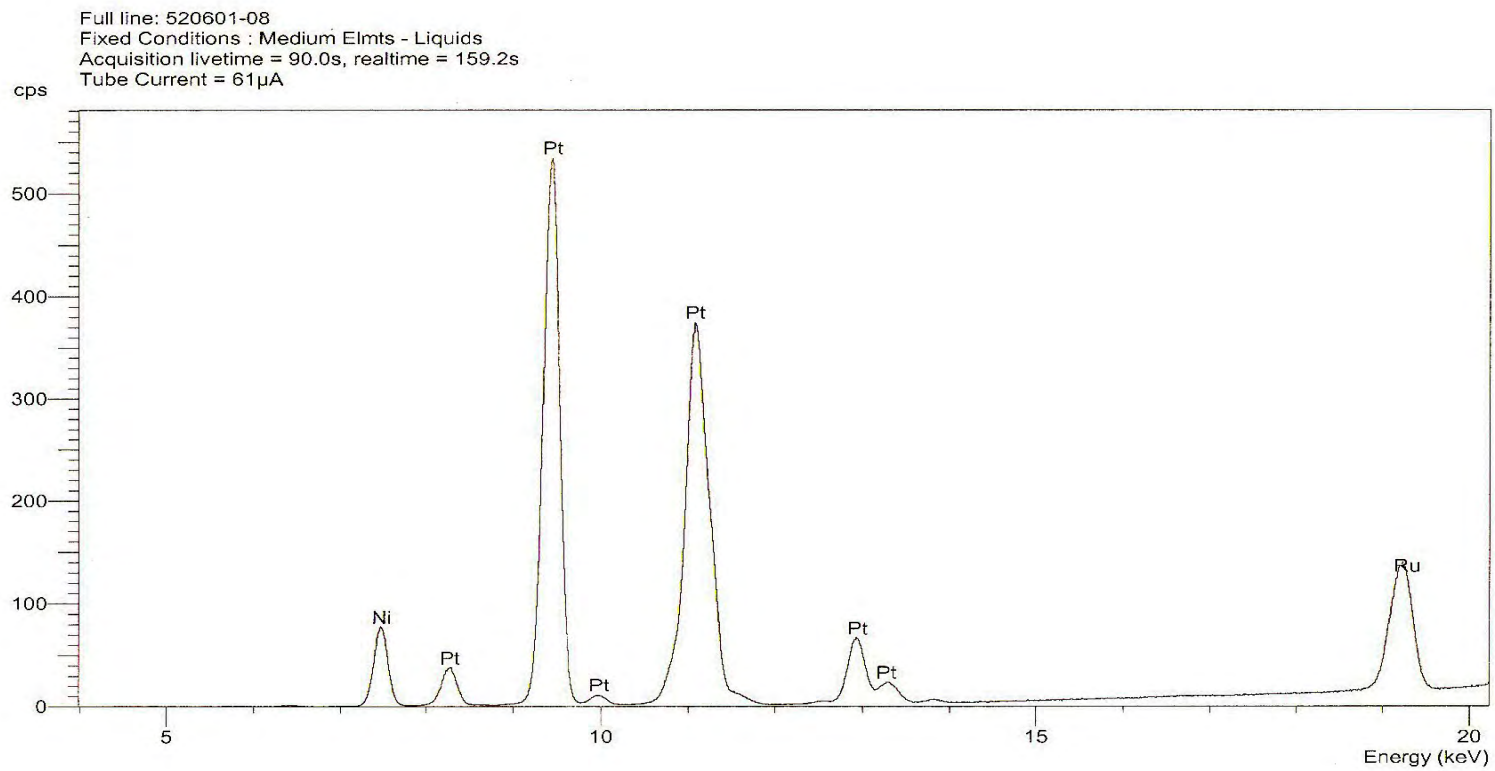


**Figure 9A** XRF-EDX spectrum of PtRuNi-CNT catalyst with Pt-to-Ru-to-Ni mole ratio 2:1:0.5

**VITA**

- Name** : Miss Rattana Cheerapradit
- Date of Birth** : Sep 17, 1983
- Place of Birth** : Suphanburi, Thailand
- Graduated** : 2002–2006 Bachelor Degree of Science  
(General Science), Kasetsart University
- 2006–2009 Master Degree in the Program of  
Petrochemistry and Polymer Science,  
Chulalongkorn University
- Home address:** 11, Moo 3, Tambol Paknum, Amphur Lungsuan,  
Chumporn 86150, Thailand
- Poster Presentation** : 2008 The Science Forum 2008, Bangkok
- 2008 5th Thailand materials Science and  
Technology Conference, Bangkok
- 2008 The 34th Congress on Science and  
Technology of Thailand (STT34),  
Bangkok
- Oral Presentation** : 2009 PACCON Pure and Applied Chemistry  
International Conference 2009,  
Phitsanulok